

**Design of cell culture substrates
for large-scale preparation of neural cells**

Shuhei Konagaya

2013

Contents

General Introduction	1
References	9

Chapter 1

Array-based functional screening of growth factors toward optimizing neural stem cell microenvironments

1.1	Introduction	17
1.2	Materials and methods	19
	Preparation of His-tagged growth factors	
	Preparation of growth factor arrays	
	Surface plasmon resonance imaging	
	Isolation and culture of NSCs	
	Cell culture on growth factor arrays	
	Immunostaining	
	Cluster analysis	
1.3	Results	25
	Preparation of His-tagged growth factors	
	Preparation of growth factor arrays	
	Cell proliferation	
	Cell differentiation	
	Cluster analysis	
1.4	Discussion	36
	References	39

Chapter 2

Design of culture substrates for large-scale expansion of neural stem cells

2.1	Introduction	45
2.2	Materials and methods	48
	Plasmid construction	
	Protein expression and purification	

	Preparation of glass-based culture modules	
	Surface anchoring of EGF-PSt on polystyrene	
	Determination of immobilized EGF-His and EGF-PSt	
	Surface plasmon resonance analysis	
	Spectroscopic analysis of immobilized EGF-His and EGF-PSt	
	Isolation of NSCs	
	Expansion of NSCs	
	Determination of cell number	
	Immunocytochemical staining	
	Differentiation culture	
	Analysis of EGF receptor expression	
2.3	Results	58
	Preparation of EGF-His and EGF-PSt	
	Surface anchoring of EGF-His to glass	
	Surface anchoring of EGF-PSt to polystyrene	
	NSC proliferation on a substrate with anchored EGF-His	
	NSC proliferation on polystyrene with anchored EGF-PSt	
	Expression of EGFR	
2.4	Discussion	69
	References	72

Chapter 3

Selective and rapid expansion of human neural progenitor cells on a substrate with terminally-anchored growth factors

3.1	Introduction	75
3.2	Materials and methods	76
	Protein expression and purification	
	Immobilization of EGF-His and bFGF-His on the glass surface	
	Surface characterization	
	hNPC Culture	
	Cell proliferation assay	
	Immunostaining	
	Differentiation culture	
	Reverse transcriptase-polymerase chain reaction (RT-PCR)	
	Flow cytometry	

3.3	Results	84
	Immobilization of EGF-His and bFGF-His	
	Secondary structure analysis of immobilized EGF-His and bFGF-His	
	Expression of EGFR and FGFR1	
	Cell proliferation on growth factor-immobilized substrates	
	Immunofluorescent staining	
	Subculture of expanded cells	
3.4	Discussion	91
	References	94

Chapter 4

Effect of surface-immobilized extracellular matrices on the proliferation of neural progenitor cells derived from induced pluripotent stem cells

4.1	Introduction	97
4.2	Materials and methods	98
	Preparation of ECM array	
	Quantification of immobilized ECM	
	Mouse iPS cells	
	Array-based assay	
	Human iPS cells	
	Expansion differentiation of hNPCs	
	Immunostaining	
	Reverse transcriptase-polymerase chain reaction (RT-PCR)	
	Reverse phase high performance liquid chromatography (HPLC)	
4.3	Results	105
	Immobilization of ECM proteins	
	Induction of miPS cells to neural lineage miPS cells	
	Array based screening of ECMs for NPC expansion	
	Expansion of hiPS-derived NPC on laminin substrate	
	Differentiation of hNPC into dopamine neurons	
4.4	Discussion	112
	References	115

Chapter 5

Induction of dopamine neurons derived from human induced pluripotent stem cells in microcapsule

5.1	Introduction	121
5.2	Materials and methods	123
	Human iPS cell culture and differentiation to dopamine neuron	
	Formation of cell aggregates	
	Agarose microencapsulation	
	DA secretion and high-performance liquid chromatography (HPLC)	
	Immunofluorescence	
	Reverse transcription polymerase chain reaction (RT-PCR)	
	Collection of cell aggregates from microbeads and adherent culture	
	Function of cell aggregates in microbeads after cryopreservation	
5.3	Results	130
	Differentiation of human iPS cells into dopamine neuron	
	Agarose microencapsulation	
	Long-term culture	
	Dopamine production	
	Cryopreservation of encapsulated DA neuron	
5.4	Discussion	136
	References	140
	Summary	145
	List of Publications	149
	Acknowledgements	151

Abbreviations

APTES	3-aminopropyltriethoxysilane
BCA	bicinchoninic acid
BDNF	brain-derived neurotrophic factor
bFGF	basic fibroblast growth factor
BSA	bovine serum albumin
BrdU	5-bromo-2'-deoxyuridine
CD	circular dichroism
cDNA	complementary DNA
CNS	central nervous system
CNTF	ciliary neurotrophic factor
DA	dopamine
DMEM/F12	Dulbecco's modified eagle medium:nutrient mixture F-12
DOPAC	3,4-dihydroxyphenylacetic acid
ECM	extracellular matrix
EDTA	ethylenediamine-N,N,N',N'-tetraacetic acid
EGF	epidermal growth factor
EGFR	epidermal growth factor receptor
ES cell	embryonic stem cell
FBS	fetal bovine serum
FGFR	fibroblast growth factor receptor
GDNF	glial cell line-derived neurotrophic factor

HBSS	Hanks' balanced salt solution
HE	hematoxylin-eosin
HEPES	4-(2-hydroxyethyl)-1-piperazineethanesulfonic acid
His	oligohistidine
HPLC	high performance liquid chromatography
IGF-1	insulin-like growth factor-1
IgG	immunoglobulin G
iPS cell	induced pluripotent stem cell
KSR	knockout serum replacement
LM	laminin
MIR-IRAS	multiple internal reflection-infrared absorption spectroscopy
NSC/NPC	neural stem cell/ neural progenitor cell
NTA	N-(5-amino-1-carboxypentyl) iminodiacetic acid
PBS	phosphate buffer saline
PD	Parkinson's disease
PLO	poly-L-ornithine
RT-PCR	reverse transcriptase-polymerase chain reaction
SAM	self-assembled monolayer
SDS-PAGE	sodium dodecylsulfate-polyacrylamide gel electrophoresis
SPR	surface plasmon resonance
TH	tyrosine hydroxylase
Tween-20	polyoxyethylene sorbitan monolaurate

General Introduction

Cell replacement therapy has been regarded as a promising way to treat Parkinson's disease (PD), type I diabetes, and other cell degenerative diseases [1, 2]. Stem cells derived from tissues and pluripotent stem cells have the ability to self-renew and differentiate into multiple different types of cells. Stem cells are considered as a potential cell source for cell replacement therapy [3, 4]. In fetal and adult tissues, there are several kinds of stem cells, including mesenchymal stem cells [5], hematopoietic stem cells [6], and neural stem cells (NSCs) [7]. In addition to these tissue-derived stem cells, embryonic stem (ES) cells can be derived from mouse [8] and [9] human embryos. ES cells can expand without limit, and they maintain their pluripotency *in vitro*; thus, as replacement cells, they can differentiate into all cell types in the adult body [10, 11]. However, the preparation of ES cells involves destruction of an embryo. This has given rise to ethical concerns and controversy about the development and use of human ES cells in cell replacement therapy. Recently, Yamanaka et al. established induced pluripotent stem (iPS) cells, which are cells reprogrammed to behave like stem cells [12, 13]. These iPS cells display the pluripotency of ES cells, and are considered an alternative cell source for cell replacement therapy.

NSCs are found in fetal and adult neural tissues in the central nervous system (CNS) [14]. During development, NSCs generate neurons, astrocytes, and oligodendrocytes, which are then organized to nervous tissues. NSCs also contribute to neurogenesis in the adult CNS [15, 16]. To date, numerous studies have used NSCs cultured *in vitro* to investigate the molecular and cellular mechanisms underlying mammalian CNS development [17, 18]. In addition, NSCs and neural progenitor cells

(NPCs) have been examined as potential sources for cell replacement therapy in various CNS disorders [19, 20], including neurodegenerative diseases [21], ischemia [22], traumatic injury of the brain [23], and spinal cord injuries (SCI) [24, 25]. For example, brain tissues from aborted human fetuses were transplanted into the brains of patients with PD [26]. In addition, in Switzerland, NSCs are currently being tested in clinical trials for the treatment of SCI [27].

The outcome of the therapy depends on the fate of transplanted cells in the host brain or spinal cord. However, various difficulties remain to be overcome. It is difficult to obtain a sufficient number of cells to treat human patients. In addition, the quality and quantity of cells are not well controlled. Cells must be available for treating the patient in a timely fashion. To address these issues, many studies have extensively investigated methods of cell expansion, differentiation, and cryopreservation. Research in biomaterials can contribute to the development of substrates for stem cell cultures [28-30]. From the clinical point of view, the culture substrate must be free from xeno-proteins, chemically-defined, and inexpensive. Currently, several kinds of culture substrates have been designed for the large-scale expansion of ES cells and iPS cells [31-33]. These substrates include extracellular matrix (ECM) components [31], synthetic polymers [32], and short peptides [33] that facilitate cell adhesion.

The aim of this thesis was to develop cell culture substrates for cells that can be used in cell replacement therapies for CNS disorders. Array-based screening of growth factors and neurotrophic factors was conducted to identify the best candidate for including in a culture substrate to enhance the expansion of NSCs (Chapter 1). Based on the result of this screening, growth factor-immobilized culture substrates were designed and prepared. Then, these culture substrates were evaluated for their efficacy in the

expansion of NSCs derived from rat fetal brain (Chapter 2) and NPCs derived from human fetal brain (Chapter 3). In Chapter 4, surface-immobilized ECM components were evaluated for their effects on the proliferation of NPCs derived from human iPS cells. Chapter 5 is concerned with the preparation of dopamine (DA) neurons for the treatment of PD.

Chapter 1 describes an array-based method for screening growth factors in preparation of creating a suitable environment for NSC expansion. Arrays display a panel of biologically-active substances on a flat plate, which facilitates screening multiple samples in parallel [34]. To gain insight into the effects of various growth factors and their combinations on the behaviors of NSCs, cell culture assays were performed with five different growth factors, including basic fibroblast growth factor (bFGF), epidermal growth factor (EGF), insulin-like growth factor-1, brain-derived neurotrophic factor, and ciliary neurotrophic factor. These factors were prepared in *Escherichia coli* as fusion proteins with a hexahistidine sequence (His-tag). The fusion proteins were arrayed on nickel ion-functionalized chips in spots of single factors or the mixtures of two factors. NSCs isolated from the fetal rat brain were cultured on each chip in the array. Cells were examined to measure proliferation rates and their ability to differentiate into other kinds of cells. The five growth factors had different impacts on cell behaviors, but the cells behaved as expected in response to each growth factor, based on previous reports. However, NSCs grown on spots with a mixture of two different factors exhibited behaviors that could not be predicted from the individual effects of growth factors; that is, the cell behaviors were not simply the sum of responses to the individual factors. A multivariate cluster analysis was carried out to quantify cell proliferation and differentiation in response to each factor or combination. The results

showed that the effects of two growth factors interacted competitively, synergistically, or destructively, depending on the combinations. In some peculiar cases, the combined effect of two growth factors was totally different from the effects of either of the individual factors.

Chapter 2 describes the preparation of culture substrates for rat NSC expansion. NSCs have been widely used for fundamental studies and applications. However, the results have been highly dependent on the methods used for preparing NSCs *in vitro*. Currently, the standard method for obtaining NSCs is to grow them in neurosphere cultures [35]. Briefly, neural cells are dissociated from embryonic or adult tissues and cultured in suspension, where they spontaneously aggregate to form spheres; hence, they are called neurospheres. However, this method normally yields a heterogeneous population that contains both differentiated neural cells and NSCs [36]. In addition, the rate of cell expansion is insufficient for providing a large quantity of NSCs in a short time period [37]. These problems are of serious concern, because they could limit the availability of human NSCs in clinical applications or when many patients require treatment at multiple facilities. In this chapter, culture substrates were assessed for their ability to facilitate highly selective, rapid expansion of rat NSCs. Based on the results obtained in Chapter 1, a culture substrate was selected that contained EGF. The EGF sequence was fused with a hexahistidine sequence (EGF-His) or with a polystyrene-binding peptide (EGF-PSt) [38]. The engineered growth factors were immobilized on a nickel-chelated glass plate or on a polystyrene dish, respectively. NSCs obtained from fetal rat striatum were used to assess the efficacy of immobilized EGF as a culture substrate. These NSCs could be selectively expanded on the EGF-His-chelated module. This module provided higher NSC expansion efficiency than

the conventional neurosphere method. The EGF-PSt bound to the polystyrene dish also provided efficient expansion for rat NSCs. These substrates offered a straightforward means for acquiring a large quantity of pure rat NSCs.

Chapter 3 describes the expansion of human NPCs (hNPCs) on substrates that carried different growth factors. In the conventional neurosphere culture method, hNPCs proliferate at a population doubling time of 5-10 days [39,40], which is much slower than rodent cell proliferation (doubling in approximately 30 h [41]). A more efficient method is needed to expand hNPCs. Furthermore, due to the limited access to fetal tissues and the ethical issues surrounding their use, it is necessary to develop highly efficient hNPC culture methods. Here, several culture substrates were investigated for their ability to selectively expand hNPCs. Previous studies have described a clear difference in the expression pattern of growth factor receptors between rat NSCs and human NPCs. Therefore, two growth factors, EGF and bFGF, were immobilized on glass slides, either alone as single components or in a combination of two factors. The growth factor-immobilized substrates were evaluated for their ability to promote selective expansion of hNPCs. Adhesion and proliferation of hNPCs took place most efficiently on the surface with a mixture of EGF and bFGF compared to surfaces with either factor alone or a bare glass surface. The rate of hNPC proliferation was 2-fold higher on this mixed substrate compared to that achieved with the standard neurosphere culture. After 5 days of culture on the substrate, approximately 90% of the NPCs exhibited nestin expression. This indicated that the culture substrate with a mixture of EGF and bFGF was effective for selective hNPC expansion.

Chapter 4 describes the effects of surface-immobilized ECM components on the proliferation of NPCs derived from iPS cells. NPCs derived from ES or iPS cells have

been considered cell sources for cell transplantation therapies in treating central nerve disorders [42]. ECM components comprise basement membrane and serum proteins. They play important roles in cell functions, including adhesion, migration, proliferation, and differentiation [43]. It was also reported that the behaviors of neural cells are controlled by ECMs [44]. This chapter describes the investigation of nine kinds of ECM, including collagen I, collagen IV, gelatin, laminin-1, laminin-5, Matrigel, fibronectin, vitronectin, and ProNectin F, for their efficacy as a culture substrate for iPS-derived NPCs. Mouse iPS cells were differentiated into NPCs with the serum-free, floating culture method [45]. The NPCs obtained were cultured for 3 days on an array that displayed different types of ECMs. The results showed that NPCs derived from mouse iPS cells efficiently proliferated on a substrate with immobilized laminin-1, laminin-5, and Matrigel. Consequently, a laminin-1-immobilized substrate was tested for efficacy in supporting NPCs derived from human iPS cells. The human NPCs also proliferated selectively on this substrate without impairment of multipotent differentiation capability. Thus, immobilized laminin-1 was an effective substrate for the selective expansion of NPCs derived from mouse or human iPS cells.

Chapter 5 is concerned with the preparation of DA neurons for the treatment of PD. PD is neurodegenerative disease, which is mainly caused by selective loss of DA neurons in the substantia nigra [46]. In recent years, cell replacement therapy has been considered an effective method for treating PD. Brain tissues from aborted fetuses were transplanted into the substantia nigra of patients with PD [19, 26, 47]. The engraftments of DA neurons and the pathological recoveries were highly variable among different reports [47]. This variability might be due to different degrees of immaturity in DA neurons from different fetal brain tissues or an insufficient number of DA neurons in

some grafts. In addition, the shortage of donors and ethical concerns make it difficult to accept use of these cells as a standard treatment for PD. Alternatively, pluripotent stem cells, like ES cells and iPS cells have been proposed as new sources for cell transplantation therapy [48, 49]. These pluripotent cells can expand indefinitely *in vitro* in the undifferentiated state; then, they can be induced to differentiate into multiple different types of cells. Various protocols have been reported for differentiating pluripotent cells into DA neurons [50-52]. A few studies have demonstrated that PD was cured with the transplantation of DA neurons derived from ES/iPS cells [50, 51]. However, various difficulties must be overcome before DA neurons derived from ES/iPS cells can be transplanted into human patients with PD. The problem of tumor formation must be carefully considered in cell transplantation therapies that use iPS-derived cells [53, 54]. There is a risk that some undifferentiated pluripotent stem cells and NPCs may contaminate the differentiated cells prepared for transplantation; these undifferentiated cells can proliferate and overgrow in the host brain [55]. It has been proposed that the risk of tumor formation can be reduced by culturing cells for long periods *in vitro* [56, 58]. By culturing them longer, the differentiated DA neurons would be as mature as possible. However, this approach is difficult in practice, because mature neurons are very weak and easily damaged by mechanical and enzymatic stress. To overcome these difficulties, it is necessary to establish improved culture methods for preparing DA neurons. This chapter describes a method that involves enclosing DA neuronal precursor cells into agarose microbeads and promoting maturation by culturing for a long time period. In this method, aggregates of NPCs derived from hiPS cells were enclosed in agarose microbeads. Then, approximately 66% of the cells differentiated into tyrosine hydroxylase-positive neurons within the agarose microbeads. The cells

released dopamine for more than 40 days. These DA neurons grown in microbeads could be handled without specific protocols, because the microbeads protected the fragile dopamine neurons from mechanical stress. In addition, microbeads containing cells can be cryopreserved. Therefore, agarose microencapsulation provides a good supporting environment for the preparation and storage of DA neuronal cells.

The aim of this thesis was to develop biomaterials for the preparation of neural cells, which can be used in cell transplantation therapy. NSCs isolated from rat and human fetal brains were selectively expanded on growth factor-immobilized substrates. In the case of NPCs derived from human iPS cells, laminin-1 proved to be an effective substrate for selective expansion. Furthermore, agarose microbeads provided a suitable environment for the preparation and storage of differentiated DA neurons. The author believes that the contents in this thesis will have a beneficial impact on the field of stem cell-based regenerative medicine.

References

- [1] Kim SU, de Vellis J. Stem Cell-Based Cell Therapy in Neurological Diseases: A Review. *J Neurosci Res* 2009;87:2183–200.
- [2] Fiorina P, Shapiro AM, Ricordi C, Secchi A. The clinical impact of islet transplantation. *Am J Transplant* 2008;8:1990–7.
- [3] Trounson A, Thakar RG, Lomax G, Gibbons D. Clinical trials for stem cell therapies. *BMC Med* 2011;9:52.
- [4] Martino G, Pluchino S. The therapeutic potential of neural stem cells. *Nat Rev Neurosci* 2006;7:395–406.
- [5] Pittenger MF, Mackay AM, Beck SC, Jaiswal RK, Douglas R, Mosca JD, et al. Multilineage potential of adult human mesenchymal stem cells. *Science* 1999;284:143–7.
- [6] Ratajczak MZ, Gewirtz AM. The biology of hematopoietic stem cells. *Semin Onco* 1995;22:210–7.
- [7] Gage FH. Mammalian neural stem cells. *Science* 2000;287:1433-8.
- [8] Evans MJ, Kaufman MH. Establishment in culture of pluripotential cells from mouse embryos. *Nature* 1981;292:154–6.
- [9] Thomson JA, Itskovitz-Eldor J, Shapiro SS, Waknitz MA, Swiergiel JJ, Marshall VS, et al. Embryonic stem cell lines derived from human blastocysts. *Science* 1998;282:1145–7.
- [10] Smith AG. Embryo-derived stem cells: Of mice and men. *Annu Rev Cell Dev Biol* 2001;17:435–62.

- [11] Murry CE, Keller G. Differentiation of embryonic stem cells to clinically relevant populations: Lessons from embryonic development. *Cell* 2008;132:661–80.
- [12] Takahashi K, Yamanaka S. Induction of pluripotent stem cells from mouse embryonic and adult fibroblast cultures by defined factors. *Cell* 2006;126:663–76.
- [13] Takahashi K, Tanabe K, Ohnuki M, Narita M, Ichisaka T, Tomoda K, et al. Induction of pluripotent stem cells from adult human fibroblasts by defined factors. *Cell* 2007;131:861–72.
- [14] Temple S. The development of neural stem cells. *Nature* 2001;414:112–7.
- [15] Ma DK, Bonaguidi MA, Ming GL, Song H. Adult neural stem cells in the mammalian central nervous system. *Cell Res* 2009;19:672–82.
- [16] Imayoshi I, Sakamoto M, Ohtsuka T, Kageyama R. Continuous neurogenesis in the adult brain. *Dev Growth Differ* 2009;51:379–86.
- [17] Ahmed S. The culture of neural stem cells. *J Cell Biochem* 2009;106:1–6.
- [18] Falk S, Sommer L. Stage- and area-specific control of stem cells in the developing nervous system. *Curr Opin Genet Dev* 2009;19:454–60.
- [19] Björklund A, Lindvall O. Cell replacement therapies for central nervous system disorders. *Nat Neurosci* 2000;3:537–44.
- [20] Ronaghi M, Erceg S, Moreno-Manzano V, Stojkovic M. Challenges of stem cell therapy for spinal cord injury: human embryonic stem cells, endogenous neural stem cells, or induced pluripotent stem cells? *Stem Cells* 2010;28:93–9.
- [21] Feng ZL, Zhao G, Yu L. Neural stem cells and Alzheimer's disease: challenges and hope. *Am J Alzheimers Dis Other Demen* 2009;24:52–7.
- [22] Locatelli F, Bersano A, Ballabio E, Lanfranconi S, Papadimitriou D, Strazzer S, et al. Stem cell therapy in stroke. *Cell Mol Life Sci* 2009;66:757–72.

- [23] Richardson RM, Singh A, Sun D, Fillmore HL, Dietrich DW 3rd, Bullock MR. Stem cell biology in traumatic brain injury: effects of injury and strategies for repair. *Neurosurg* 2010;112:1125–38.
- [24] Ogawa Y, Sawamoto K, Miyata T, Miyano S, Watanabe M, Nakamura M, et al. Transplantation of in vitro-expanded fetal neural progenitor cells results in neurogenesis and functional recovery after spinal cord contusion injury in adult rats. *J Neurosci Res* 2002;69:925–33.
- [25] Keirstead HS, Nistor G, Bernal G, Totoiu M, Cloutier F, Sharp K, et al. Human embryonic stem cell-derived oligodendrocyte progenitor cell transplants remyelinate and restore locomotion after spinal cord injury. *J Neurosci* 2005;25:4694–705.
- [26] Freed CR, Greene PE, Breeze RE, Tsai WY, DuMouchel W, Kao R, et al. Transplantation of embryonic dopamine neurons for severe Parkinson's disease. *N Engl J Med* 2001;344:710–9.
- [27] Trounson A, Thakar RG, Lomax G, Gibbons D. Clinical trials for stem cell therapies *BMC Med* 2011;9:52.
- [28] Lutolf MP, Gilbert PM, Blau HM. Designing materials to direct stem-cell fate. *Nature* 2009;462:433–41.
- [29] Dellatore SM, Garcia AS, Miller WM. Mimicking stem cell niches to increase stem cell expansion. *Curr Opin Biotechnol* 2008;19:534–40.
- [30] Lutolf MP, Blau HM. Artificial stem cell niches. *Adv Mater* 2009;21:3255–68.
- [31] Rodin S, Domogatskaya A, Ström S, Hansson EM, Chien KR, Inzunza J, et al. Long-term self-renewal of human pluripotent stem cells on human recombinant laminin-511. *Nat Biotechnol* 2010;28:611–5.

- [32] Melkounian Z, Weber JL, Weber DM, Fadeev AG, Zhou Y, Dolley-Sonneville P, et al. Synthetic peptide-acrylate surfaces for long-term self-renewal and cardiomyocyte differentiation of human embryonic stem cells. *Nat Biotechnol* 2010;28:606–10.
- [33] Villa-Diaz LG, Nandivada H, Ding J, Nogueira-de-Souza NC, Krebsbach PH, O'Shea KS, et al. Synthetic polymer coatings for long-term growth of human embryonic stem cells. *Nat Biotechnol* 2010;28:581–3.
- [34] Underhill GH, Bhatia SN. High-throughput analysis of signals regulating stem cell fate and function. *Curr Opin Chem Biol* 2007;11:357–66.
- [35] Reynolds BA, Tetzlaff W, Weiss SA. Multipotent EGF-responsive striatal embryonic progenitor cell produces neuron and astrocytes. *J Neurosci* 1992;12:4565–74.
- [36] Deleyrolle LP, Reynolds BA. Isolation, expansion, and differentiation of adult Mammalian neural stem and progenitor cells using the neurosphere assay. *Methods Mol Biol* 2009;549:91–101.
- [37] Sommer L, Rao M. Neural stem cells and regulation of cell number. *Prog Neurobiol* 2002;66:1–18.
- [38] Kumada Y, Shiritani Y, Hamasaki K, Ohse T, Kishimoto M. High biological activity of a recombinant protein immobilized onto polystyrene. *Biotechnol J* 2009;4:1178–89.
- [39] Carpenter MK, Cui X, Hu ZY, Jackson J, Sherman S, Seiger A, et al. In vitro expansion of a multipotent population of human neural progenitor cells. *Exp Neurol* 1999;158:265–78.

- [40] Kanemura Y, Mori H, Kobayashi S, Islam O, Kodama E, Yamamoto A, et al. Evaluation of in vitro proliferative activity of human fetal neural stem/progenitor cells using indirect measurements of viable cells based on cellular metabolic activity. *J Neurosci Res* 2002;69:869–79.
- [41] Nakaji-Hirabayashi T, Kato K, Arima Y, Iwata H. Oriented immobilization of epidermal growth factor onto culture substrates for the selective expansion of neural stem cells. *Biomaterials* 2007;28:3517–29.
- [42] Robinton DA, Daley GQ. The promise of induced pluripotent stem cells in research and therapy. *Nature* 2012;481:295–305.
- [43] Kim SH, Turnbull J, Guimond S. Extracellular matrix and cell signalling: the dynamic cooperation of integrin, proteoglycan and growth factor receptor. *J Endocrinol* 2011;209:139–51.
- [44] Wojcik-Stanaszek L, Gregor A, Zalewska T. Regulation of neurogenesis by extracellular matrix and integrins. *Acta Neurobiol Exp* 2011;71:103–12.
- [45] Okada Y, Matsumoto A, Shimazaki T, Enoki R, Koizumi A, Ishii S, et al. Spatiotemporal Recapitulation of Central Nervous System Development by Murine Embryonic Stem Cell-Derived Neural Stem/Progenitor. *Cells Stem Cells* 2008;26:3086–98.
- [46] Dauer W, Przedborski S. Parkinson's Disease: Review Mechanisms and Models. *Neuron* 2003;39:889–909.
- [47] Hauser RA, Freeman TB, Snow BJ, Nauert M, Gauger L, Kordower JH, et al. Long-term evaluation of bilateral fetal nigral transplantation in Parkinson disease. *Arch Neurol* 1999;56:179–87.

- [48] Robinton DA, Daley GQ. The promise of induced pluripotent stem cells in research and therapy. *Nature* 2012;481:295–305.
- [49] Lindvall O, Kokaia Z. Prospects of stem cell therapy for replacing dopamine neurons in Parkinson's disease. *Trends Pharmacol Sci* 2009;30:260–7.
- [50] Kriks S, Shim JW, Piao J, Ganat YM, Wakeman DR, Xie Z, et al. Dopamine neurons derived from human ES cells efficiently engraft in animal models of Parkinson's disease. *Nature* 2011;480:547–51.
- [51] Rhee YH, Ko JY, Chang MY, Yi SH, Kim D, Kim CH, et al. Protein-based human iPS cells efficiently generate functional dopamine neurons and can treat a rat model of Parkinson disease. *J Clin Invest* 2011;121:2326–35.
- [52] Swistowski A, Peng J, Liu Q, Mali P, Rao MS, Cheng L, et al. Efficient generation of functional dopaminergic neurons from human induced pluripotent stem cells under defined conditions. *Stem Cells* 2010;281:893–904.
- [53] Hentze H, Graichen R, Colman A. Cell therapy and the safety of embryonic stem cell-derived grafts. *Trends Biotechnol* 2007;25:24–32.
- [54] Fong CY, Gauthaman K, Bongso A. Teratomas from pluripotent stem cells: A clinical hurdle. *J Cell Biochem* 2010;111:769–81.
- [55] Li JY, Christophersen NS, Hall V, Soulet D, Brundin P. Critical issues of clinical human embryonic stem cell therapy for brain repair. *Trends Neurosci* 2008;31:146–53.
- [56] Brederlau A, Correia AS, Anisimov SV, Elmi M, Paul G, Roybon L, et al. Transplantation of human embryonic stem cell-derived cells to a rat model of Parkinson's disease: effect of in vitro differentiation on graft survival and teratoma formation. *Stem Cells* 2006;24:1433–40.

- [57] Seminatore C, Polentes J, Ellman D, Kozubenko N, Itier V, Tine S, et al. The postischemic environment differentially impacts teratoma or tumor formation after transplantation of human embryonic stem cell-derived neural progenitors. *Stroke* 2010;41:153–9.

Chapter 1

Array-based functional screening of growth factors toward optimizing neural stem cell microenvironments

1.1 Introduction

Neural progenitor cells can be derived from various sources such as embryonic and adult brain tissues [1, 2], embryonic stem cells [3, 4], and induced pluripotent stem cells [5]. The neural progenitor cells have been extensively studied for treating neurodegenerative diseases [6, 7], ischemia [8, 9], and traumatic injury of the brain [10] and the spinal cord [11, 12] through cell transplantation. Recently, clinical trials for the treatment of spinal cord injury using ES cell-derived oligodendrocytes and neural stem cells from the fetal brain were approved in the US and Switzerland. In most cases, a suspension of progenitor cells or their aggregates have been directly infused into the brain or the spinal cord for functional restoration.

The fate of transplanted cells in the host brain or spinal cord seems to have great impact on the outcome of the therapy. However, it is not straightforward with current technologies to direct survival, proliferation, migration, differentiation, and integration of cells after transplantation. For controlling the behavior of transplanted cells, several research groups have been involved in tissue engineering approaches where injectable gels are used as a carrier for neural cells [13]. In most cases, cell

adhesive peptides [14, 15] or growth factors [16, 17] have been incorporated into carrier materials.

The utilization of cell adhesive peptides and growth factors has been inspired by natural microenvironments in which the behaviors of neural cells are precisely controlled by extracellular matrices and signaling factors. However, the diversity of these proteins makes it difficult to select the most appropriate component to be incorporated into carrier materials.

The effect of growth factors generally predominated those of extracellular matrices. To identify the best candidate, various growth factors and neurotrophic factors were combinatorially displayed on an array [18]. Neural stem cells (NSCs) were cultured on the array to screen various biomaterials without knowledge a priori on their functions. In this chapter, an array displaying multiple growth factors including basic fibroblast growth factor (bFGF), epidermal growth factor (EGF), insulin-like growth factor-1 (IGF1), brain-derived neurotrophic factor (BDNF), and ciliary neurotrophic factor (CNTF) were fabricated. Among various growth factors, these five factors were tested because previous literatures reported responsiveness of neural cells to these factors [19–23]. In addition, these factors transduce signaling through the distinct class of receptors, while some of the intracellular signaling cascades partially overlap each other.

Five growth factors were synthesized as fusion proteins with hexahistidine residues (His) and arrayed on a chip as a single component or the combination of two factors through chelate linkage with Ni^{2+} ions fixed on a chip. To achieve site-addressable presentation of these factors, an alkanethiol self-assembled monolayer (SAM) was patterned by UV irradiation [24]. The His-mediated chelating method allows

to simply immobilize different growth factors on a chip through the identical chemical reaction under mild conditions. This is of advantage because we do not need to separately optimize reaction conditions for individual proteins with different structures and stabilities. NSCs obtained from the rat embryonic striatum were cultured directly on the array for parallel functional assays.

1.2 Materials and methods

Preparation of His-tagged growth factors

Recombinant growth factors including bFGF, EGF, IGF1, BDNF, and CNTF were expressed in *Escherichia coli* as a C-terminal fusion with His. These fusion proteins are referred hereafter to as bFGF-His, EGF-His, IGF1-His, CNTF-His, and BDNF-His. The construction of expression plasmids was previously reported for EGF-His [24] and BDNF-His [17].

For bFGF-His and IGF1-His, plasmids were constructed in a similar fashion to EGF-His. In brief, the coding region of mature bFGF (154 amino acid residues, NCBI RefSeq: NM_002006) and IGF1 (70 amino acid residues, NCBI RefSeq: NM_001111283) was generated by polymerase chain reaction (PCR) using the following primers: bFGF; (forward) 5'-AGA TAT ACA TAT GGC AGC CGG GAG CAT CAC CAC-3' and (reverse) 5'-GGT GCT CGA GGC TCT TCG CAG ACA TTG GAA-3', IGF1; (forward) 5'-AGA TAT ACA TAT GGG ACC GGA GAC GCT CTG CGG-3' and (reverse) 5'-GGT GCT CGA GAG CTG ACT TGG CAG GCT TGA-3'. The sequences underlined are restriction sites for Nde I (forward primers) and Xho I

(reverse primers). The amplified DNAs were digested with Nde I and Xho I, and then unidirectionally ligated to pET22b (Novagen, Darmstadt, Germany) that had been digested by the same restriction enzymes. These plasmids were cloned in *E. coli* DH5 α to obtain pET22-bFGF and pET22-IGF1. The correctness of the insert DNAs was checked by sequencing.

In the case of CNTF (199 amino acid residues, NCBI RefSeq: NM_000614), exon 1 and exon 2 were separately amplified by PCR using a human genomic DNA as a template and then ligated each other by overlap extension and PCR. The full length DNA for the coding region of CNTF thus obtained was first cloned in *E. coli* and then amplified by PCR using the following primers: (forward) 5'-GCC CAT ATG GAA TTC GCT TTC ACA GAG CAT TCA CC-3' and (reverse) 5'-GGT GCT CGA GCA TTT TCT TGT TGT TAGC AAT ATA ATG -3'. The sequences underlined are restriction sites for Nde I (forward primers) and Xho I (reverse primers). The PCR product was inserted in the same manner as for bFGF and IGF1 to obtain pET22-CNTF. The correctness of the insert DNA was checked by sequencing.

An *E. coli* strain, BL21 CodonPlus (Stratagene, La Jolla, CA) or BL21(DE3)pLysS (Novagen), was transformed with one of the five plasmids. The proteins were expressed in the transformants using Overnight Express Autoinduction System (Novagen) as inclusion bodies (Only bFGF-His was obtained as a soluble form). The proteins, except for bFGF-His, were extracted under denatured conditions using a buffer solution containing 8M urea, purified with a Ni-chelated affinity column (His Trap HP; GE Healthcare Bio-Science Corp., Piscataway, NJ), and refolded by dialyzing against 50 mM Tris-HCl buffer (pH 8.5) containing 10 mM NaCl, 2 M L-arginine, 3.75 mM γ -L-glutamyl-L-cysteinylglycine (glutathione), and 0.375 mM glutathione

disulfide. bFGF-His was purified under non-denatured conditions without urea, and finally dialyzed against 20 mM citrate buffer of pH 5.

The purity of the proteins was checked by sodium dodecylsulfate-polyacrylamide gel electrophoresis (SDS-PAGE), while the structure of the proteins was analyzed by circular dichroism (CD) spectroscopy using JASCO J-850 spectropolarimeter as before [13]. The biological activity of EGF-His [19] and bFGF-His [20] was assessed from their activity to promote neurosphere formation. The activity of other proteins was assessed from their potential to promote neuronal (BDNF-His) [22] and astroglial (CNTF-His) [23] differentiation or the survival of IGF1-His [25].

Preparation of growth factor arrays

A patterned SAM was prepared as before [26] using a gold-coated glass plate (22 mm × 26 mm × 1 mm) as a substrate. In brief, a 1-hexadecanethiol SAM was photolithically micropatterned to create an array of 5 × 5 spots (1 mm in diameter and 2 mm in center-to-center distance) presenting a bare gold surface. Then a SAM of 11-mercapto-1-undecanoic acid was formed within the spots. The carboxylic acid on the spots was derivatized to active succinimidyl ester by reacting with N-hydroxysuccinimide in the presence of N,N'-dicyclohexylcarbodiimide. The active ester was reacted with 10 mM N-(5-amino-1-carboxypentyl) iminodiacetic acid and then with 40 mM NiSO₄ to form Ni²⁺ chelate [24]. His-tagged growth factors were diluted with phosphate buffered saline (PBS) to the concentration of 50 µg/mL. These solutions were manually pipetted to the Ni²⁺-chelated spots (approximately 100 nL per

spot) under sterile conditions and kept at room temperature for 2 h to allow for chelation between the surface-bound Ni²⁺ and the His. As a control, pure PBS was used instead of a protein solution. As another control, laminin-1 was physically adsorbed to some of the spots by pipetting 50 µg/mL laminin solution. Finally, the array was washed with PBS and immediately used for later experiments.

Surface plasmon resonance imaging

Surface plasmon resonance (SPR) imaging was performed to detect immobilized proteins on an array as reported before [18]. The details of a home-made SPR imaging apparatus were reported elsewhere [27]. In brief, a protein array prepared as described above was mounted on a triangular glass prism. A p-polarized, collimated white light was radiated to the back side of the array through the prism at a constant incident angle ca. 0.5 degree smaller than the angle for the occurrence of surface plasmon resonance at the region between spots on the array. To obtain a two-dimensional reflection image, reflected light was passed through a narrow band interference filter (center wavelength: 905 nm) and then collected with a CCD camera. The resulting reflection image represents local changes in the refractive index in the vicinity of the sample surface, and hence, reflects the distribution of protein over the array. The imaging was carried out in air at room temperature.

Isolation and culture of NSCs

The striatum was isolated from fetus (E16) of Fischer 344 rats, and dissociated into single cells by treating with 0.05 % trypsin solution containing 0.53 mM ethylenediamine- N,N,N',N'-tetraacetic acid (EDTA). All experiments were performed according to the guidelines of the Animal Welfare Committee of the Institute. The cells obtained were suspended in DMEM/F12 (1:1) (Invitrogen Corp., Carlsbad, CA) containing 2% (v/v) B27 supplement (Invitrogen), 5 µg/mL heparin, 100 U/mL penicillin, 100 µg/mL streptomycin, 20 ng/mL bFGF (Wako Pure Chemical Industries, Osaka, Japan), and 20 ng/mL EGF (Wako Pure Chemical Industries), and cultured for 4–5 d at 37 °C under 5% CO₂ atmosphere to form neurospheres [28].

Cell culture on growth factor arrays

Neurosphere forming cells at passage 2 were dissociated into single cells by treating with 0.05% trypsin solution containing 0.53 mM EDTA and suspended in DMEM/F12 (1:1) containing 2% (v/v) B27 supplement, 5 µg/mL heparin, 100 unit/mL penicillin, and 100 µg/mL streptomycin. Then the cells were plated onto the protein array at a density of 5.0×10^4 cells/cm² and cultured for 4–5 d at 37 °C under 5% CO₂ atmosphere. In some experiments, fetal bovine serum (FBS, 1% v/v) and retinoic acid (1 µM) were added to the medium to promote cell differentiation. For assessing cell proliferation, 5-bromo-2'-deoxyuridine (BrdU) was added to the medium to the concentration of 50 µM for 12 h prior to fixation.

Immunostaining

The expression of marker proteins as well as the incorporation of BrdU was analyzed by immunologically staining cells as previously reported [29]. In brief, cells were fixed with a solution containing paraformaldehyde and glutaraldehyde followed by permeabilization with Triton X-100 solution and blocking with Blocking One reagent (Nacalai Tesque, Kyoto, Japan). Primary antibodies used were specific for nestin (1:200, mouse monoclonal, Rat 401, BD Biosciences, San Jose, CA), β -tubulin III (1:500, rabbit polyclonal, Covance, Princeton, NJ), glial fibrillar acidic protein (GFAP, 1:200, mouse monoclonal G-A-5, Millipore, Billerica, MA), RIP (1:1000, mouse monoclonal, Millipore), and BrdU (1:100, mouse monoclonal, Dako, Glostrup, Denmark). Secondary antibodies used were Alexa Fluor 594 anti-mouse IgG and Alexa Fluor 488 anti-rabbit IgG (1:500, Molecular Probes, Inc., Eugene, OR). Cell nuclei were counterstained with Hoechst 33258 (Dojindo Laboratories, Kumamoto, Japan). The localization of secondary antibodies and the Hoechst dye was analyzed with a fluorescent microscope (BX51 TRF, Olympus Corp., Tokyo, Japan). Micrographs (magnification: $\times 100$) of every spot were used to determine the fluorescent intensity for a circular region (original diameter: 1 mm) on the spot using the Image J software (National Institutes of Health, Bethesda, MD). The fluorescent intensities measured on cells immunofluorescently stained for BrdU, nestin, β -tubulin III, and GFAP were first normalized by fluorescent intensity measured for the respective areas in the Hoechst images to compensate variation in cell numbers and then by the fluorescent intensity for immunofluorescently stained cells on the laminin spot on the identical array to compensate experiment-to-experiment deviations in the background fluorescent intensity. The normalized intensities were averaged for independent three experiments and log-scaled (base 2). The mean values were scaled to a unit standard deviation.

Cluster analysis

Cluster analysis was performed for a data set obtained from immunostaining to identify phenotypic structure of growth factor attributes. The log-scaled fluorescent intensities were subjected to cluster analysis using a square Euclidian distance and the Ward's hierarchical clustering method [30] in which clusters were combined so as to minimize an increase in the error sum of squares at each clustering step. The error sum of squares is given by the following equation:

$$\text{Error sum of squares} = \sum_i \sum_j \sum_k |X_{ijk} - \bar{x}_{i \cdot k}|^2$$

where X_{ijk} is the scaled fluorescent intensity for marker k and growth factor condition j belonging to cluster i . $\bar{x}_{i \cdot k}$ is the centroid of cluster i . Clustering was continued until all data were merged into a single cluster.

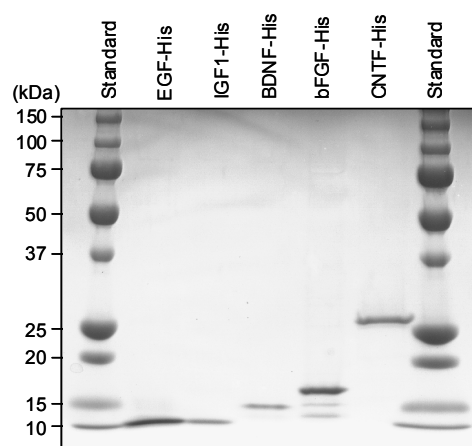


Fig. 1. SDS-PAGE analysis for His-tagged growth factors. Molecular weight standards were electrophoresed at both sides.

1.3 Results

Preparation of His-tagged growth factors

Among the His-tagged growth factors expressed in *E. coli*, only bFGF-His was obtained as a soluble form. On the other hand, rest of the growth factors were obtained as inclusion bodies. Figure 1 shows the result of SDS-PAGE analysis for these proteins. All the proteins were separated as a distinct band. The molecular weight of the proteins estimated from their mobility is in good agreement with that predicted from amino acid sequences (predicted molecular weight in kDa: bFGF-His, 18; EGF-His, 7; IGF1-His, 9; BDNF-His, 15; CNTF-His, 24).

The secondary structure of His-tagged growth factors was analyzed by CD spectroscopy. For comparison, commercially available cognate growth factors with no His-tag were analyzed under the same conditions. The results are shown in Fig. 2. In general, all of the His-tagged growth factors gave spectra similar to the cognate factors. The spectra of bFGF-His, EGF-His, and BDNF-His show a positive Cotton effect at 230 nm, suggesting the presence of β -turn structure. The spectra of EGF-His and BDNF-His are also consistent with our previous observation [31, 17]. The spectra of IGF1-His and CNTF-His exhibit a negative Cotton effects at 208 and 220 nm, which is characteristic for α -helical structure. In fact, CNTF is a typical four-bundled helix protein [32], while IGF1 contains an α -helix of 8 amino acid residues [33]. All these CD spectra gave evidence for the proper refolding of the His-tagged growth factors.

The biological activity of the growth factors was assayed using a neurosphere forming cells. The results are shown in Fig. 3. It was observed that, when EGF-His and bFGF-His were separately added in a medium, the formation of neurospheres was

promoted in both cases. On the other hand, addition of BDNF-His promoted neuronal differentiation of neurosphere forming cells in an adherent culture, whereas CNTF-His promoted glial differentiation. In the case of IGF1-His, cells survived longer periods in a medium with IGF1-His than in a control medium. These results show that all of the His-tagged growth factors synthesized here were biologically active.

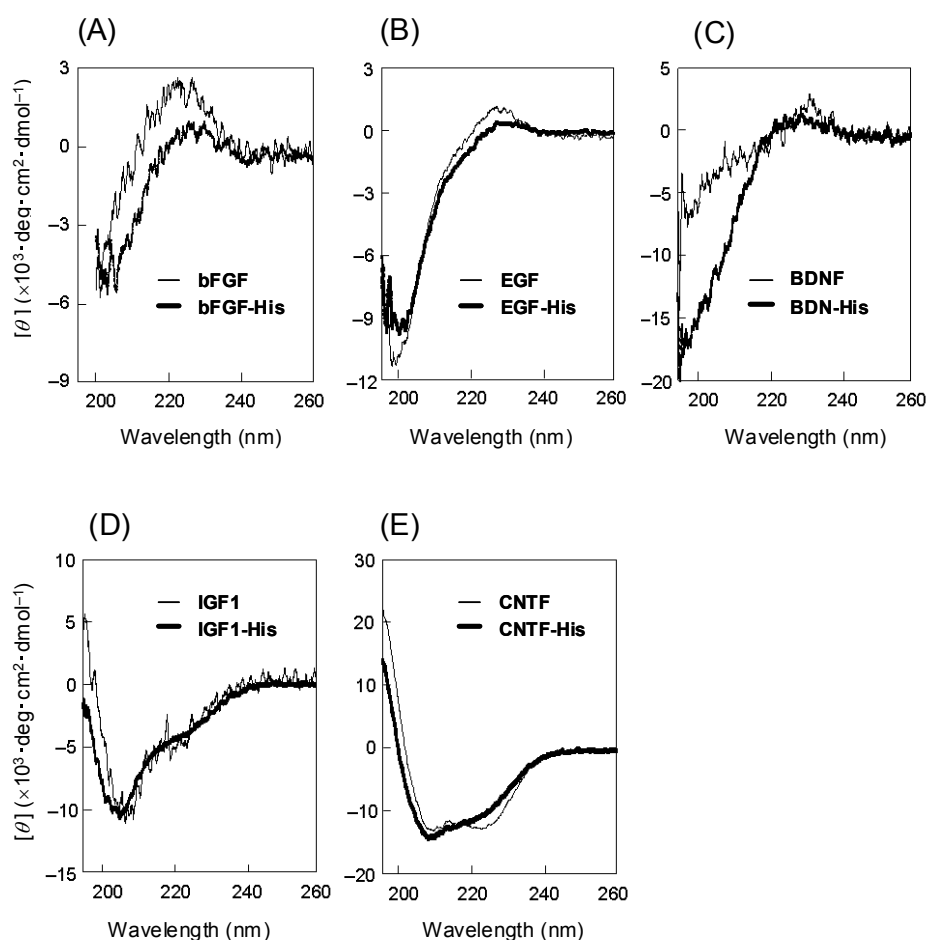


Fig. 2. Far-UV circular dichroism spectra of His-tagged growth factors and cognate growth factors with no His-tag. Mean residual molar ellipticity is shown as a function of wavelength. (A) bFGF-His and bFGF, (B) EGF-His and EGF, (C) BDNF-His and BDNF, (D) IGF1-His and IGF1, and (E) CNTF-His and CNTF.

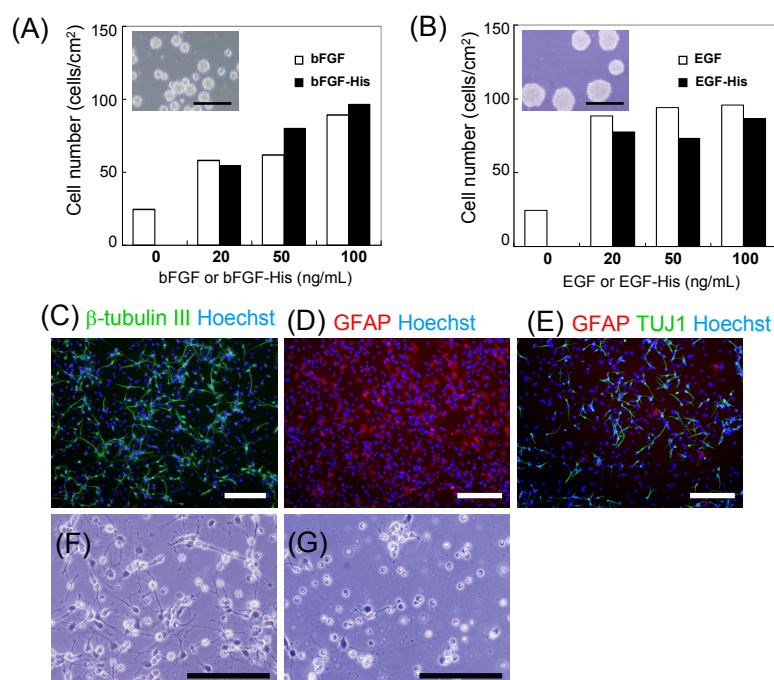


Fig. 3. The results of biological activity assays performed with His-tagged growth factors synthesized in this study. (A, B) The results of neurosphere forming assays in the presence of (A) bFGF-His or (B) EGF-His. These proteins were separately added in a medium to a concentration of 10, 50, or 100 ng/mL. The number of cells were determined by the MTT assay 4 d after seeding. Commercially available EGF and bFGF were used for comparison. Inserts represent representative phase contrast micrographs of neurospheres formed after 4-d culture in the presence of 50 ng/mL EGF-His or bFGF-His. Note that neurosphere formation was promoted by adding EGF-His or bFGF-His in a dose dependent manner, with a cell growth rate similar to the case with commercial products. These results show that EGF-His and bFGF-His were biologically active. (C–E) Fluorescent micrographs of neurons and astrocytes differentiated from neurosphere forming cells cultured on laminin-coated substrates for 4 d in a medium containing (C) BDNF-His (250 ng/mL), (D) CNTF-His (50 ng/mL), and (E) no His-tagged growth factor (control). Cells were immunologically stained using antibody to a neuronal marker β -tubulin III (green) and an astrocyte marker GFAP (red). Nuclei were counterstained with Hoechst (blue). Note that the larger number of neurons and astrocytes are seen in a culture with BDNF-His and CNTF-His, respectively, than control. (F,G) Phase contrast micrographs of neurosphere forming cells cultured for 3 d in a medium containing IGF1-His (100 ng/mL). Cells were cultured on laminin-coated substrates for 3 d in DMEM/F12 (1:1) containing 5 μ g/mL heparin, 100 U/mL penicillin, 100 μ g/mL streptomycin (F) with or (G) without IGF1-His. Insulin-free B27 (Invitrogen) was added so as to exclude the effect of insulin. Note that cells survived longer periods in the IGF1-His-containing medium than in control, indicating the biological activity of IGF1-His. Scale bar: (A, B) 200 μ m, and (C–G) 100 μ m.

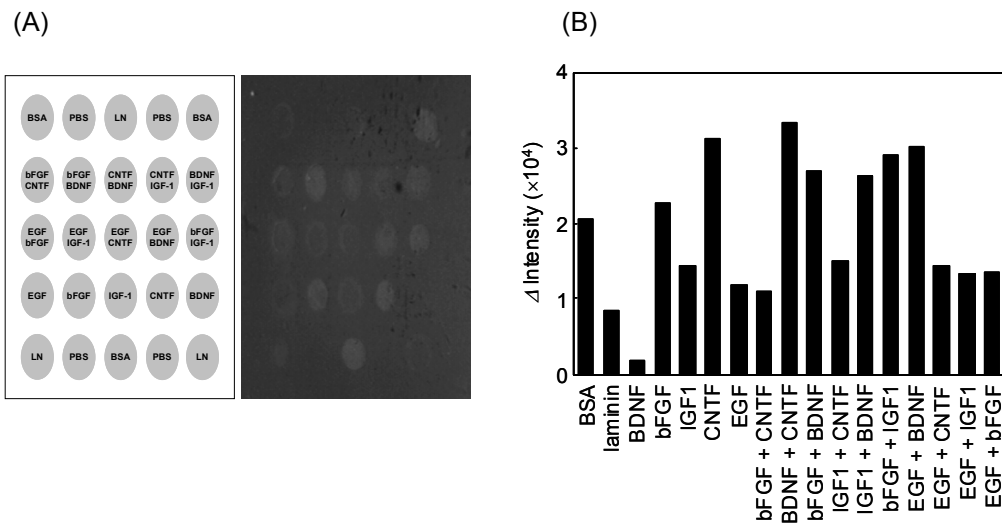


Fig. 4. Surface plasmon resonance imaging analysis of immobilized-growth factors. (A) Surface plasmon resonance image of the array displaying various His-tagged growth factors as a single component or a combination of two different factors. For simplicity, the abbreviation of -His is omitted from each growth factor symbol. LN and BSA: laminin (LN) and bovine serum albumin (BSA) were physically adsorbed to the spots as controls. PBS: control spots that had been treated with phosphate buffered saline containing no protein. (B) The results of SPR imaging analysis for the surface-anchored growth factors. The intensity of reflected light was determined on two cognate spots and averaged.

Preparation of growth factor arrays

His-tagged growth factors were arrayed on a patterned substrate as a single component or a combination of two factors (molar ratio = 1 : 1). The array was imaged with an SPR apparatus, and the intensity of light reflected from each spot was determined as a measure for immobilized proteins. The SPR image is shown in Fig. 4A and the intensity of reflected light is shown in Fig. 4B. As can be seen, all proteins and their combinations were successfully immobilized onto the spots. The observed variation in the light intensity may be attributed to several effects such as accessibility of His and the molecular sizes of the growth factors.

Cell proliferation

Figure 5A shows the phase contrast images of cells cultured on the protein array for 5 d in a serum free medium but supplemented with B27 and antibiotics. As is seen, cells adhered to and proliferated on all the spots. The exception was the spots treated with PBS, on which few cells are seen to adhere. Cell densities after 5-d culture were varied depending on the immobilized factors, suggesting that the factors had impacts on cell adhesion and proliferation. Cell density was slightly lower on the spot with bFGF-His, CNTF-His, and bFGF-His/CNTF-His in combination compared to the other spots with growth factors. In addition, as shown in Fig. 5B, cells had distinct morphologies depending on the growth factors immobilized. This result led us to assume that the immobilized factors had an effect on the specification of cell fate.

To examine the effect of growth factors on cell proliferation, an analogue of deoxythymidylic acid, BrdU, was incorporated into daughter DNA newly synthesized during DNA replication. Figure 6A shows the fluorescent micrographs of cells immunologically stained using an antibody to BrdU. The average fluorescent intensity measured on every spot is shown in Fig. 6B. Obviously the spot with EGF-His, bFGF-His, or EGF-His/bFGF-His in combination most abundantly contains cells stained in red among the spots on the array. Cells on the spots with EGF-His/IGF1-His, EGF-His/BDNF-His, EGF-His/CNTF-His, and bFGF-His/IGF1-His (the spots that contain at least bFGF-His or EGF-His as one of the co-immobilized proteins) were stained in red more markedly than on the spots with IGF1-His, BDNF-His, or CNTF-His alone. These results suggest that EGF and bFGF are most potent activators for cell proliferation.

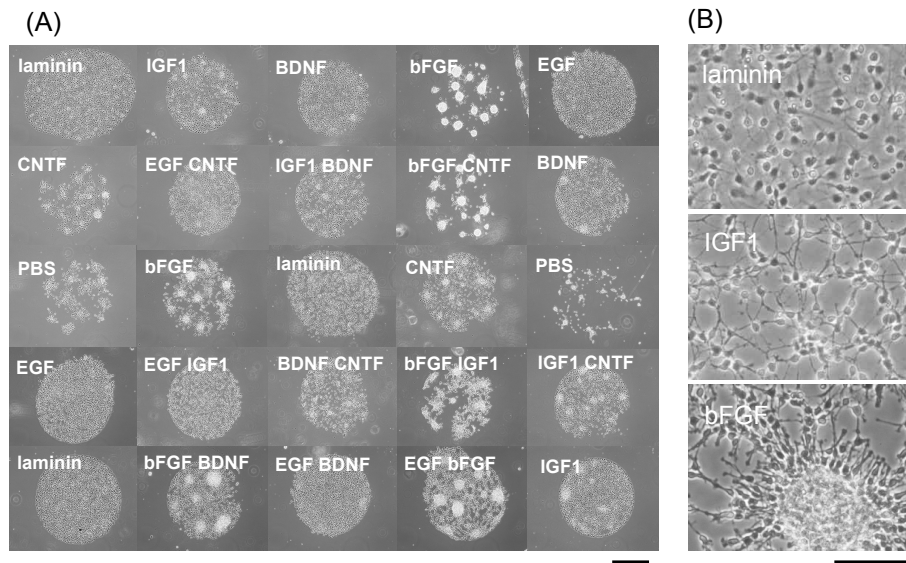


Fig. 5. Phase contrast micrographs of cells cultured for 5 days on the growth factor array. (A) Low magnification images for all the spots on a single array. Identification of a spot is indicated in the image. PBS: control spots that were exposed to pure PBS instead of a protein solution. (B) High magnification images of cells on the representative spots. Scale bar: (A) 500 μm and (B) 100 μm .

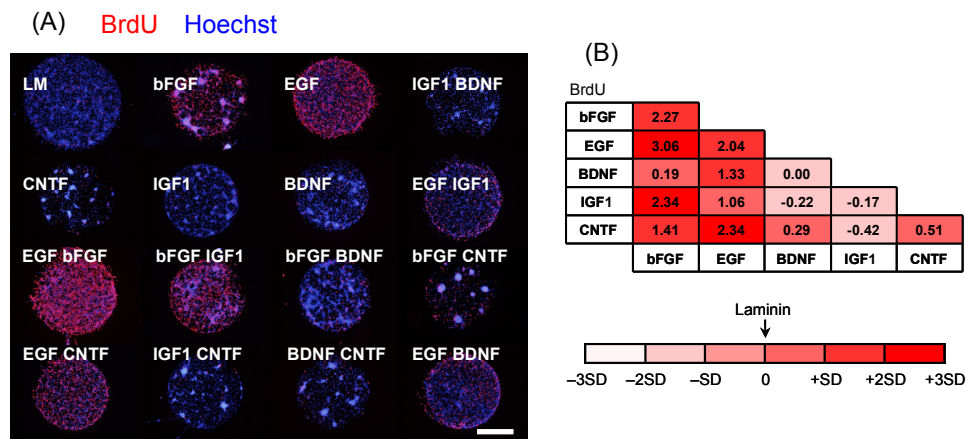


Fig. 6. Effect of various growth factors on cell proliferation. (A) Fluorescent micrographs of cells treated with BrdU followed by immunostaining using anti-BrdU antibody (red). Nuclei were counterstained with Hoechst (blue). Identification of a spot is indicated in the image. Scale bar: 500 μm . (B) Intensity of red fluorescence (BrdU) determined for every spot. The log-scaled fluorescent intensity ($n = 3$) is shown in a similar way to a league table, i.e., one of the factors shown in the left column was co-immobilized with others shown on the bottom line. Each box is shaded depending on the deviation in the fluorescent intensity compared to the control laminin spot (see scale to the bottom of the figure).

Cell differentiation

To examine the effect of growth factors on differentiation, cells were cultured on the array in a medium containing 1% FBS and 1 μ M retinoic acid. Generally, serum and retinoic acid are known to promote differentiation of NSCs [34, 35], giving rise to reduced expression of nestin, a marker for NSCs. After 5-d culture, cells were immunologically stained using antibodies to markers for NSCs (nestin), neurons (β -tubulin III), astrocytes (GFAP), and oligodendrocytes (RIP). Fluorescent micrographs are shown in Fig. 7. The quantitative data are shown in Fig. 10 for nestin, β -tubulin III, and GFAP. In the case of RIP (Fig. 7D), reliable data could not be obtained due to a small number of stained cells.

As shown Figs. 7A and 9A, cells on the spots with bFGF-His alone or as one of the two components abundantly expressed nestin even in the presence of FBS and retinoic acid. The expression of nestin was most strongly promoted on the spot with bFGF-His and EGF-His in combination. Other partners co-presented with bFGF-His had little effects on nestin expression. Though the effect was less obvious than bFGF-His, EGF-His also promoted nestin expression compared to the case with BDNF-His, IGF1-His, and CNTF-His. These results suggest that both bFGF-His and EGF-His promote the proliferation of NSCs.

As shown in Figs. 7B and 9B, the expression of β -tubulin III was elevated on the spot with BDNF-His or IGF1-His alone and as one of the two components, with little effects of co-presented partners. These results indicate that neuronal differentiation was promoted on the spots with BDNF-His and IGF1-His. In addition, cells on the spots with bFGF-His alone or bFGF-His/CNTF-His in combination abundantly expressed

β -tubulin III, though the spot with bFGF-His also promoted proliferation of NSCs as described above.

Figures 7C and 9C show the results with regard to the expression of GFAP. It is obvious that cells on the spots with CNTF-His alone most abundantly expressed GFAP among the spots on the array, suggesting the enhanced differentiation of cells to glial lineage, especially to astrocytes. However, the GFAP expression was reduced depending on the partners co-presented with CNTF-His. Strikingly, a few cells expressed GFAP on the spot with bFGF-His alone.

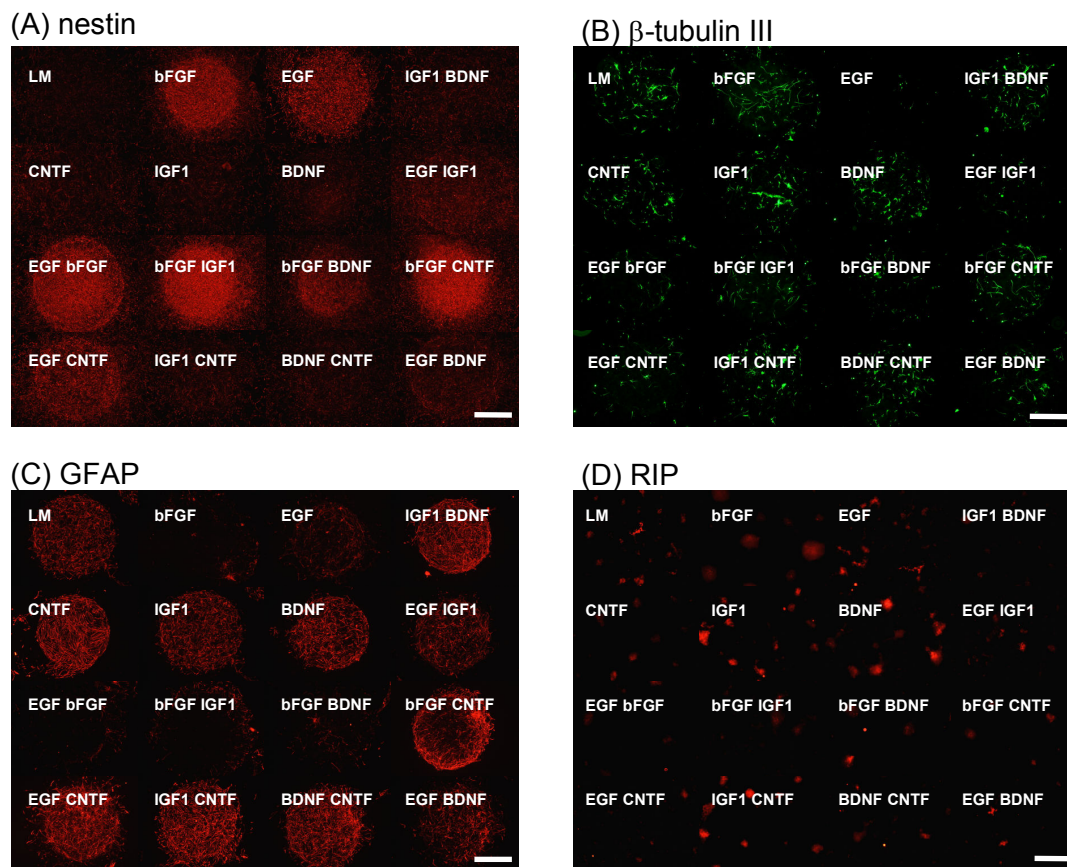


Fig. 7. Fluorescent micrographs of cells stained using antibodies to (A) nestin, (B) β -tubulin III, (C) GFAP, and (D) RIP. To induce differentiation, 1% FBS and 1 μ M retinoic acid were added to the culture medium. Identification of a spot is indicated in the image. Scale bar: (A–B) 500 μ m and (D) 200 μ m.

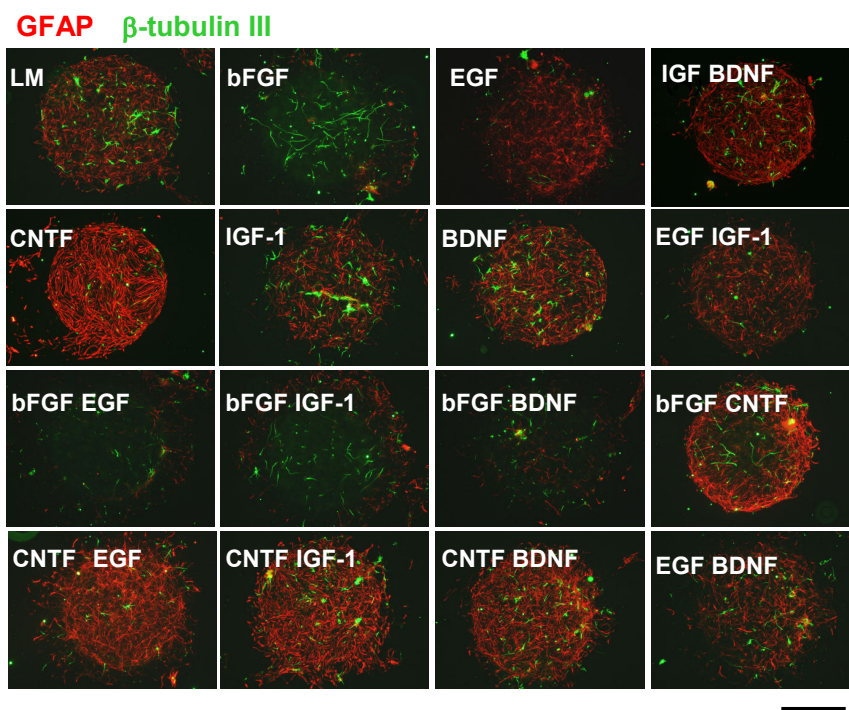


Fig. 8. Merged image for β -tubulin III (green) and glial fibrillar acidic protein (GFAP) (red). For simplicity, the abbreviation of -His is omitted from each growth factor symbol. LN: laminin was physically adsorbed to the spots as a control. The individual images are shown in Fig. 7 B and C in the main body of this article. Scale bar: 500 μ m.

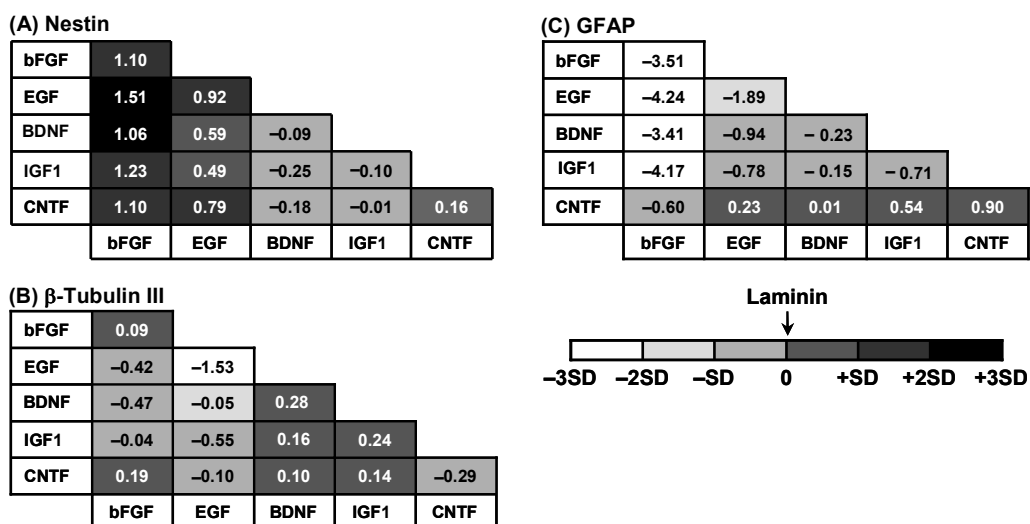


Fig. 9. Fluorescent intensity determined for every combination of growth factors. Fluorescently stained markers: (A) nestin, (B) β -tubulin III, and (C) GFAP. The log-scaled fluorescent intensity ($n = 3$) is shown in a similar way to Fig. 6B.

Cluster analysis

A hierarchical cluster analysis was performed for a data set obtained from immunofluorescent staining of BrdU, nestin, β -tubulin III, and GFAP for 15 different growth factor conditions. The resulting dendrogram is shown in Fig. 10. It can be seen that 15 conditions are joined into three major clusters from A to C. Taking the immunostaining results described above into consideration, the cluster A appears to contain growth factor conditions that promote proliferation of NSCs, while the other conditions are grouped based on the similarity in their potential of inducing astrocytes and neurons in clusters B and C, respectively.

Strikingly, growth factor combinations such as EGF-His/BDNF-His and EGF-His/IGF1-His were joined in cluster B, in spite that each growth factor alone was grouped in the other cluster (EGF-His in cluster A, BDNF-His and IGF1-His in cluster C).

In the case of bFGF-His/BDNF-His and bFGF-His/IGF1-His, these growth factor conditions were grouped in the same cluster (cluster A) as bFGF-His alone. Similarly, bFGF-His/CNTF-His and EGF-His/CNTF-His were grouped in the same cluster (cluster B) as CNTF-His alone, and BDNF-His/CNTF-His and IGF1-His/CNTF-His were grouped in the same cluster (cluster C) as BDNF-His or IGF1-His alone. As is seen in Fig. 8, the effect of major components in these combinations, such as bFGF-His, CNTF-His, BDNF-His, and IGF1-His, was mostly reduced by co-presenting with other factors.

It should also be noted that the number of proliferating NSCs was elevated with the bFGF-His/EGF-His combination (grouped in cluster A) compared to bFGF-His or

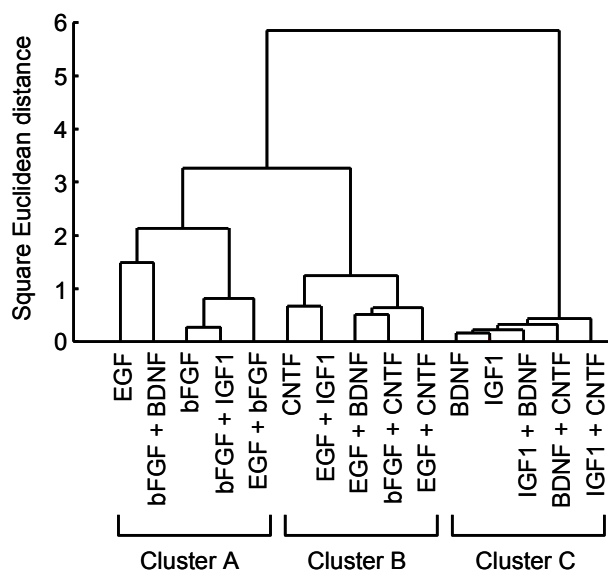


Fig. 10. Dendrogram obtained from the hierarchal cluster analysis for 15 different growth factor conditions.

EGF-His alone (These single components were also grouped in cluster A). This result suggests the synergistic effect of these growth factors. In contrast, the BDNF-His/IGF1-His combination (cluster C) exhibited slightly reduced differentiation into neurons in comparison to individual factors (both grouped in cluster C).

1.4 Discussion

Rationally designing biomaterials that provide microenvironments optimized for controlling NSC fates and functions may be achieved through incorporation of functional polypeptides that present proper signaling cues toward the cells. In light of this prospect, cell array-based functional analyses were carried out to screen five growth factors and their combinations (total fifteen different conditions).

According to the results of array-based assays, five growth factors have an apparent impact on cell behaviors. bFGF-His and EGF-His promote the self-renewal of NSCs, while EGF-His inhibits differentiation of the cells into neuronal and glial lineages. In the case of IGF1-His and BDNF-His, both factors act as activators for neuronal differentiation, whereas CNTF-His for glial differentiation. These findings are overall in accordance with the effects previously reported in other literatures for these growth factors added to culture media [19–23].

However, in this case with surface-bound growth factors, cells expressing cognate receptors may be selectively captured on the array [29], leading to the enrichment of cells responsive for the factors. In addition, the surface-bound form of growth factors may have influence on the kinetics of receptor-growth factor complex internalization and thus on downstream signaling in the cells. However, it appears that these aspects rather reflect possible incidents within carrier materials incorporating growth factors.

The array-based assay combined with cluster analysis enables us with simply studying the effect of two different factors co-presented on a single spot. It is interesting to note that, in some cases such as EGF-His/BDNF-His and EGF-His/IGF1-His, cell behaviors cannot be predicted from the effect of individual growth factors as a single component. In other cases, the influence by one of the factors apparently predominated over that by the co-presented partner. A synergistic effect was also observed a synergistic effect in the case of bFGF-His/EGF-His. This may be implicated in the fact that the maturation of NSCs is promoted by their sequential actions [36] in which bFGF promotes the expression of EGF receptors to increase responsiveness of the cells to EGF.

Accordingly, array-based assay provided deep insights into the effects of growth factors on the proliferation and differentiation of NSCs. The combinatorial effects of growth factors are rather complicated, but the findings obtained here will serve to rationally design carrier materials in which cellular microenvironments are fine-tuned by incorporating growth factors for achieving proper cell fates and functions. It appears that this complexity is attributed to the interference between partially-overlapping intracellular signaling cascades. Therefore, the results also provide a basis for deeper investigations on the crosstalk between growth factor receptors.

References

- [1] Ishibashi S, Sakaguchi M, Kuroiwa T, Yamasaki M, Kanemura Y, Shizuko I, et al. Human neural stem/progenitor cells, expanded in long-term neurosphere culture, promote functional recovery after focal ischemia in Mongolian gerbils. *J Neurosci Res* 2004;78:215–23.
- [2] Johansson CB, Momma S, Clarke DL. Identification of a neural stem cell in the adult mammalian central nervous system. *Cell* 1999;96:25–34.
- [3] Kawasaki H, Mizuseki K, Sasai Y. Induction of Midbrain dopaminergic neurons from ES cells by stromal cell–derived inducing activity. *Neuron* 2000;28:31–40.
- [4] Kim JH, Auerbach JM, Rodriguez-Gomez JA, McKay R. Dopamine neurons derived from embryonic stem cells function in an animal model of Parkinson's disease. *Nature* 2002;418:50–6.
- [5] Wernig M, Zhao JP, Pruszak J, Hedlund E, Fu D, Soldner F, et al. Neurons derived from reprogrammed fibroblasts functionally integrate into the fetal brain and improve symptoms of rats with Parkinson's disease. *Proc Natl Acad Sci* 2008;105:5856–61.
- [6] Takagi Y, Takahashi J. Dopaminergic neurons generated from monkey embryonic stem cells function in a Parkinson primate model. *J Clin Invest* 2005;115:102–9.
- [7] Feng ZL, Zhao G, Yu L. Neural stem cells and Alzheimer's disease: challenges and hope. *Am J Alzheimers Dis Other Demen* 2009;24:52–7.
- [8] Locatelli F, Bersano A, Ballabio E, Lanfranconi S, Papadimitriou D, Strazzer S, et al. Stem cell therapy in stroke. *Cell Mol Life Sci* 2009;66:757–72.

- [9] Daadi MM, Maag AL, Steinberg GK. Adherent self-renewable human embryonic stem cell-derived neural stem cell line: Functional engraftment in experimental stroke model. *PLoS One* 2008;3:e1644.
- [10] Richardson RM, Singh A, Sun D, Fillmore HL, Dietrich DW 3rd, Bullock MR. Stem cell biology in traumatic brain injury: effects of injury and strategies for repair. *Neurosurg* 2010;112:1125–38.
- [11] Ogawa Y, Sawamoto K, Miyata T, Miyano S, Watanabe M, Nakamura M, et al. Transplantation of in vitro-expanded fetal neural progenitor cells results in neurogenesis and functional recovery after spinal cord contusion injury in adult rats. *J Neurosci Res* 2002;69:925–33.
- [12] Keirstead HS, Nistor G, Bernal G, Totoiu M, Cloutier F, Sharp K, et al. Human embryonic stem cell-derived oligodendrocyte progenitor cell transplants remyelinate and restore locomotion after spinal cord injury. *J Neurosci* 2005;25:4694–705.
- [13] Cooke MJ, Vulic K, Shoichet MS. Design of biomaterials to enhance stem cell survival when transplanted into the damaged central nervous system. *Soft Matter* 2010;6:4988–98.
- [14] Hiraoka M, Kato K, Nakaji-Hirabayashi T, Iwata H. Enhanced survival of neural cells embedded in hydrogels composed of collagen and laminin-derived cell adhesive peptide. *Bioconjugate Chem* 2009;20:976–83.
- [15] Potter W, Kalil RE, Kao WJ. Biomimetic material systems for neural progenitor cell-based therapy. *Front Biosci* 2008;13:806–21.
- [16] Han Q, Jin W, Xiao Z, Ni H, Wang J, Kong J, et al. The promotion of neural regeneration in an extreme rat spinal cord injury model using a collagen scaffold

- containing a collagen binding neuroprotective protein and an EGFR neutralizing antibody. *Biomaterials* 2010;31:9212–20.
- [17] Nakaji-Hirabayashi T, Kato K, Iwata H. Hyaluronic acid hydrogel loaded with genetically-engineered brain-derived neurotrophic factor as a neural cell carrier. *Biomaterials* 2009;30:4581–9.
- [18] Nakajima M, Ishimuro T, Kato K, Ko I-K, Hirata I, Arima Y, et al. Combinatorial protein display for the cell-based screening of biomaterials that direct neural stem cell differentiation. *Biomaterials* 2007;28:1048–60.
- [19] Wong RWC, Guillaud L. The role of epidermal growth factor and its receptors in mammalian CNS. *Cytokine Growth Factor Rev* 2004;15:147–56.
- [20] Mason I. Initiation to end point: the multiple roles of fibroblast growth factors in neural development. *Nat Rev Neurosci* 2007;8:583–96.
- [21] Ye P, D'Ercole AJ. Insulin-like growth factor actions during development of neural stem cells and progenitors in the central nervous system. *J Neurosci Res* 2006;83:1–6.
- [22] Ahmed S, Reynolds BS, Weiss S. BDNF enhances the differentiation but not the survival of CNS stem cell-derived neuronal precursors. *J Neurosci* 1995;15:5765–78.
- [23] Lillien LE, Sendtner M, Raff MC. Extracellular matrix-associated molecules collaborate with ciliary neurotrophic factor to induce type-2 astrocyte development. *J Cell Biol* 1990;111:635–44.
- [24] Kato K, Sato H, Iwata H. Immobilization of histidine-tagged recombinant proteins onto micropatterned surfaces for cell-based functional assays. *Langmuir* 2005;21:7071–5.

- [25] Erickson RI, Paucar AA, Jackson RL, Visnyei K, Kornblum H. Roles of insulin and transferrin in neural progenitor survival and proliferation. *J Neurosci Res.* 2008;86:1884–94.
- [26] Ko I-K, Kato K, Iwata H. Parallel analysis of multiple surface markers expressed on rat neural stem cells using antibody microarrays. *Biomaterials* 2005;26:4882–91.
- [27] Arima Y, Ishii R, Hirata I, Iwata H. Development of surface plasmon resonance imaging apparatus for high-throughput study on protein–surface interactions. *e-J Surf Sci Nanotech* 2006;4:201–7.
- [28] Reynolds BA, Tetzlaff W, Weiss SA. A multipotent EGF-responsive striatal embryonic progenitor cell produces neurons and astrocytes. *J Neurosci* 1992;12:4565–74.
- [29] Nakaji-Hirabayashi T, Kato K, Arima Y, Iwata H. Oriented immobilization of epidermal growth factor onto culture substrates for the selective expansion of neural stem cells. *Biomaterials* 2007;28:3517–29.
- [30] Ward JH. Hierarchical grouping to optimize an objective function. *J Am Stat Assoc* 1963;58:236–44.
- [31] Nakaji-Hirabayashi T, Kato K, Iwata H. Surface-anchoring of spontaneously dimerized epidermal growth factor for highly selective expansion of neural stem. *Bioconjugate Chem* 2009;20:102–10.
- [32] Krüttgen A, Grötzinger J, Kurapkat G, Weis J, Simon R, Thier M, et al. Human ciliary neurotrophic factor: a structure-function analysis. *Biochem J* 1995;309:215–20.

- [33] Hua QX, Narhi L, Jia W, Arakawa T, Rosenfeld R, Hawkins N, et al. Native and non-native structure in a protein-folding intermediate: spectroscopic studies of partially reduced IGF-I and an engineered alanine model. *J Mol Biol* 1996;259:297–313.
- [34] Palmer TD, Ray J, Gage FH. FGF-2-responsive neuronal progenitors reside in proliferative and quiescent regions of the adult rodent brain. *Mol Cell Neurosci* 1995;6:474–86.
- [35] Takahashi J, Palmer TD, Gage FH. Retinoic acid and neurotrophins collaborate to regulate neurogenesis in adult-derived neural stem cell cultures. *J Neurobiol* 1999;38:65–81.
- [36] Okada Y, Matsumoto A, Shimazaki T, Enoki R, Koizumi A, Ishii S, et al. Spatiotemporal recapitulation of central nervous system development by murine embryonic stem cell-derived neural stem/progenitor cells. *Stem Cells* 2008;26:3086–98.

Chapter 2

Design of culture substrates for large-scale expansion of neural stem cells

2.1 Introduction

Neural stem cells (NSCs), capable of self-renewal and differentiation into multiple cell types, are found in embryonic and adult tissues in the central nervous system (CNS) [1]. During development, NSCs generate neurons, astrocytes, and oligodendrocytes to organize nervous tissues and are considered to contribute to the neurogenesis in the adult CNS [2,3]. To date, numerous studies have been made with NSCs cultured in vitro to investigate the molecular and cellular mechanisms underlying mammalian CNS development [4,5]. In addition, NSCs have been utilized as one of the potential sources for the cell replacement therapy of CNS disorders [6, 7].

All of these fundamental and applied studies largely rely on the capability of culturing NSCs in vitro. Currently, the most standard method to obtain NSCs is so-called neurosphere culture [8, 9], in which neural cells dissociated from embryonic or adult tissues are cultured in suspension in the presence of basic fibroblast growth factor (bFGF) and epidermal growth factor (EGF). As a result, growth factor-responsive cells proliferate to generate cell aggregates, neurospheres, in which NSCs are enriched.

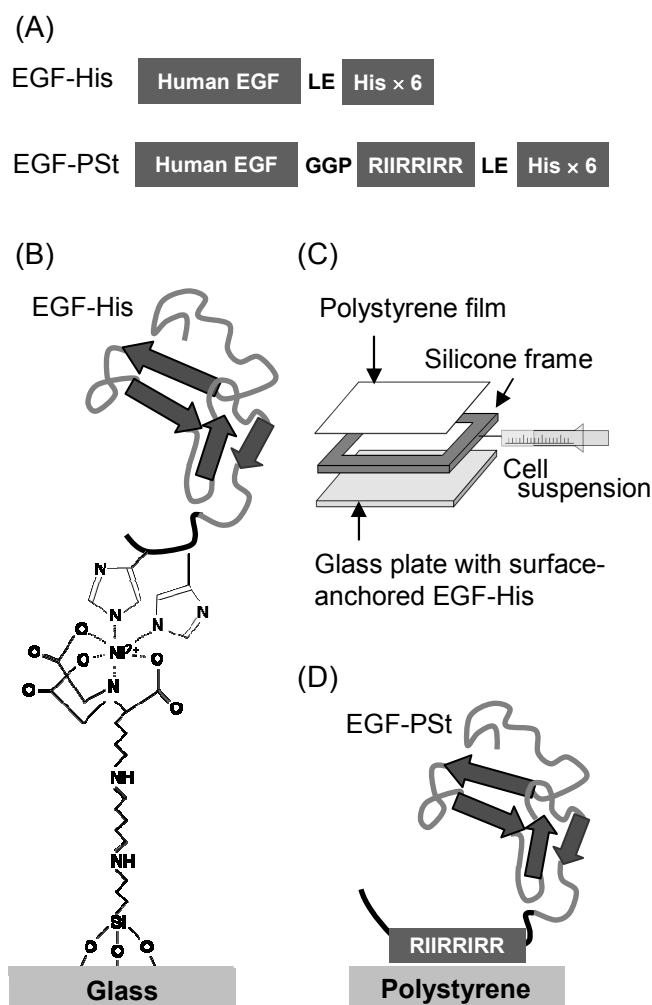
Though the neurosphere culture is widely employed, there are still limitations associated with this method. The most critical problems may be heterogeneity of cell

populations in a neurosphere. The content of cells expressing a marker for NSCs, nestin, reaches only 50 – 60% of total cells in a neurosphere [10]. The rest of cells are more differentiated cells in neuronal and glial lineages. Such heterogeneity makes it difficult to solely investigate the behaviors of NSCs, and also limits the controlled processing of NSCs for cell transplantation therapy. In addition, a growth rate is limited in neurosphere culture, probably because of the fact that differentiated cells present in neurospheres have reduced potential of proliferation [11]. Accordingly, it appears that the neurosphere culture method is inefficient for the production of NSCs.

In this chapter, culture substrates were developed to overcome these limitations. According to the results of chapter 1, bFGF-His and EGF-His promote the self-renewal of NSCs, while EGF-His inhibits differentiation of the cells into neuronal and glial lineages. EGF was used for a culture substrate that enables highly efficient expansion of NSCs in adherent culture. On the substrate, EGF, a strong mitogen for NSCs [8], was immobilized for selectively capturing NSCs and transducing proliferative signaling in the captured NSCs. To avoid denaturation of EGF upon immobilization and detachment of immobilized EGF during cell culture, a hexahistidine sequence (His) was fused to the C-terminus of EGF [12, 13] and then the engineered EGF (EGF-His) was anchored under mild conditions through the coordination of His with a Ni²⁺-bearing substrate.

The method for surface-anchoring EGF opened a way to fabricate culturewares that allow for large-scale expansion of pure NSCs. The present study was undertaken to construct culture modules with surface areas much larger than the laboratory-scale substrate [10, 12]. For uniformly anchoring EGF-His over a larger area, attempts were made to utilize a glass plate with amine functionalities at the surface. It also seems that no requirement for a gold layer is advantageous to the general use of the technique. In

this chapter, the surface-anchoring method was further applied to conventional polystyrene dishes. For simple fabrication, a nonapeptide (RIIRRIRR) bearing an affinity for polystyrene [14] (designated this peptide as PSt tag hereafter) was fused to EGF. The EGF-PSt was then anchored to the surface of a polystyrene dish by simply exposing the dish to the EGF-PSt solution.



Scheme 1. (A) Structure of EGF-His and EGF-PSt. The sequence LE comes from the plasmid. The sequence GGP was inserted as a linker. His: hexahistidine. (B) Illustration for the oriented immobilization of EGF-His onto a glass surface. (C) Illustration of a culture module fabricated using a glass plate with surface-anchored EGF-His. (D) Illustration for the surface anchoring of EGF-PSt onto a polystyrene surface.

2.2 Materials and methods

Plasmid construction

The preparation of an expression vector for EGF-His (pET22-EGF) was described elsewhere [13]. For the construction of plasmid for EGF-PSt, a coding sequence for EGF was amplified from pET22-EGF by polymerase chain reaction (PCR) using a sense primer, 5'-agatatacatatgaatagtactctgaatgtcccctg-3', and an antisense primer,

5'-ggtgctcgagTCGTCGGATCCTTCGGATGATGATACGtgacctccgcgcagttcccaccacttcag-3' (both synthesized by Invitrogen, Carlsbad, CA). The antisense primer contained a sequence for PSt tag (uppercase letter) [14] and a linker peptide GGP (underlined). PCR was performed under the following cycling conditions: initial denaturation for 5 min at 94 °C; 30 cycles of denaturation for 30 s at 94 °C, annealing for 30 s at 55 °C, and extension for 30 s at 72 °C; final extension for 7 min at 72 °C. The DNA fragment thus obtained was ligated into the Nde I – Xho I site of pET22b (Novagen, Darmstadt, Germany). The plasmid, pET22-EGF-PSt, was then cloned in *Escherichia coli* (*E. coli*) DH5 α (Toyobo Co., Ltd., Osaka, Japan). The correctness of the insert was confirmed by sequencing.

Protein expression and purification

EGF-His was expressed, purified, and refolded as previously reported [13] and stored in solution at –80 °C until use. For the preparation of EGF-PSt, *E. coli* strain

BL21-CodonPlus (Stratagene, La Jolla, CA) was transformed with pET22-EGF-PSt to obtain a clone harboring the plasmid. The transformant was cultured in Terrific Broth (TB) medium containing 100 µg/mL ampicillin at 37 °C for 30 min. Then, 1 mM isopropyl β-D-thiogalactoside (Novagen) was added to the culture to induce gene expression followed by additional culture for 4 h. Alternatively, Overnight Express™ autoinduction system (Merck KGaA, Darmstadt, Germany) with a TB medium was used for spontaneous protein expression for 24 h at 25 °C. EGF-PSt expressed as inclusion bodies was extracted with 20 mM phosphate buffer (pH 7.4) containing 8 M urea, 5 mM 2-mercaptoethanol, and 20 mM imidazole and purified by Ni-chelate affinity chromatography using a His Trap HP column (GE Healthcare Bio-Science Corp., Piscataway, NJ). EGF-PSt was stored in solution containing 8 M urea, 5 mM 2-mercaptoethanol, and 500 mM imidazole at 4 °C. The purity and the molecular size of EGF-His and EGF-PSt were analyzed by sodium dodecylsulfate-polyacrylamide gel electrophoresis (SDS-PAGE). The concentration of these proteins was determined using micro BCA kit (Pierce Biotechnology Inc., Rockford, IL). The structure of EGF-His and EGF-PSt are depicted in Scheme 1A.

Preparation of glass-based culture modules

As shown in Scheme 1B, EGF-His was anchored to the glass surface. First a glass plate (60 mm × 60 mm × 1 mm) was treated with a piranha solution (concentrated sulfuric acid : 30% hydrogen peroxide solution = 7 : 3 by volume) for 15 min at room temperature to remove organic impurities and subsequently treated with an aqueous solution containing 2 M hydrochloric acid and 1.5 M hydrogen peroxide solution for 15

min at room temperature to introduce silanol groups on the surface [15]. After thorough washing with water and drying with nitrogen gas, the glass plate was immersed in toluene containing 5% (v/v) 3-aminopropyltriethoxysilane (APTES, Shin-Etsu Chemical Co., Ltd., Tokyo, Japan) for 1 h at room temperature followed by washing with ethanol and water. Subsequently, the glass plate was heated at 80 °C in vacuo for 3 h to complete condensation of APTES. The glass plate with amines on the surface was immersed in 10% (v/v) aqueous glutaraldehyde solution for 30 min at room temperature to introduce aldehyde. After washing the plate with water, the surface was exposed to 10 mM solution of N-(5-amino-1-carboxypentyl) iminodiacetic acid (NTA, Dojindo Laboratories, Kumamoto, Japan) for 3 h at room temperature to introduce NTA through the formation of Schiff base. Subsequently, the glass plate was immersed in 40 mM NiSO₄ for 30 min to chelate Ni²⁺ ions to the NTA introduced. To verify the above reactions, static contact angles of water were measured by the sessile drop method using a CA-X contact angle meter (Kyowa Interface Science Co., Ltd., Saitama, Japan). After extensive washing with water, the surface was exposed to 50 µg/mL EGF-His solution in PBS for 1 h at room temperature to allow for the immobilization of EGF-His by coordination of the surface-bound Ni²⁺ with the His and then washed with PBS to remove unbound EGF-His.

To fabricate a culture module, a silicon frame (thickness: 1 mm) was adhered to the EGF-immobilized glass plate, and a polystyrene film (thickness: 75 µm) was adhered to the other side of the silicone frame as shown in Scheme 1C. A culture area within the silicone frame was 25 cm², and a chamber volume created between the glass plate and the polystyrene film was 2.5 mL. The module thus obtained was immediately used for cell culture as described below.

EGF-His was also immobilized onto rectangular glass plates (22 mm × 26 mm × 0.5 mm) or glass discs (diameter: 15 mm, thickness: 0.15 mm) in the same manner as described above. These samples were used to determine the amount of immobilized EGF-His and the number of cells proliferated on the substrate, respectively.

Surface anchoring of EGF-PSt on polystyrene

An EGF-PSt solution containing 8 M urea was diluted 4-times with PBS containing 0.05% Tween 20 (final EGF-PSt concentration: 50 µg/mL) [14]. The diluted solution (3 mL) was added to a 10 cm-polystyrene tissue culture dish (Asahi Glass Co., Ltd. Tokyo, Japan) and kept at room temperature to allow for the binding of EGF-PSt to the surface of a polystyrene dish (Scheme 1D). After 1 h, the dish was washed with PBS and further soaked in PBS at room temperature for more than 2 h to promote refolding of the bound EGF-PSt.

Determination of immobilized EGF-His and EGF-PSt

The surface density of immobilized EGF-His and EGF-PSt was determined using a microBCA protein assay kit (Pierce Biotechnology, Inc., Rockford, IL). A silicone frame having a square window (inner area: 3 cm²) was placed on the EGF-His- or EGF-PSt-anchored surface. The microBCA reaction mixture (250 µL) was pipetted within the window, and the temperature was kept at 37 °C for 2 h to allow coloring reaction. The absorbance was measured at 562 nm for the resultant solution using a spectrophotometer (DU 640, Beckman Coulter, Brea, CA). The amount of immobilized

protein was determined using bovine serum albumin (BSA) as a standard.

Surface plasmon resonance analysis

Polystyrene (MW = 125000–25000, Polyscience, Inc., Warrington, PA) was dissolved in toluene to a concentration of 1% and spin-coated onto a gold-evaporated glass plate at 6000 rpm for 60 s. The surface of a polystyrene film was treated with plasma for 30 s using a plasma generator (PA-300AT, O-kuma Engineering Co, Ltd., Fukuoka, Japan) operated at 5 Pa and 30 W. The plate was then mounted to the surface plasmon resonance (SPR) apparatus [16]. The light reflectance was continuously monitored at 37 °C and an incident angle 0.5 degree smaller than the resonance angle during the following procedures: After equilibrating with PBS (pH 7.4) in a flow cell, the polystyrene surface was exposed to PBS containing 50 µg/mL EGF-PSt, 2 M urea, 0.0375% Tween 20, 5 mM 2-mercaptoethanol, and 25 mM imidazole (pH 7.4) for 90 min followed by circulation of pure PBS (pH 7.4) for 120 min. In control experiments, plasma treatment was omitted to examine the effects of surface hydrophilicity on the binding of EGF-PSt. The reflectance was converted to the resonance angular shift. The angular shift observed before and after the circulation of EGF-PSt was converted to the amount of EGF-PSt bound to the surface, assuming that unit angular shift corresponds to a protein density of 1.1 µg/cm² [16].

Spectroscopic analysis of immobilized EGF-His and EGF-PSt

The secondary structure of EGF-His and EGF-PSt at surface was analyzed by

multiple internal reflection-infrared absorption spectroscopy (MIR-IRAS) under water [15]. A cleaned Si plate (0.5 mm × 11 mm × 35 mm) with 45° bevels on both sides was soaked in an aqueous solution containing 2 M HCl and 1.5 M H₂O₂ at room temperature for 20 min to introduce Si–OH on the surface. The plate was reacted with APTES, glutaraldehyde, NTA, and Ni²⁺ ion as described above. Alternatively, a thin polystyrene layer was formed by spin coating a 1% polystyrene (MW = 125000–25000, Polyscience, Inc) solution in toluene at 6000 rpm for 60 s. The polystyrene surface was then treated with oxygen plasma generated at a pressure of 5 Pa and an electronic power of 30 W for 60 s to enhance hydrophilicity of the surface. These modified plates were mounted to an IR spectrometer (FTLA-2000, ABB Inc., Zurich, Switzerland) equipped with a flow cell. PBS containing 50 µg/mL EGF-His or EGF-PSt was injected into the flow cell and kept for 60 min to anchor the protein. An IR light beam from an interferometer was focused at a normal incidence to the bevel of the Si plate and penetrated through the plate with internal reflection of ca. 80 times. The light exiting from the other bevel was focused to a liquid nitrogen-cooled mercury–cadmium–telluride detector. Spectra were recorded at an accumulation of 1024 scans and a resolution of 4 cm⁻¹. A sample chamber was continuously purged with dry nitrogen gas. The Ni²⁺–NTA-bound surface or the surface with a hydrophilic polystyrene layer was used as a reference. Immobilization reactions were carried out in H₂O-based solutions, whereas all measurements were carried out under D₂O. Spectra were analyzed using a GRAMS/AI software (Thermo Galactic, MA). Second-derivative spectral analysis was carried out to establish the position of the overlapping components of an amide I' band (the prime notation designates a deuterated condition) and assign them to different secondary structures [17]. The contribution of each component to the amide I' band was determined by Gaussian curve-fitting. Fitting

adjustment was repeated until a synthetic curve matched the experimental one with a precision factor of $\leq 1\%$.

Isolation of NSCs

The striatum was isolated from fetus (E16) of Fischer 344 rats and dissociated into single cells by treating with 0.05% trypsin solution containing 0.53 mM ethylenediamine-N,N,N',N'-tetraacetic acid (EDTA). All experiments were performed according to the guidelines of the Animal Welfare Committee of the Institute. The cells obtained were cultured in DMEM/F12 (1:1) (Invitrogen Corp., Carlsbad, CA) containing 2% (v/v) B27 supplement (Invitrogen), 5 $\mu\text{g}/\text{mL}$ heparin, 100 U/mL penicillin, 100 $\mu\text{g}/\text{mL}$ streptomycin, 20 ng/mL bFGF, and 20 ng/mL EGF for 4–5 d to form neurospheres [8]. According to our previous study [10], 50–60% of neurosphere-forming cells express nestin, a marker for undifferentiated neural stem cells.

Expansion of NSCs

Neurospheres at passage 2 were dissociated into single cells by treating with 0.05% trypsin-EDTA solution containing 0.53 mM EDTA. The cells were suspended in DMEM/F12 (1:1) containing 2% (v/v) B27 supplement, 5 $\mu\text{g}/\text{mL}$ heparin, 100 U/mL penicillin, 100 $\mu\text{g}/\text{mL}$ streptomycin. The cell suspension was infused by a syringe into the module at a density of 3.0×10^4 cells per square centimeter of a glass surface (total 7.50×10^5 cells per module). Alternatively, cells were seeded to the EGF-PSt-bound

polystyrene dish at a density of 3.0×10^4 cells/cm². The cells were cultured in an incubator at 37 °C under 5% CO₂ atmosphere. Every 4 d, cells were washed gently with DMEM/F12 (1:1) medium to remove weakly adhering cells, and observed with a phase contrast optical microscope (Diaphot 300, Nikon Corp., Tokyo, Japan).

Determination of cell number

EGF-His was anchored to the surface of glass discs as described above. The discs were placed in a 24-well polystyrene culture plate. In the case of EGF-PSt, the protein was anchored to each well of a 24-well polystyrene culture plate in the same manner as described above. Dissociated neurosphere-forming cells were seeded to these wells at a density of 3.0×10^4 cells/cm² and cultured for 1–5 d. The number of cells was determined every 24 h using a cell count reagent SF (Nacalai Tesque, Kyoto, Japan) according to the manufacturer's instructions. The cells were incubated for 3 h at 37 °C under 5% CO₂ by which tetrazolium salt was converted into formazan by NADH-catalyzed reduction in living cells. The concentration of formazan was determined from the absorbance at 450 nm on the resulting solution. The cell number was determined using a calibration curve obtained from various numbers of neurosphere forming cells.

Immunocytochemical staining

Cells cultured on the substrates were fixed with PBS containing 4% paraformaldehyde and 0.1% glutaraldehyde, and permeabilized by treating with 0.5%

Triton X-100 solution for 20 min at room temperature. Then the cells were treated with a Blocking One reagent (Nacalai Tesque) for 2 h to block nonspecific adsorption of antibodies, followed by binding of primary antibodies to nestin (1:200, mouse monoclonal, Rat 401, BD Biosciences, San Jose, CA) and β -tubulin III (1:500, rabbit polyclonal, Covance, Princeton, NJ) for 1 h at room temperature. After washing with PBS containing 0.05% Tween 20, cells were treated with Alexa Fluor 594 anti-mouse IgG and Alexa Fluor 488 anti-rabbit IgG (both from Molecular Probes, Inc., Eugene, OR) at a dilution of 1:500 for 1 h at room temperature and washed with PBS containing 0.05% Tween 20. Then, cell nuclei were counterstained with 1 μ g/mL Hoechst 33258 (Dojindo). The localization of secondary antibodies was analyzed with a fluorescent microscope (BX51 TRF, Olympus Optical Co., Ltd., Tokyo, Japan). The cells reactive for antibodies to nestin and β -tubulin III were counted on the merged images with nuclei staining. The original images were recorded at a magnification of $\times 200$, and individual cells were carefully identified on the merged images enlarged with a computer software. Cells were counted on three different sights on the same sample, and these data were averaged. The data are shown as mean \pm standard deviation for five independent samples.

Differentiation culture

NSCs at passage 6 were harvested from EGF-immobilized substrates by pipetting, and seeded on laminin coated dishes at a density of 3.0×10^4 cells/cm². To induce neuronal and astroglial differentiation, cells were cultured for 5 days in DMEM/F12 (1:1) containing 5 μ g/mL heparin, 100 U/mL penicillin, 100 μ g/mL

streptomycin, 1% (v/v) FBS, and 1 μ M retinoic acid and then immunofluorescently stained using antibody to glial fibrillar acidic protein (GFAP, 1:200, mouse monoclonal G-A-5, Millipore, Billerica, MA) and β -tubulin III (1:500, rabbit polyclonal, Covance) in a similar fashion to that described above. To induce oligodendroglial differentiation, cells were cultured for 5 days in DMEM/F12 (1:1) containing 2% (v/v) B27 supplement, 5 μ g/mL heparin, 100 U/mL penicillin, 100 μ g/mL streptomycin, and 50 ng/ml insulin like growth factor-1 and then immunofluorescently stained using antibody to oligodendrocyte marker O4 (1:200, mouse monoclonal 81, Millipore) in a similar fashion to that described above.

Analysis of EGF receptor expression

Cells were harvested from substrates with surface anchored EGF-His and EGF-PSt by pipetting. Then the cells were starved for EGF by incubating in a serum-free medium for 2–3 h. Subsequently, cells were fixed with PBS containing 4% paraformaldehyde and blocked with 1% BSA to prevent non-specific adsorption of antibody. Then the cells were reacted with antibody to EGF receptor (EGFR; 1:100, rabbit polyclonal, Abcam, Cambridge, UK) for 1 h at room temperature followed by washing with PBS containing 1% BSA to remove unreacted antibody. Subsequently, the cells were reacted with secondary antibody (1:250, Alexa Fluor 488 anti-rabbit IgG, Molecular Probes Inc., Eugene, OR) for 1 h at room temperature and washed with PBS containing 1% BSA to remove unreacted antibody. The population of fluorescently active cells was determined using Guava EasyCyte Mini (Millipore) equipped with a 488 nm diode laser. Data from approximately 50000 cells were used to generate a

histogram. Cells harvested from the substrates and exposed only to secondary antibody were used as a negative control. On the other hand, the neuroendocrine cell line PC12 derived from rat pheochromocytoma (Health Science Research Resources Bank, Tokyo, Japan) was used as a positive control, because the cells are known to express EGFR [18]. PC12 cells were stained using the primary and secondary antibodies as described above. Data from the control experiments were used to set the threshold to discriminate EGFR expressing cells.

2.3 Results

Preparation of EGF-His and EGF-PSt

Figure 1 shows the results of SDS-PAGE analysis carried out for EGF-His and EGF-PSt. EGF-His is separated as a single band around 7 kDa, being in accordance with the molecular weight predicted from the amino acid sequence (61 amino acid residues). CD spectroscopy and a biological assay gave results similar to our previous observation (Data not shown).

EGF-PSt is separated as a single band in SDS-PAGE analysis but the mobility is slightly higher than that predicted from the amino acid sequence (73 amino acid residues). The observed shift may be attributed to the larger binding capacity of the cationic PSt tag for SDS, which might enhance the swelling of the molecules and hence cause the enlarged size of the polypeptide. Because EGF-PSt was present in the denatured form in 8 M urea solution, we did not perform CD measurements and biological activity assays.

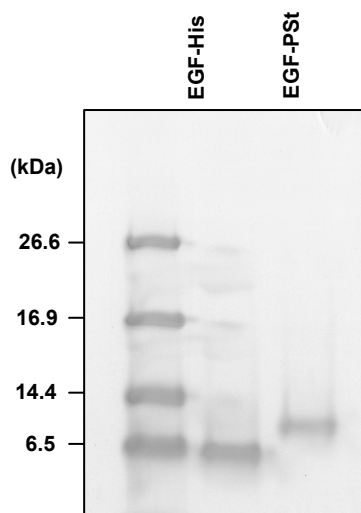


Fig. 1. SDS-PAGE analysis of EGF-His and EGF-PSt. A molecular weight standard was electrophoresed in a lane at the left side.

Table 1

Water contact angles measured on a bare glass surface and glass surfaces reacted with APTES and NTA.

Surface	Contact angle (degree) ^{a)}
Glass	< 10
Glass-APTES	70.2 ± 2.0
Glass-APTES-GA-NTA ^{b)}	60.4 ± 3.8

a) Contact angle measured on 10 different positions of a single sample were averaged and expressed as the mean ± standard deviation. ^{b)} GA: glutaraldehyde.

Surface anchoring of EGF-His to glass

Table 1 shows water contact angles measured on a bare glass surface and glass surfaces after reaction with APTES and NTA. The initially-hydrophilic glass surface turned to be relatively hydrophobic after reaction with APTES, being in consistent with previous observation by Wang H, et al [19]. A further reaction with glutaraldehyde and

NTA reduced the contact angle by approximately 10 degree, suggesting that carboxylic acid was introduced to the surface.

Nickel ions were chelated to the NTA-bound surface, and EGF-His was further coordinated to the surface bearing NTA-Ni²⁺. The amount of coordinated EGF-His determined after extensive washing with PBS was $0.53 \pm 0.10 \mu\text{g}/\text{cm}^2$ by the micro BCA assay. MIR-IRAS analysis was carried out on the surface obtained after reaction with EGF-His. As shown in Fig. 2A, the spectrum exhibited strong absorption at amide I' (1600–1700 cm⁻¹) and amide II' (1510–1580 cm⁻¹) bands, indicating the presence of EGF-His at surface. The composition of characteristic secondary structures was determined from the amide I' band (Fig. 2B). The result is shown in Table 2. The surface-anchored EGF-His contained β -sheet and β -turn structures at a similar content to those in the native EGF in solution [17] and also in EGF-His anchored to a Ni²⁺-bound surface created on an alkanethiol self-assembled monolayer [15].

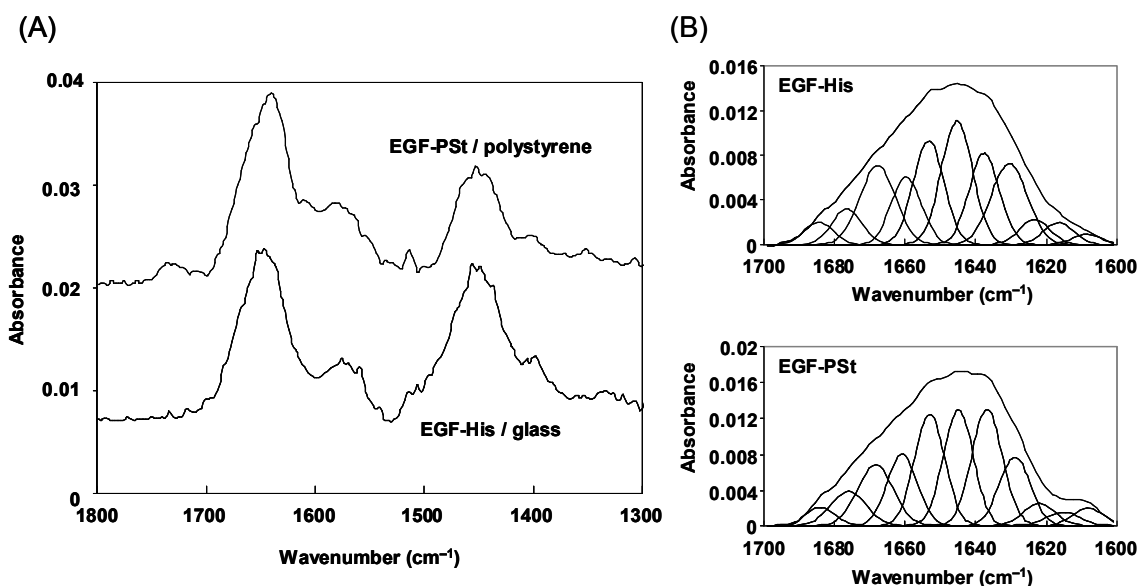


Fig. 2. MIR-IRAS analysis of the glass surface with anchored EGF-His and the polystyrene surface with anchored EGF-PSt. (A) Spectra are shown for 1300–1800 cm⁻¹ region which include amide I' and amide II' bands. (B) Absorption at amide I' band together with individual Gaussian components.

Table 2

The fraction of secondary structures in surface-anchored EGF-His and EGF-PSt determined by Gaussian curve-fitting.

Protein	Secondary structure				
	β -Sheet	Loop	Reverse turn	Random coil	Side chain
EGF-His	35.7	14.9	26.3	18.5	3.2
EGF-PSt	37.4	16.4	24.0	17.0	2.3
EGF ^{a)}	40.6	13.0	25.0	16.5	4.9

^{a)} Secondary structure of native EGF in solution reported by Yang *et al* [17].

Surface anchoring of EGF-PSt to polystyrene

Figure 3A shows the SPR sensorgrams recorded during the exposure of plasma-treated polystyrene surface to the solution of EGF-PSt. As can be seen, after large drift due to a urea containing medium, the resonance angle gradually increased to reach a plateau level. After 90 min circulation, the EGF-PSt solution was switched with pure PBS to wash the surface. The resonance angle immediately reduced due to a reduction in the refractive index of the medium. After this period, the resonance angle did not significantly change, indicating that EGF-PSt firmly bound to the polystyrene surface. The surface density of EGF-PSt estimated from the resonance angular shift after PBS washing was $1.29 \mu\text{g}/\text{cm}^2$. This is in good agreement with the result of microBCA assays ($1.05 \mu\text{g}/\text{cm}^2$) for EGF-PSt bound to the sensor surface. However, on a polystyrene dish, the density of surface-anchored EGF-PSt was determined to be $0.45 \pm 0.08 \mu\text{g}/\text{cm}^2$ by the microBCA method. This discrepancy is probably because of higher surface hydrophilicity of the sensor than the polystyrene dish. It was reported that the affinity between polystyrene and the polystyrene binding peptide correlated

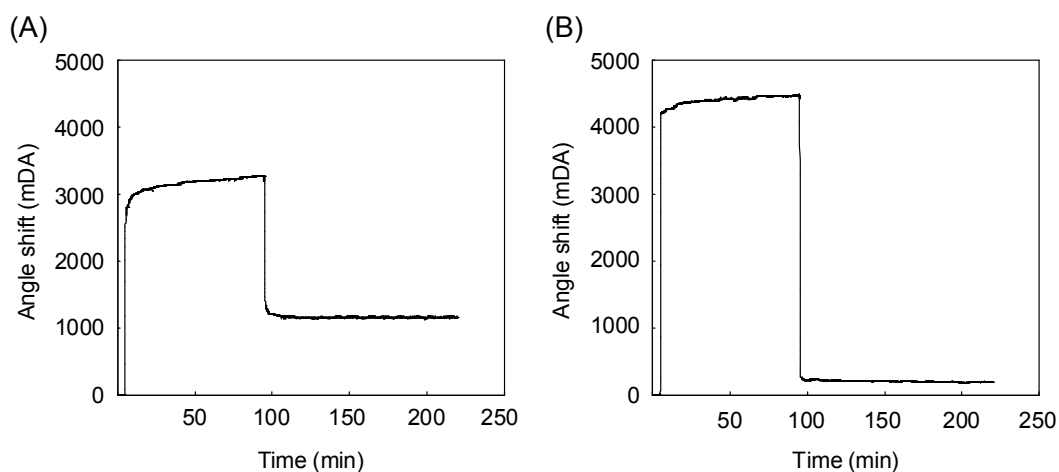


Fig. 3. (A) SPR sensorgrams recorded during the exposure of a plasma-treated polystyrene surface to the solution of EGF-PSt and subsequent washing with PBS. (B) Sensorgrams are also shown for control experiment in which EGF-PSt was circulated over the bare polystyrene surface (not treated with plasma)

with the hydrophilicity of a polystyrene surface [14]. This is in accordance with the result shown in Fig. 3B. The hydrophobic surface of naive polystyrene that had not been treated with plasma showed a lower binding capacity for EGF-PSt.

An MIR-IRAS spectrum recorded for the polystyrene surface with anchored EGF-PSt is shown in Fig. 2, and the composition of secondary structures determined from the amide I' band is shown in Table 2. Similar to the case with EGF-His, the surface-anchored EGF-PSt contained β -sheet and β -turn structures at a similar content to those in the native EGF in solution. This result suggests structural integrity of EGF-PSt anchored to the surface.

NSC proliferation on a substrate with anchored EGF-His

Dissociated neurosphere-forming cells were seeded to the glass-based substrate

with surface-anchored EGF-His (small-scale substrates). It was observed that approximately 50% of total cells were adhered to the surface. As shown in Fig. 4, a cell number increased on the EGF-His/glass substrate to reach at 1×10^6 cells/cm² after 5-d culture. On the other hand, the number of cells increased during the initial 4 d in neurosphere culture, and decreased at day 5. The observed reduction in proliferation rate may be due to cell necrosis in the core of neurospheres caused by limited oxygen supply. In Table 3, a fold increase in cell number after 5-d culture and an apparent doubling time are shown for the EGF-His/glass system and neurosphere culture. As can be seen, adherent culture on the EGF-His/glass substrate resulted in much faster proliferation of cells than neurosphere culture.

As shown in Fig. 5A, dissociated neurosphere-forming cells were injected into a module. A polystyrene film was placed on the top face to allow for necessary gas exchange. This construction facilitated highly homogeneous distribution of cells seeded in the module as well. In addition, the modular design permitted us to culture cells in a closed system. As shown in Fig. 5B, cells adhered and proliferated in the module, exhibiting their morphology similar to the case with the EGF-His-anchored gold substrate [10]. After 4-d culture, 5×10^6 cells could be obtained per module. These cells could be subcultured with new modules. During 6 passages by sub-culturing every 4 d, the average number of cells harvested after each subculture reached $5.4 \pm 1.7 \times 10^6$ cells per module, though cell proliferation slightly retarded after 7 passages.

Figure 5C shows the fluorescent micrograph of cells cultured in the module and then immunologically stained for nestin, a marker for NSCs, and β -tubulin III, a marker for differentiated neurons. As can be seen, a majority of cells are positive for nestin but not for β -tubulin III. This result indicates that cells proliferated in the module while

maintain the undifferentiated state. The number of cells with a phenotype of nestin⁺ β -tubulin III⁻ was determined to be 95% of total cells. This is marked contrast to the population obtained by neurosphere culture, in which nestin expressing cells are contained at 50–60% of total cells [10]. In addition, the cells obtained after 6 passages could be differentiated into three major lineages including neuron, astrocyte, and oligodendrocyte under appropriate conditions (Fig. 6), demonstrating that the cells still held multipotency.

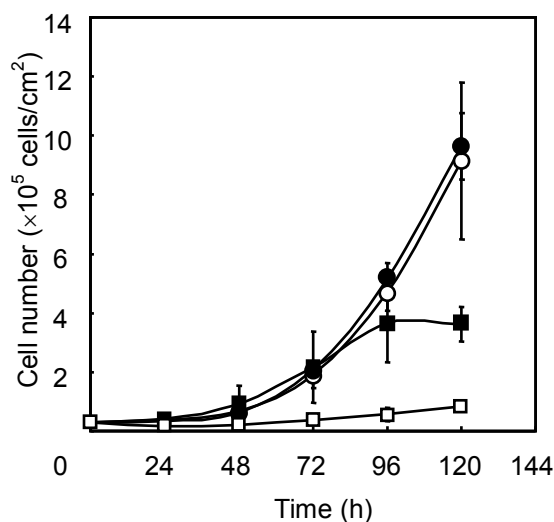


Fig. 4. Proliferation of neurosphere forming cells on (○) the glass with anchored EGF-His, (●) polystyrene with anchored EGF-PSt, and (□) bare polystyrene. Results are also shown for (■) neurosphere culture. Data are expressed as the mean \pm standard deviation ($n = 3$).

Table 3

Fold increase in a cell number after 5-d culture and the apparent doubling time determined for various culture systems.

Culture system	Fold increase in cell number	Apparent doubling time ^{a)}
	after 5 d	(h)
EGF-His / glass (adherent)	30.5 \pm 8.8	20.6 \pm 0.5
EGF-PSt / polystyrene (adherent)	32.1 \pm 3.7	19.4 \pm 0.7
Neurosphere culture (floating)	8.7 \pm 2.0	30.7 \pm 3.9

^{a)} Determined from the growth curve for 2 – 5 d after seeding.

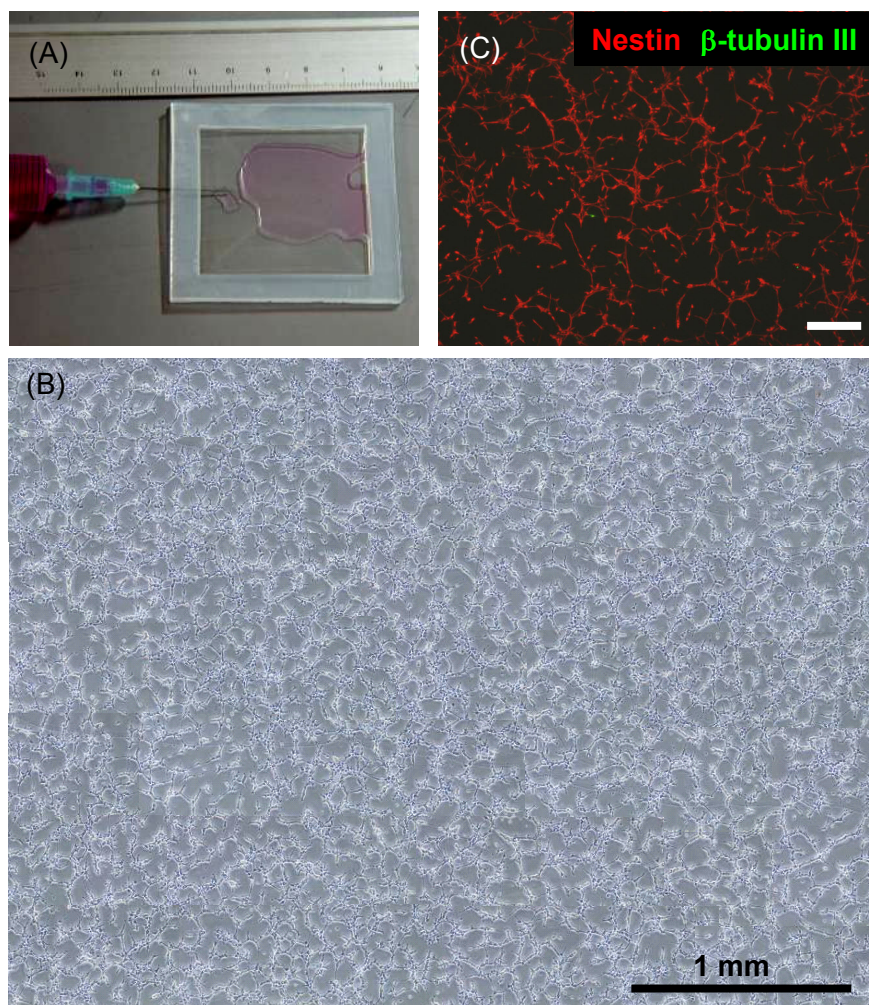


Fig. 5. Selective expansion of NSCs on the glass substrate with surface-anchored EGF-His. (A) Photograph of a culture module fabricated with the EGF-His/glass substrate, a silicone frame, and an upper film made of polystyrene. (B) Phase contrast micrograph of cells cultured for 4 d in the module. (C) Fluorescent micrograph of cells immunologically stained using antibody to nestin (red) and β -tubulin III (green). Scale bar: (B) 1 mm and (C) 100 μ m.

NSC proliferation on polystyrene with anchored EGF-PSt

Figure 7A shows the phase contrast micrograph of cells cultured for 3 d in a polystyrene dish with surface-anchored EGF-PSt. It is seen that cells adhered to the dish

and extended processes with a morphology similar to the cells on the EGF-His/glass substrate. In contrast, cells adhered to neither the bare polystyrene dish (Fig. 7B) nor the polystyrene dish that had been treated with EGF-His carrying no PS peptide (Fig. 7C). Furthermore, a film made of polyethylene or poly(ethylene terephthalate) could not support cell adhesion even after treatment with EGF-PSt (data not shown). These results as a whole indicate that EGF-PSt binds exclusively to the polystyrene surface and that cells are trapped on the surface through interactions with bound EGF-PSt.

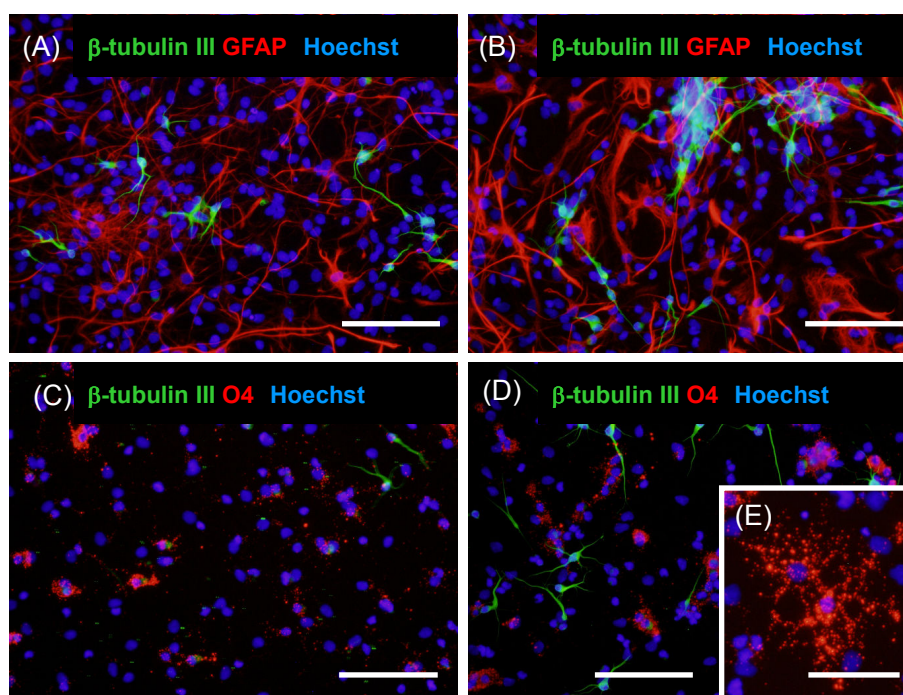


Fig. 6. Differentiation of NSCs into neurons, astrocytes, and oligodendrocytes. NSCs expanded on substrates with (A, C) EGF-His or (B, D) EGF-PSt were subjected to differentiation culture (see Material and methods for details). (A, B) Fluorescent micrographs of cells stained for GFAP (red), β -tubulin III (green), and nuclei (blue). (C, D) Fluorescent micrographs of cells stained for O4 (red), β -tubulin III (green), and nuclei (blue). (E) High magnification image of O4 positive cells in D. Scale bar: (A – D) 100 μ m and (E) 50 μ m.

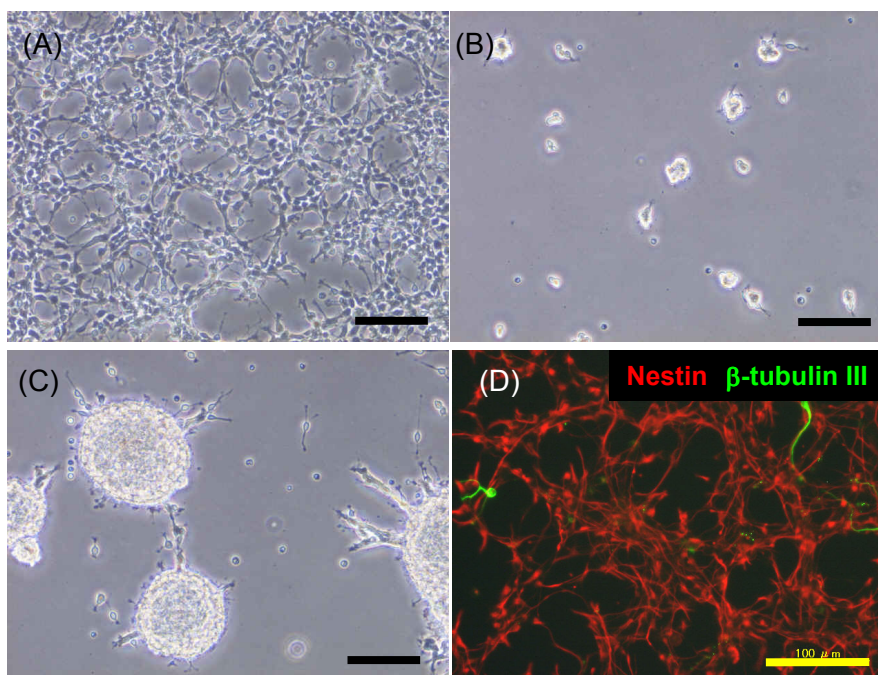


Fig. 7. Selective expansion of NSCs in a polystyrene dish with surface-anchored EGF-PSt. Phase contrast micrographs are shown for cells cultured for 4 d on (A) polystyrene with anchored EGF-PSt, (B) polystyrene treated with EGF-His, and (C) untreated polystyrene. (D) Fluorescent micrograph of cells cultured for 4 d in the EGF-PSt/polystyrene dish and then immunofluorescently stained using antibody to nestin (red) and β -tubulin III (green). Scale bar: 100 μ m.

As shown in Fig. 4, the number of cells increased on the EGF-PSt/polystyrene surface at a rate similar to that on the EGF-His/glass surface, with a comparable doubling time as well (Table 3). A greater part of the proliferated cells expressed nestin, while a few cells expressed β -tubulin III (Fig. 7D). The content of nestin expressing cells was determined to be $96.0 \pm 1.5\%$ of total cells. As shown in Fig. 6 B and D, the NSCs after 6 passages held multipotency.

Expression of EGFR

Flow cytometry analysis of neurosphere forming cells was carried out for the

expression of EGFR before and after adherent culture on the EGF-His/glass or EGF-PSt/polystyrene substrates. As shown in Fig. 8A, neurospheres contained 63% EGFR-positive cells. Neurospheres were dissociated into single cells and seeded to the EGF-His/glass or EGF-PSt/polystyrene substrates. After incubation for 15 h, non-adhering cells were removed by washing with PBS and then adherent cells were mechanically harvested for flow cytometry. As can be seen, the content of EGFR-positive cells in the total adherent cells was 96% on the EGF-His/glass (Fig. 8B) and 95% on the EGF-PSt/polystyrene (Fig. 8C). These results indicate that EGFR-positive cells were enriched on these surfaces, suggesting the selective entrapment of EGFR-positive cells through receptor–ligand interactions. In particular, cell adhesion was largely inhibited by the addition of 200 ng/mL soluble EGF to a medium (data not shown). The content of EGFR-positive cells was kept at a high level (approx. 90%) on the both substrates after culture for 4 d.

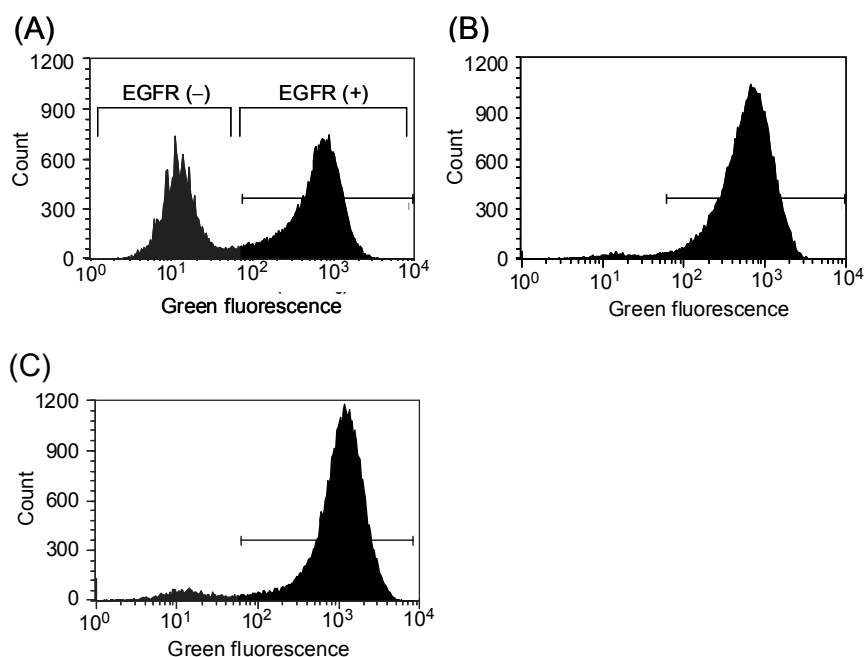


Fig. 8. Flow cytometry analysis for the expression of EGFR on neurosphere forming cells (A) before and after culture for 15 h on (B) EGF-His/glass and (C) EGF-PSt/polystyrene.

2.4 Discussion

Pure sources rich in NSCs are invaluable for various applications including fundamental study on brain development, cell-based drug screening, neurotoxicity testing, and cell-based therapy for CNS disorders. The glass- and polystyrene-based culture substrates reported here provide more efficient methods for obtaining pure NSC sources than the standard neurosphere culture. What is unique with our methods is to perform adherent cell culture on the substrates to which engineered EGF is surface-anchored.

One of the culture substrates developed in this study utilizes a glass plate as a substrate. The glass surface is first modified with an organosilicone compound, APTES, to introduce amine functionality and then with NTA to chelate Ni^{2+} ions. Finally, EGF-His is coordinated to the Ni^{2+} ions on the glass surface. Contact angle measurements, MIR-IRAS analysis, and the protein assay provided evidence for the reaction with APTES and NTA and the immobilization of EGF-His on the glass surface.

The culture module constructed with a silicone frame and a polystyrene membrane greatly facilitates homogeneous distribution of seeded cells, allowing cultivation of a large number of cells under identical conditions. In addition, the module requires a smaller volume of a medium than the standard cell culture systems. More importantly, the modular system is of great advantage to further scaling up and cell processing in a closed system for safe use in cell transplantation therapy.

After a single passage (4 d) in the culture module, we successfully obtained 5×10^6 cells per module with an NSC content of 95%. The cells could be subcultured up to passage 6, while retained multi-lineage differentiation potential. Accordingly, a cell

number can be expanded in principle ~10,000 fold after 5 passages. Taking into consideration that neurosphere forming cells originally contain nestin expressing NSCs at a content of no more than 60% [10], our module enables for NSCs to proliferate in a highly selective manner. As is shown by flow cytometry analyses (Fig. 8), EGFR expressing cells are trapped on the EGF-anchored surface most likely through the EGF-EGFR interaction. This entrapment leads to the enrichment of NSCs at the surface, because the majority of nestin-expressing NSCs co-express EGFR [20]. It is plausible that the ligation of EGFR on the entrapped NSCs activates EGFR signaling to promote proliferation of the cells.

Another culture substrates developed in this study is prepared by surface-anchoring EGF-PSt to a commercially-available tissue culture polystyrene dish. Analyses by MIR-IRAS, SPR, and protein assays revealed that EGF-PSt was immobilized on the polystyrene surface. The anchoring procedure is quite simple on account of the polystyrene-binding nonapeptide. The peptide was originally identified by screening phage display library with polystyrene as a binding substrate [14]. The high affinity for polystyrene allows us to anchor EGF-PSt on a polystyrene dish even in the presence of 2 M urea and subsequently refold the EGF-PSt anchored to the surface. Therefore, it is not required to eliminate urea from the solvent before anchoring, which is also convenient for EGF-PSt that is prone to precipitate when dissolved in urea-free solution at relatively high concentration.

On the EGF-PSt-anchored polystyrene dish, neurosphere forming cells proliferated to yield approximately 3×10^7 cells per 10-cm dish with an NSC content of 96%. Similar to the culture module fabricated using the EGF-His/glass substrate, the EGF-PSt/polystyrene dish permits more efficient expansion of NSCs than neurosphere

culture. The simple procedure for the fabrication of the cultureware using a commercial polystyrene dish makes easily available to prepare a large quantity of pure NSCs in standard laboratories. Further study is currently under way to apply these technologies for the selective expansion of human neural progenitor cells. Neural progenitor cells of human origin are known to proliferate much more slowly than rodent NSCs. A method for the efficient expansion of human neural progenitors will boost their clinical application for the treatment of CNS disorders.

References

- [1] Temple S. The development of neural stem cells. *Nature* 2001;414:112–7.
- [2] Ma DK, Bonaguidi MA, Ming GL, Song H. Adult neural stem cells in the mammalian central nervous system. *Cell Res* 2009;19:672–82.
- [3] Imayoshi I, Sakamoto M, Ohtsuka T, Kageyama R. Continuous neurogenesis in the adult brain. *Dev Growth Differ* 2009;51:379–86.
- [4] Ahmed S. The culture of neural stem cells. *J Cell Biochem* 2009;106:1–6.
- [5] Falk S, Sommer L. Stage- and area-specific control of stem cells in the developing nervous system. *Curr Opin Genet Dev* 2009;19:454–60.
- [6] Björklund A, Lindvall O. Cell replacement therapies for central nervous system disorders. *Nat Neurosci* 2000;3:537–44.
- [7] Ronaghi M, Erceg S, Moreno-Manzano V, Stojkovic M. Challenges of stem cell therapy for spinal cord injury: human embryonic stem cells, endogenous neural stem cells, or induced pluripotent stem cells? *Stem Cells* 2010;28:93–9.
- [8] Reynolds BA, Tetzlaff W, Weiss SA. Multipotent EGF-responsive striatal embryonic progenitor cell produces neuron and astrocytes. *J Neurosci* 1992;12:4565–74.
- [9] Deleyrolle LP, Reynolds BA. Isolation, expansion, and differentiation of adult Mammalian neural stem and progenitor cells using the neurosphere assay. *Methods Mol Biol* 2009;549:91–101.
- [10] Nakaji-Hirabayashi T, Kato K, Arima Y, Iwata H. Oriented immobilization of epidermal growth factor onto culture substrates for the selective expansion of neural stem cells. *Biomaterials* 2007;28:3517–29.

- [11] Sommer L, Rao M. Neural stem cells and regulation of cell number. *Prog Neurobiol* 2002;66:1–18.
- [12] Nakaji-Hirabayashi T, Kato K, Iwata H. Surface-anchoring of spontaneously dimerized epidermal growth factor for highly selective expansion of neural stem cells. *Bioconjugate Chem* 2009;20:102–10.
- [13] Kato K, Sato H, Iwata H. Immobilization of histidine-tagged recombinant proteins onto micropatterned surfaces for cell-based functional assays. *Langmuir* 2005;21:7071–5.
- [14] Kumada Y, Shiritani Y, Hamasaki K, Ohse T, Kishimoto M. High biological activity of a recombinant protein immobilized onto polystyrene. *Biotechnol J* 2009;4:1178–89.
- [15] Nakaji-Hirabayashi T, Kato K, Iwata H. Essential role of structural integrity and firm attachment of surface-anchored epidermal growth factor in adherent culture of neural stem cells. *Biomaterials* 2008;29:4403–8.
- [16] Hirata I, Morimoto Y, Murakami Y, Iwata H, Kitano E, Kitamura H, Ikada Y. Study of complement activation on well-defined surface using surface plasmon resonance. *Colloids Surf B Biointerfaces* 2000;18:285–92.
- [17] Yang CH, Wu PC, Huang YB, Tsai YH. A new approach for determining the stability of recombinant human epidermal growth factor by thermal Fourier transform infrared (FTIR) microspectroscopy. *J Biomol Struct Dyn* 2004;22:101–10.
- [18] Santos SD, Verveer PJ, Bastiaens PI. Growth factor-induced MAPK network topology shapes Erk response determining PC-12 cell fate. *Nat Cell Biol* 2007;9:324–30.

- [19] Wang H, Chen SF, Li LY. Improved method for the preparation of carboxylic acid and amine terminated self-assembled monolayers of alkanethiolates. *Langmuir* 2005;21:2633–6.
- [20] Ko IK, Kato K, Iwata H. Parallel analysis of multiple surface markers expressed on rat neural stem cells using antibody microarrays. *Biomaterials* 2005;26:4882–91.

Chapter 3

Selective and rapid expansion of human neural progenitor cells on a substrate with terminally-anchored growth factors

3.1 Introduction

Human neural progenitor cells (hNPCs) have been the focus of intense research with the goal of developing new stem cell-based treatments for spinal cord injuries and for neurodegenerative disorders such as Parkinson's disease. Many animal studies [1, 2] have shown that transplantation of hNPCs and their derivatives into the brain or spinal cord provides effective and safe treatments for these injuries and diseases. Recently, a phase I/II clinical trial began in Switzerland for the treatment of spinal cord injuries using fetal-derived hNPCs [3].

hNPCs are capable of self-renewal and of differentiation into multiple lineages, including neurons, astrocytes, and oligodendrocytes [4]. hNPCs can be obtained using the neurosphere culture method [5], in which cells from fetal or adult brain tissues are cultured in serum-free medium supplemented with basic fibroblast growth factor (bFGF) and/or epidermal growth factor (EGF). During culture, cells spontaneously form aggregates (neurospheres) that contain hNPCs. Cells with properties that are similar to

hNPCs can also be derived from human embryonic stem cells [6] and induced pluripotent stem cells [7] through neurosphere culture.

Although neurosphere culture is widely employed, the low rate of cell proliferation (doubling time 5-10 days [5, 8]) limits the availability of hNPCs; this rate is much slower than the doubling time of rodent cells (approximately 30 h [9]). This problem, as well as limited access to fetal tissues and ethical issues regarding their use, will become a serious concern, especially when hNPCs are clinically applied to many patients at multiple facilities. Therefore, an alternative method is critical for the efficient expansion of hNPCs obtained from minimal biopsy specimens.

In chapter 4, neural stem cells obtained from the fetal rat striatum (rNSCs) proliferated selectively and rapidly in an adherent culture on the substrate onto which epidermal growth factor (EGF) was immobilized. In this chapter, similar strategy was employed to the expansion of hNPCs. Due to a difference in the expression pattern of growth factor receptors between rNSCs and hNPCs, the growth factors EGF and bFGF were immobilized on glass substrates as a single component or in combination. These growth factor-immobilized substrates were evaluated for the selective expansion of hNPCs.

3.2 Materials and methods

Protein expression and purification

The preparation of EGF and bFGF carrying hexahistidine residues at their C-termini (EGF-His and bFGF-His, respectively) was previously reported [11]. Briefly,

complementary DNA (cDNA) was obtained for human EGF and human bFGF by polymerase chain reaction (PCR) using human cDNA libraries as templates and specific primers carrying restriction sites. The resulting DNA fragments were inserted into the multiple cloning site of the pET22 vector (Novagen, Darmstadt, Germany) upstream of the His-tag. These protein factors were expressed in *Escherichia coli*. EGF-His, obtained as inclusion bodies, was extracted under denatured conditions, purified over a Ni-chelated affinity column (His Trap HP; GE Healthcare Bio-Science Corp., Piscataway, NJ, USA), and refolded by dialyzing against solutions of reduced and oxidized glutathione. bFGF-His was obtained in soluble form and was purified under non-denaturing conditions. The purity of the proteins was checked by sodium dodecylsulfate-polyacrylamide gel electrophoresis (SDS-PAGE), while the structure of the proteins was analyzed by circular dichroism (CD) spectroscopy. Protein concentrations were determined using the Micro BCA Kit (Thermo, Waltham, MA, USA). Biological activity was assessed using neurosphere-forming cells. The EGF-His and bFGF-His solutions were stored at -80 °C until use.

Immobilization of EGF-His and bFGF-His on glass surfaces

EGF-His and bFGF-His were immobilized on glass surfaces through chelation of Ni²⁺ with a His-tag, as previously described [9]. Briefly, cleaned glass plates (22 mm × 26 mm × 0.5 mm; Matsunami Glass Ind. Ltd., Osaka, Japan) were immersed in 5% (v/v) 3-aminopropyltriethoxysilane (APTES; Shin-Etsu Chemical Co., Ltd., Tokyo, Japan) in toluene for 1 h at room temperature, then washed with ethanol and water. The plates were placed in a vacuum oven and heated to 80 °C for 3 h to obtain glass plates

surface-modified with APTES, which carries an amine at its terminus. The APTES-modified glass plates were immersed in 10% (v/v) aqueous glutaraldehyde (Nacalai Tesque, Kyoto, Japan) for 30 min at room temperature to introduce aldehyde groups; the plates were then washed with water to remove unreacted glutaraldehyde. Then, a 10 mM aqueous solution of *N*-(5-amino-1-carboxypentyl) iminodiacetic acid (NTA, Dojindo Laboratories, Kumamoto, Japan) was dispensed onto the activated surface, the plates were kept at room temperature for 2 h, and then the plates were washed with water to remove unreacted NTA. The glass plate was immersed in 40 mM NiSO₄ for 30 min at room temperature to form Ni²⁺ chelate, and then the plates were washed with water. EGF-His and/or bFGF-His in phosphate-buffered saline (50 µg/mL) was plated onto the Ni²⁺-chelated surface and kept for 1 h at room temperature to allow immobilization of the His-tagged proteins. These proteins were immobilized as a single component or in combination (molar ratio = 1:1).

Surface characterization

The surface density of immobilized EGF-His and bFGF-His was determined using the Micro BCA kit. A silicone frame with a square window (area: 3 cm²) was placed on the EGF-His-immobilized surface. The Micro BCA reaction mixture (250 µL) was pipetted in the window, and the temperature was kept at 37 °C for 2 h to allow development of the colorimetric reaction. The absorbance of the resultant solution was measured at 562 nm using a spectrophotometer (DU 640, Beckman Coulter). The amount of immobilized protein was determined using bovine serum albumin (BSA) as a standard.

The secondary structures of the immobilized proteins were analyzed by CD spectroscopy. EGF-His or bFGF-His was immobilized on quartz slides (35 mm × 9 mm × 0.5 mm) as described in section 2.2. Eighteen slides carrying immobilized EGF-His or bFGF-His were stacked and inserted in a quartz cuvette (40 × 10 × 10 mm³) containing 5 mM Tris-HCl (pH = 8.0). The CD spectra were obtained at 20 °C using a J-850 spectropolarimeter (JASCO Corp., Tokyo, Japan). As controls, the CD spectra of commercially available EGF (Wako Pure Chemical Industries, Osaka, Japan) and bFGF (Wako) were recorded in solution.

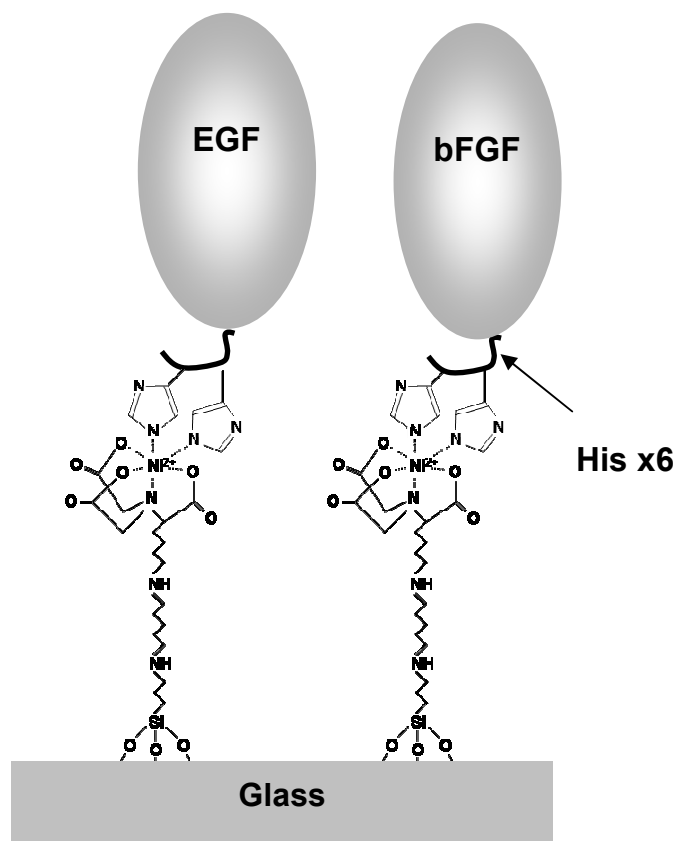


Fig. 1. Schematic representation of the surface immobilization of EGF-His and bFGF-His via chelate linkages.

hNPC culture

hNPCs (Lonza, Basel, Switzerland) isolated from fetal brain tissue (17-19 weeks gestation) were suspended in Dulbecco's Modified Eagle Medium/nutrient F12 (DMEM/F12, 1:1; Invitrogen Corp., Carlsbad, CA, USA) containing 0.6% glucose, 5 mM 4-(2-hydroxyethyl)-1-piperazineethanesulfonic acid (HEPES), 2% (v/v) B27 supplement (Invitrogen), 100 U/mL penicillin, 100 mg/mL streptomycin, 20 ng/mL bFGF (Wako), 20 ng/mL EGF (Wako), and 10 ng/mL leukemia inhibitory factor (Millipore, Billerica, MA, USA). Cells were cultured for 5-7 days to form neurospheres; the neurospheres from passages 2-5 were used for the following experiments. Neurospheres were dissociated into single cells by treatment with Accutase (Millipore) and then resuspended in DMEM/F12 (1:1) containing 0.6% glucose, 5 mM HEPES, 2% (v/v) B27 supplement, 100 U/mL penicillin, and 100 mg/mL streptomycin. The cells were seeded onto the substrates with immobilized EGF-His and/or bFGF-His at a density of 3.0×10^4 cells/cm².

Cell proliferation assay

EGF-His and bFGF-His were immobilized onto the surfaces of glass disks (diameter: 15 mm) as described in section 2.2. The disks were placed in each well of a 24-well polystyrene culture plate. Neurosphere-forming cells were seeded at a density of 3.0×10^4 cells/cm² and cultured for 1, 3, and 5 days in DMEM/F12 (1:1) containing 0.6% glucose, 5 mM HEPES, 2% (v/v) B27 supplement, 100 U/mL penicillin, and 100

mg/mL streptomycin. The number of cells was determined using Cell Count Reagent SF (Nacalai Tesque) according to the manufacturer's instructions.

Immunostaining

Cells were immunofluorescently stained as described previously [9]. Primary antibodies were specific for nestin (1:200, mouse monoclonal; BD Biosciences, San Jose, CA, USA), β -tubulin III (1:500, rabbit polyclonal; Covance, Princeton, NJ, USA), glial fibrillar acidic protein (GFAP; 1:200, mouse monoclonal G-A-5; Millipore), and RIP (1:1000, mouse monoclonal; Millipore). The secondary antibodies used were Alexa Fluor 594 anti-mouse IgG and Alexa Fluor 488 anti-rabbit IgG (1:500; Molecular Probes, Inc., Eugene, OR, USA). Cell nuclei were counterstained with Hoechst 33258 (Dojindo Laboratories, Kumamoto, Japan). Localization of secondary antibodies and the Hoechst dye was analyzed with a fluorescent microscope (BX51 TRF; Olympus Corp., Tokyo, Japan). All cells were counted on the fluorescent micrograph following Hoechst staining. The cells reactive for antibodies to nestin and β -tubulin III were counted on the merged image with nuclear staining.

Differentiation culture

hNPCs at passage 6 were harvested from the EGF/bFGF co-immobilized substrates by pipetting, then seeded onto laminin-coated dishes at a density of 3.0×10^4 cells/cm². To induce neuronal differentiation, cells were cultured for 5 days in DMEM/F12 (1:1) containing 100 U/mL penicillin, 100 μ g/mL streptomycin, 2% (v/v)

B27 supplement, and 50 ng/mL brain-derived neurotrophic factor; the cells were then immunofluorescently stained for β -tubulin III as described in section 2.6. To induce astroglial differentiation, cells were cultured for 5 days in DMEM/F12 (1:1) containing 100 U/mL penicillin, 100 μ g/mL streptomycin, and 1% (v/v) fetal bovine serum, then immunofluorescently stained for GFAP as described in section 2.6. To induce oligodendroglial differentiation, cells were cultured for 5 days in DMEM/F12 (1:1) containing 2% (v/v) B27 supplement, 100 U/mL penicillin, 100 μ g/mL streptomycin, 50 ng/mL insulin-like growth factor-1, and 10 ng/mL platelet-derived growth factor-AA, and then immunofluorescently stained for RIP as described in section 2.6.

Reverse transcriptase-polymerase chain reaction (RT-PCR)

Total RNA was extracted from neurosphere-forming cells at passage 2 with the SV Total RNA Isolation System (Promega Corp., Madison, WI, USA); this RNA was reverse-transcribed using the Transcriptor First Strand cDNA Synthesis Kit (Roche Applied Science, Mannheim, Germany) primed with oligo(dT)₁₈. The resulting first-strand cDNA was amplified by PCR using the following specific primers [15]: EGF receptor (EGFR), sense 5'-TGC TGA CTA TGT CCC GCC ACT GGA-3', antisense 5'-TGT GAG GTG GTC CTT GGG AAT TTG G-3'; FGF receptor 1 (FGFR1), sense 5'-GTT ACC CGC CAA GCA CGT ATA C-3', antisense 5'-CGA GCT CAC TGT GGA GTA TCC ATG-3'; and glyceraldehyde-3-phosphate dehydrogenase (GAPDH), sense 5'-ACC ACA GTC CAT GCC ATC AC-3', antisense 5'-TCC ACC ACC CTG TTG CTG TA-3'. The reaction mixtures (20 μ L) containing 1 μ L cDNA template, 5 U Takara Ex Taq DNA polymerase (Takara Bio Inc., Shiga, Japan), 0.5 μ M

sense primer, and 0.5 μ M antisense primer were subjected to 30 cycles of PCR under the following thermal cycling conditions: denaturation at 94 °C for 30 s, annealing at 55 °C (EGFR) or 58 °C (FGFR1) for 30 s, extension at 72 °C for 30 s. RT-PCR products were analyzed by 2% agarose gel electrophoresis with ethidium bromide staining.

Flow cytometry

Neurospheres were starved for EGF and bFGF by incubation in serum-free medium for 2-3 h. Neurospheres were dissociated into single cells by treatment with Accutase (Millipore), then blocked with 1% BSA to prevent non-specific adsorption of antibody. The cells were reacted with antibody against EGFR (1:100, mouse monoclonal; Abcam, Cambridge, MA, USA) or FGFR1 (1:100, rabbit polyclonal; Abcam) for 1 h at room temperature, then washed with phosphate-buffered saline containing 1% BSA to remove unreacted antibody. Subsequently, the cells were reacted with secondary antibody (Alexa Fluor 488 anti-mouse IgG or Alexa Fluor 488 anti-rabbit IgG antibody; Molecular Probes) for 1 h at room temperature and washed with phosphate-buffered saline containing 1% BSA to remove unreacted antibody. The population of fluorescently active cells was analyzed using a Guava EasyCyte Mini flow cytometer (Millipore) equipped with a 488-nm diode laser. Data from approximately 10,000 cells were used to generate a histogram. Cells harvested from the substrates and exposed only to secondary antibody were used as negative controls. Data from the control experiments were used to set the threshold for identifying EGFR- or FGFR1-expressing cells.

3.3 Results

Immobilization of EGF-His and bFGF-His

EGF-His and bFGF-His were expressed and purified following the method previously reported [14]. SDS-PAGE and biological assays yielded results similar to our previous observations (data not shown). His-tagged growth factors were immobilized onto the surfaces of glass substrates; Ni ions were chelated to the NTA-bound surface, and the growth factors were further coordinated to the surface bearing NTA-Ni²⁺ (Fig. 1). The amounts of immobilized factors were $0.53 \pm 0.10 \mu\text{g}/\text{cm}^2$ (EGF-His), $0.55 \pm 0.12 \mu\text{g}/\text{cm}^2$ (bFGF-His), and $0.34 \pm 0.04 \mu\text{g}/\text{cm}^2$ (EGF-His + bFGF-His).

Secondary structure of immobilized EGF-His and bFGF-His

The secondary structures of the immobilized growth factors were analyzed by CD spectroscopy. Since the amount of growth factor immobilized onto a single glass plate was insufficient for obtaining an accurate CD spectrum, 18 glass plates with immobilized EGF-His or bFGF-His were stacked and inserted into a quartz cuvette. Ultraviolet light was passed perpendicular through every surface of the stacked glass plates to acquire an accumulated spectrum. For comparison, the soluble forms of the cognate proteins in solution were analyzed over the same wavelength range (Fig. 2). The spectra of the immobilized EGF-His and bFGF-His exhibited a positive Cotton effect at 230 nm, suggesting the presence of β -turn structure. Both immobilized growth

factors produced spectra similar to the soluble forms of their respective proteins and to those proteins lacking a His-tag. These results suggest that the immobilized EGF-His and bFGF-His were folded into proper structures on the glass surface.

Expression of EGFR and FGFR1 on cells

Flow cytometry and semi-quantitative RT-PCR were employed to evaluate the expression of EGFR and FGFR1 on neurosphere-forming cells. Only 17.4% of the neurosphere-forming cells expressed EGFR (Fig. 3A), but 96.5% of the cells expressed FGFR1 (Fig. 3B). These observations of low levels of EGFR expression and high levels

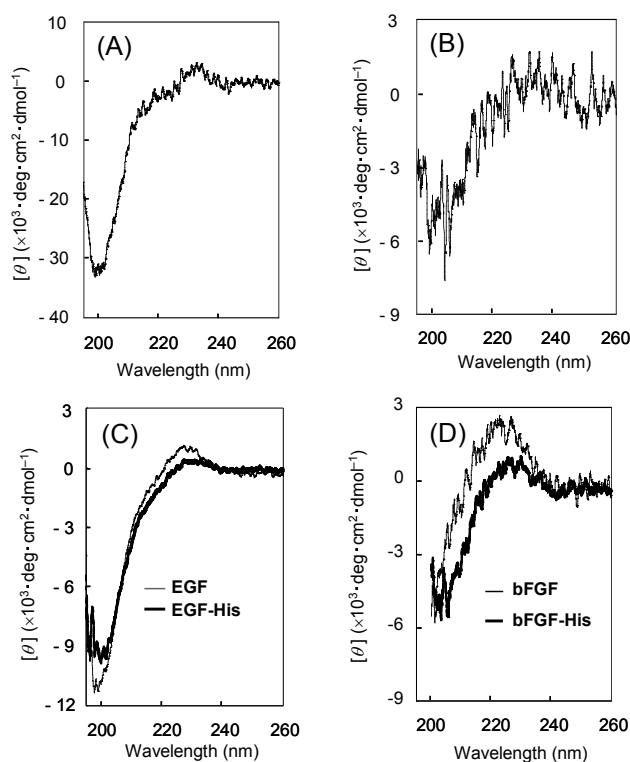


Fig. 2. Far-ultraviolet CD spectra of immobilized growth factors and cognate growth factors in solution. (A) Immobilized EGF-His, (B) Immobilized bFGF-His, (C) EGF and EGF-His in solution, and (D) bFGF and bFGF-His in solution.

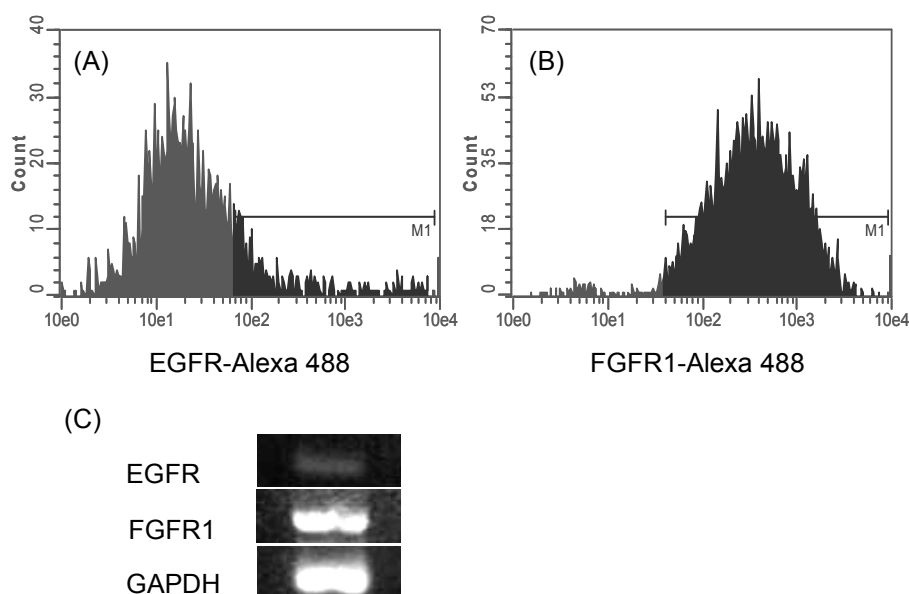


Fig. 3. Analysis of receptor expression by neurosphere-forming cells. (A, B) Flow cytometry using antibodies against (A) EGFR and (B) FGFR1. (C) RT-PCR using specific primers for EGFR, FGFR1, and GAPDH.

of FGFR1 expression were in good agreement with the results from RT-PCR (Fig. 3C); a strong band was seen for FGFR1, and a trace band was detected for EGFR.

Cell proliferation on growth factor-immobilized substrates

Dissociated neurosphere-forming cells were seeded onto growth factor-immobilized substrates and cultured for 5 days. A limited number of cells were seen on the surface with immobilized EGF-His (Fig. 4A). On the other hand, many cells were observed on the surface with immobilized bFGF-His (Fig. 4B); these cells extended neurites and were uniformly distributed over the surface. Many cells also

appeared on the surface with co-immobilized EGF-His and bFGF-His (Fig. 4C). These cells formed bundles of neurites that were similar to those observed in adherent culture of rat NSCs on EGF-His-immobilized substrates [9, 10]. Cell adhesion and proliferation were nearly undetectable on the control surface without immobilized growth factors (Fig. 4D).

We determined the numbers of cells that proliferated during 5 days on the surfaces with or without immobilized growth factors, as well as the number of cells that grew in neurospheres (Fig. 5). Cell numbers increased 5-fold and 4-fold on the bFGF-His- and bFGF-His/EGF-His-immobilized surfaces, respectively. These increases were significantly higher than those determined for the EGF-His-immobilized surface

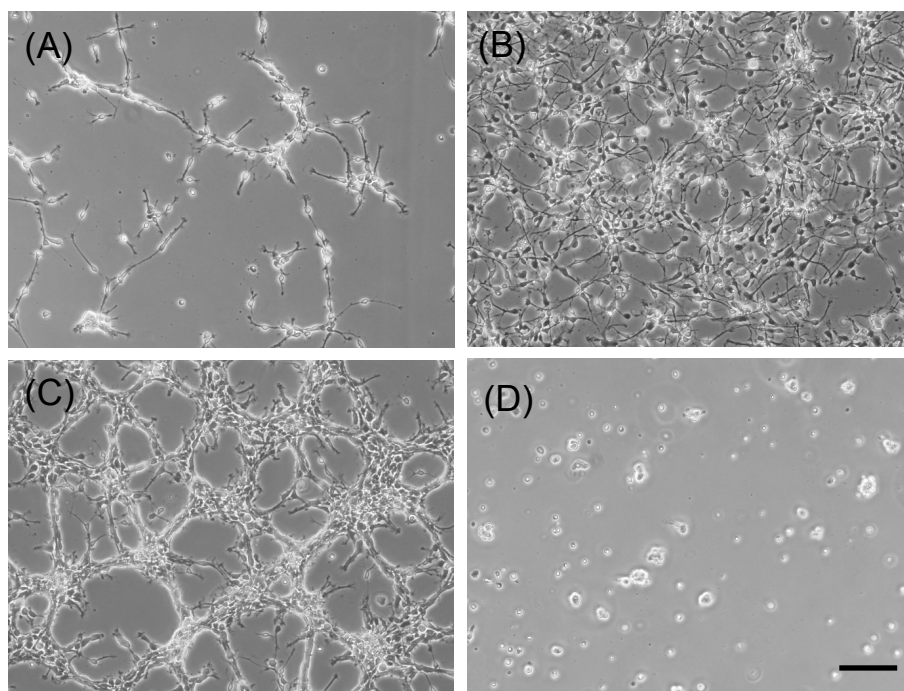


Fig. 4. Phase contrast micrographs of cells cultured for 5 days on substrates with immobilized (A) EGF-His, (B) bFGF-His, and (C) EGF-His/bFGF-His, and on (D) a Ni-bound surface without growth factors. Scale bar: 100 μ m.

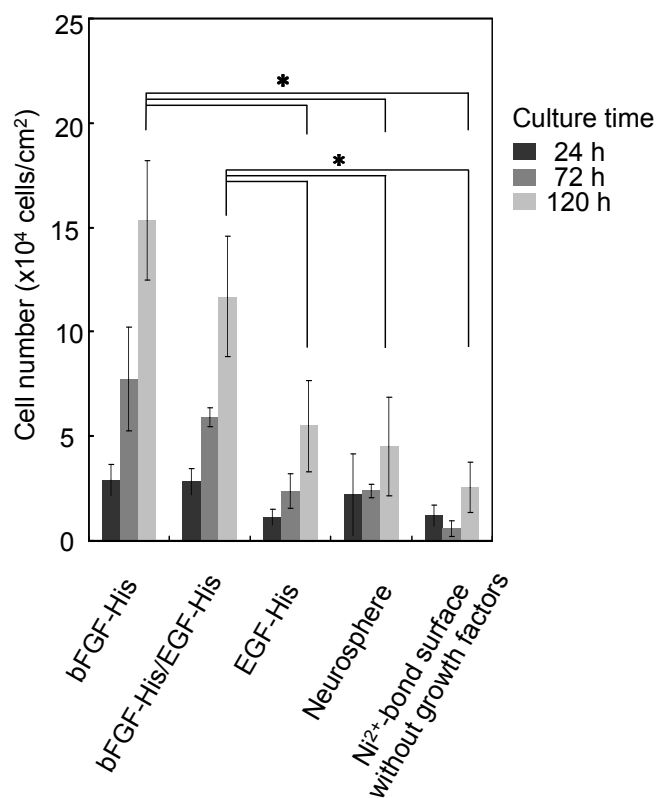


Fig. 5. Proliferation of neurosphere-forming cells on substrates with and without immobilized growth factors. Results are also shown for neurosphere culture. Data are expressed as the mean \pm standard deviation ($n = 3$). An asterisk represents statistical significance ($p < 0.01$, Student's t -test).

and the Ni-bound surface without growth factors. Importantly, the cell numbers after 5 days of culture were approximately 4- and 3-fold greater on the bFGF-His- and bFGF-His/EGF-immobilized surfaces, respectively, than in neurospheres.

Immunofluorescence

Figure 6 contains fluorescent micrographs of cells cultured on bFGF-His- and bFGF-His/EGF-His-immobilized surfaces that were immunologically stained for nestin,

a marker for NPCs, and β -tubulin III, a marker for differentiated neurons. We did not perform immunological staining of cells on the EGF-His-immobilized surface and the surface without growth factor because cell proliferation was limited on these surfaces (section 3.4). Relatively few nestin-expressing progenitor cells were seen on the bFGF-His-immobilized surface, while many β -tubulin III-expressing neurons were observed on this surface (Fig. 6A). The nestin-expressing cells represented $68.7 \pm 8.9\%$ of the total cell population on this type of surface ($n = 6$). In contrast, most cells expressed nestin on the bFGF-His/EGF-His-co-immobilized surface, while only a few cells expressed β -tubulin III (Fig. 6B). The nestin-expressing cells made up $92.2 \pm 2.1\%$ of the total cell population ($n = 4$).

Taken together, the immunofluorescence experiments and the proliferation assays (section 3.4) indicate that among the substrates studied here, co-immobilization of EGF-His and bFGF-His provided the most efficient substrate with respect to the selectivity and the rate of hNPC proliferation.

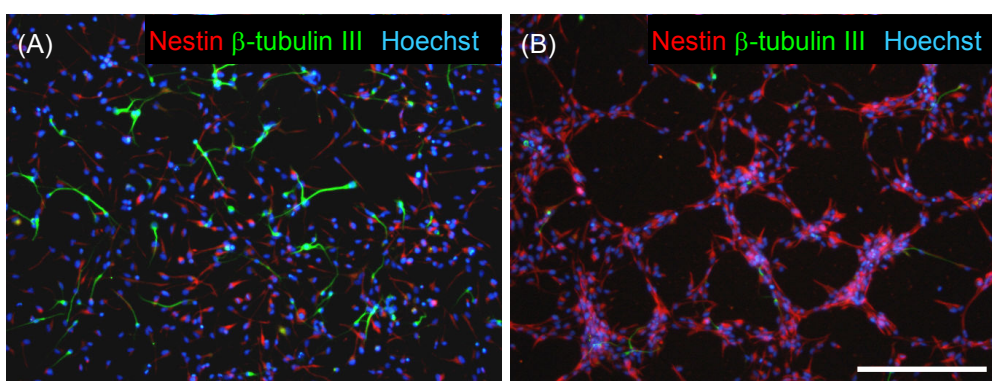


Fig. 6. Fluorescent micrographs of cells cultured for 4 days on substrates immobilized with (A) bFGF-His alone or (B) EGF-His/bFGF-His. Cells were immunofluorescently stained using antibodies against nestin (red) and β -tubulin III (green). Cell nuclei were counterstained with Hoechst dye (blue). Scale bar: 100 μ m.

Subculture of expanded cells

The EGF-His/bFGF-His-co-immobilized substrate was further examined for long-term culture of hNPCs. Cumulative cell numbers were calculated from the fold-increases determined after every passage onto fresh EGF-His/bFGF-His-co-immobilized substrates (Fig. 7). Cell numbers linearly increased during 6 passages of subculture every 4 days. The proliferation rate was almost constant over these 6 passages, with an average doubling time of 74.8 h. In addition, the majority of the expanded cells expressed the neural progenitor cell marker nestin, as assessed by immunofluorescence (data not shown). The cells harvested after 6 passages were further cultured under differentiation conditions; these cells were able to differentiate into three major lineages found in the central nervous system (Fig. 8), neurons, astrocytes, and oligodendrocytes, demonstrating that the cells remained multipotent after 6 passages on EGF-His/bFGF-His-co-immobilized substrates.

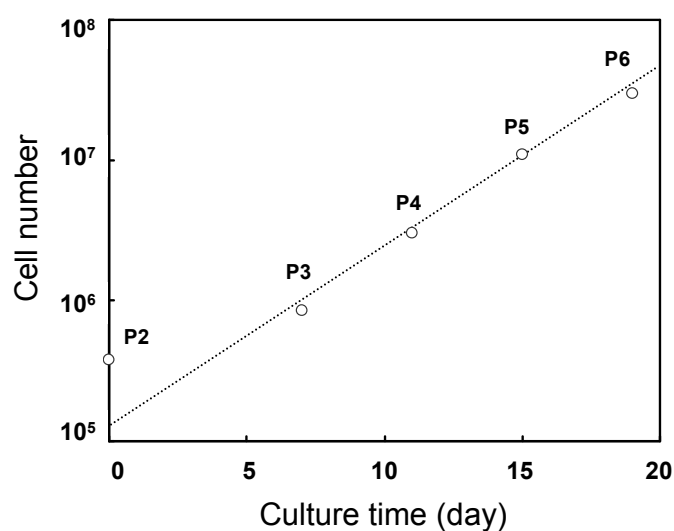


Fig. 7. Long-term culture of hNPCs on substrate with co-immobilized EGF-His/bFGF-His. Cumulative cell numbers are calculated from the fold increase determined for every passage (P).

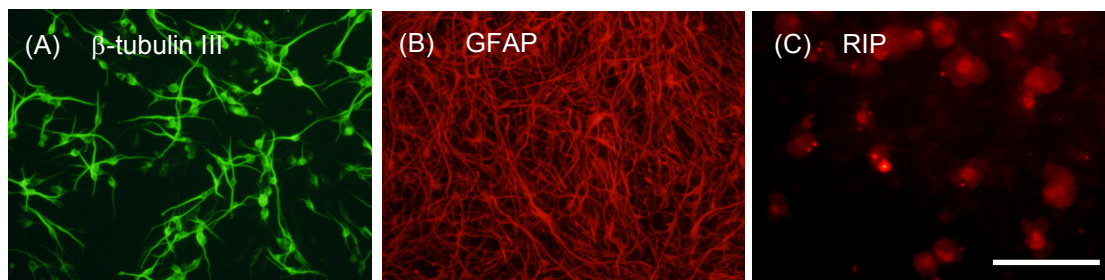


Fig. 8. Fluorescent micrographs of cells immunologically stained using antibodies against (A) β -tubulin III, (B) GFAP, and (C) RIP. hNPCs at passage 6 were subjected to differentiation culture (see Material and Methods). Scale bar: 100 μ m.

3.4 Discussion

The culture substrate with co-immobilized both EGF-His and bFGF-His permitted selective and rapid proliferation of hNPCs. The rate of hNPC proliferation was found to be two times greater on the EGF-His/bFGF-His-immobilized substrate than in standard neurosphere culture. In addition, the percentage of nestin-positive hNPCs (92.2%) was much higher on this substrate than in neurosphere culture (67.5%). hNPCs could be subcultured for at least 6 passages (Fig. 7), retaining their capacity for multipotent differentiation (Fig. 8). Taken together, these observations suggest that an adherent culture on our substrate may be a suitable alternative method for the production of hNPCs.

In an attempt to accelerate the growth of hNPCs, one of the effective strategies may be to selectively culture hNPCs. In the case of neurosphere culture, heterogeneous cell aggregates contain differentiated cells [10] with reduced proliferation potential, as well as neural stem/progenitor cells. Since it appears that the differentiated cells affect the

growth rate of the total population, we speculated that a population containing a higher percentage of hNPCs would grow faster than cells in neurospheres.

A similar hypothesis was supported by our previous investigation of rNSCs [9, 11]. We fabricated a culture substrate with surface-immobilized EGF-His to selectively capture rNSCs expressing EGFR at a high frequency [9]. rNSCs were selectively captured on the EGF-His-immobilized substrate through EGF-EGFR interactions [12]. The captured rNSCs proliferated on the substrate, due to the mitogenic activity of EGF, while retaining their undifferentiated state. As a result, we obtained a population rich in rNSCs (>98%) two times faster than in neurosphere culture [9, 10]. In the case of human neurosphere-forming cells, as in the present study, the pattern of growth factor receptor expression differed from that in the rat neurosphere cells used in our previous study. Here, human neurosphere cells expressed low levels of EGFR but high levels of FGFR1 (Fig. 3). The observed difference in EGFR and FGFR1 expression may have been caused by the isolation of the hNPCs from the 17-19-week-old fetal brain, an earlier stage of neurogenesis than the source of rNSCs isolated from the E16 fetal rat brain. It is likely that the observed pattern of growth factor receptor expression is directly due to differences in cell adhesion to the substrates (Fig. 4). Cell adhesion effectively took place only on the substrates with immobilized bFGF-His (substrates with bFGF alone and EGF-His/bFGF-His), suggesting that cells initially bind to the substrate via bFGF-FGFR1 interactions.

Strikingly, of the substrates studied here, hNPCs were most selectively expanded on the EGF-His/bFGF-His substrate (Figs. 4-6). The selectivity of hNPC proliferation was much higher on this substrate than on the substrate with bFGF-His alone, even though the cells were not expected to effectively interact with immobilized

EGF-His due to the limited expression of EGFR at the time of cell seeding. This finding may contribute to the observations that the activation of FGFR1 by ligand binding promotes the expression of EGFR [13] and that EGFR activation generates signals for maintaining the undifferentiated state of hNPCs [8]. Such a cascade may underlie the requirement for co-immobilized EGF-His on the substrate.

Another important aspect of our substrate is that growth factors are surface-immobilized through chelate linkages between the fixed Ni^{2+} ions and the histidine residues fused to the proteins (Fig. 1). CD spectroscopy (Fig. 2) indicated that anchoring of EGF and bFGF at their C-termini is of great advantage for maintaining the secondary structure of these proteins. We previously observed a similar effect regarding the secondary structure of surface-anchored EGF-His via multiple internal reflection-infrared absorption spectroscopy [14]. This outcome is in marked contrast to that following covalent immobilization of EGF-His onto the substrate surface through standard carbodiimide chemistry, which led to considerable deterioration of the secondary structure of EGF-His [14]. In addition, the stability of chelate linkages under cell culture conditions is important for establishing adherent culture.

References

- [1] Martino G, Pluchino S. The therapeutic potential of neural stem cells. *Nat Rev Neurosci* 2006;7:395–406.
- [2] Kim SU, de Vellis J. Stem cell-based cell therapy in neurological diseases: a review. *J Neurosci Res* 2009;87:2183–200.
- [3] Trounson A, Thakar RG, Lomax G, Gibbons D. Clinical trials for stem cell therapies *BMC Med* 2011;9:52.
- [4] Gage FH. Mammalian neural stem cells. *Science* 2000;287:1433–8.
- [5] Carpenter MK, Cui X, Hu ZY, Jackson J, Sherman S, Seiger A, Wahlberg LU. In vitro expansion of a multipotent population of human neural progenitor cells. *Exp Neurol* 1999;158:265–78.
- [6] Reubinoff BE, Itsykson P, Turetsky T, Pera MF, Reinhartz E, Itzik A, et al. Neural progenitors from human embryonic stem cells. *Nat Biotechnol* 2001;19:1134–40.
- [7] Shofuda T, Fukusumi H, Kanematsu D, Yamamoto A, Yamasaki M, Arita N, et al. A method for efficiently generating neurospheres from human-induced pluripotent stem cells using microsphere arrays. *Neuroreport*. 2013;24:84–90.
- [8] Nelson AD, Suzuki M, Svendsen CN. A high concentration of epidermal growth factor increases the growth and survival of neurogenic radial glial cells within human neurosphere cultures. *Stem Cells* 2008;26:348–55.
- [9] Nakaji-Hirabayashi T, Kato K, Arima Y, Iwata H. Oriented immobilization of epidermal growth factor onto culture substrates for the selective expansion of neural stem cells. *Biomaterials* 2007;28:3517–29.

- [10] Kato K, Sato H, Iwata H. Immobilization of histidine-tagged recombinant proteins onto micropatterned surfaces for cell-based functional assays. *Langmuir* 2005;21:7071–5.
- [11] Ko IK, Kato K, Iwata H. Parallel analysis of multiple surface markers expressed on rat neural stem cells using antibody microarrays. *Biomaterials* 2005;26:4882–91.
- [12] Ciccolini F, Svendsen CN. Fibroblast growth factor 2 (FGF-2) promotes acquisition of epidermal growth factor (EGF) responsiveness in mouse striatal precursor cells: identification of neural precursors responding to both EGF and FGF-2. *J Neurosci* 1998;18:7869–80.
- [13] Nakaji-Hirabayashi T, Kato K, Iwata H. Essential role of structural integrity and firm attachment of surface-anchored epidermal growth factor in adherent culture of neural stem cells. *Biomaterials* 2008;29:4403–8.

Chapter 4

Effect of surface-immobilized extracellular matrices on the proliferation of neural progenitor cells derived from induced pluripotent stem cells

4.1 Introduction

Neural progenitor (NPC) cells have potencies of self-renewal and differentiation to neuronal and glial lineages. They are considered as one of the promising cell sources for the treatment of central nervous system (CNS) disorders such as Parkinson's disease [1], spinal cord injury [2], and traumatic brain injury [3]. NPCs isolated from fetal human brain tissues have been transplanted for the treatment of a patient with Parkinson's disease [4]. However, the limitation of donor cells and ethical concerns make this therapy difficult to be clinically applied.

Embryonic stem (ES) cells and induced pluripotent stem (iPS) cells are other candidates of a cell source for stem cell-based transplantation therapies [5]. These cells can unlimitedly expand *in vitro* and differentiate to multiple types of functional cells. Recently, two clinical trials using human ES-derived cells were started [6, 7]. However, because establishment of an ES cell line requires destruction of human embryos, an ethical problem still remains in the clinical use of human ES cells.

iPS cells might overcome the difficulties mentioned above for brain-derived NPCs and ES cells. Because iPS cells are reprogrammed from somatic cells, there is no

need to destroy human embryos for the establishment of cell lines. Many protocols have been reported for the differentiation of iPS cells into neural cell lineages [8, 9]. It was further demonstrated that differentiated neural cells derived from iPS cells successfully integrated into the animal brain and spinal cord [10, 11]. In addition, autologous iPS cells might be useful for studying mechanisms underlying the progression of CNS disorders and searching effective treatments for these diseases [12]. Most of the applications mentioned above require the culture method that allows to maintain the differentiated state of NPCs. However, current technology is not sufficient to do this, and thus it is highly needed to develop an appropriate culture method.

To optimize extracellular microenvironments surrounding NPCs, in this chapter, protein arrays [13, 14] were fabricated with various extracellular matrices (ECMs) and utilized them to screen using mouse iPS (miPS) cells for the best components to be immobilized onto culture substrates. Our idea is based on the fact that ECMs play pivotal roles in the maintenance of various stem and progenitor cells in native tissues. [15] and behaviors of neural cells [16]. Finally, a candidate ECM was tested as a culture substrate for the expansion of NPCs derived from human iPS (hiPS) cells.

4.2 Materials and methods

Preparation of ECM arrays

ECMs were covalently immobilized onto glass surfaces. First, amine groups were introduced on a glass surface (22 mm × 26 mm) by treating the glass with

aminopropyltriethoxysilane (APTES, Shin-Etsu Chemical Co., Ltd., Tokyo, Japan). The glass plate with amines on the surface was immersed in 10% (v/v) aqueous glutaraldehyde solution for 1 h at room temperature to introduce aldehyde groups. After washing the plate with water, a silicon frame was mounted on the top of glass plate to make a microwell array (5 × 4 wells of 2 mm in diameter). Phosphate buffered saline (PBS) containing 50 µg/mL collagen I (Col-I, Cellmatrix type I, Nitta Gelatin, Inc., Osaka, Japan), collagen IV (Col-IV, Cellmatrix type IV, Nitta Gelatin), gelatin (Gel, Sigma, St. Louis, MO), laminin-1 (LM-1, Invitrogen Corp., Carlsbad, CA), Matrigel (BD Biosciences, San Jose, CA), fibronectin (FN, BD Bioscience), vitronectin (VN, Sigma), and ProNectin F (Sanyo Chemical Industries Ltd., Kyoto Japan) and 2 µg/mL laminin-5 (LM-5, Oriental Yeast Co., Ltd., Tokyo, Japan) were separately pipetted to different spots (approx. 800 µL for each spot) to form through Schiff base between aldehyde and proteins. After 1 h, the glass plate was washed with PBS to remove unbound proteins.

Quantification of immobilized ECMs

ECMs were separately immobilized onto the entire surface of a glass plate (22 × 26 × 0.5 cm³) through the similar chemistry as described above. The surface density of immobilized ECMs was determined using a micro BCA protein assay kit (Pierce Biotechnology, Inc., Rockford, IL). A silicone frame having a square window (inner area: 4 cm²) was placed on the ECM-immobilized surface. The micro BCA reaction mixture (150 µL) was pipetted within the window, and the temperature was kept at 37 °C for 2 h to allow for coloring reaction. The absorbance was measured at 562 nm for

the resultant solution using a spectrophotometer (SpectraMax™ 2Me, Molecular Devices, LLC, Sunnyvale, CA). The amount of immobilized protein was determined using bovine serum albumin (BSA) as a standard.

Mouse iPS cells

Mouse iPS (miPS) cells (20D17) [18] were obtained from Riken cell bank, Ibaraki, Japan and maintained on a feeder layer of mouse embryonic fibroblasts (MEF) in DMEM/F12 containing 15% fetal bovine serum, 0.1 mM MEM non-essential amino acid, 0.1 mM 2-mercaptoethanol, 10 µg/mL leukemia inhibitory factor, 100 U/mL penicillin, and 100 µg/mL streptomycin. For differentiation, miPS cells were dissociated into single cells by treating with 0.05% trypsin solution containing 0.53 mM ethylenediamine-*N,N,N',N'*-tetraacetic acid (EDTA). The cells were cultured on gelatin coated dish for 40 minutes and then unattached miPS cells were collected. For primary aggregate culture, miPS cells were suspended in DMEM/F12 (1:1) containing 2% (v/v) B27 supplement, 5 µg/mL heparin, 100 U/mL penicillin, 100 µg/mL streptomycin, 20 ng/mL EGF, and 20 ng/mL and bFGF 10 nM retinoic acid, and then seeded on a tissue culture dish coated with Pluronic F127 (Sigma) at a density of 8.5×10^3 cells/cm². Every 5–7 days, aggregates were dissociated into single cells by treating with AccuMax (Innovative Cell Technologies, Inc, San Diego, CA) containing 0.05% trypsin, and subcultured to form second aggregates. Dissociation and aggregation were repeated to obtain aggregates at fourth generation.

Array-based assays

Aggregates of miPS cells (7 days after subculture for fourth generation) were dissociated into single cells by treating with AccuMax containing 0.05% trypsin. The cells were suspended in DMEM/F12 (1:1) containing 2% (v/v) B27 supplement, 5 µg/mL heparin, 100 U/mL penicillin, 100 µg/mL streptomycin, 20 ng/mL EGF, and 20 ng/mL bFGF. The cells were seeded to an ECM array at a density of 2.0×10^4 cells/cm² and cultured for 3 days at 37 °C under 5% CO₂ atmosphere.

Human iPS cells

hiPS cells (253G1 [18] and 201B7 [19]) were obtained from Riken cell bank and maintained on a feeder layer of SNL 76/7 cells (ECACC, Salisbury, UK) as previously reported [20]. hiPS cells were differentiated to neural progenitor cells by serum-free floating culture of embryoid body-like aggregates (SFEB) culture method [21]. Undifferentiated hiPS cells were cultured for 3 h in a medium containing 50 µM ROCK inhibitor (Y-27632, Wako, Osaka, Japan). Subsequently, hiPS cells were dissociated into single cells by treating with AccuMax. The cells were suspended in DMEM/F12 containing 2 mM L-glutamine, 5% Knockout-serum replacement (KSR, invitrogen), 10 µM SB 431542 (Wako), and 2 µM dorsomorphin (Wako). The cells were seeded to a round-bottom 96 well plate at a density of 9.0×10^3 cells/well. During first 4 days, 10 µM ROCK inhibitor was added to the culture medium. After 10 days, medium was changed to DMEM/F12 (1:1) containing 2% (v/v) B27 supplement, 100 U/mL penicillin, 100 µg/mL streptomycin, and 10 ng/mL bFGF, and cultured for 5 days. At day 15, cell aggregates were plated on a LM-1/poly-L-ornithine (PLO, Sigma)

coated dish. After 5 days of culture, colonies with neural rosette structure were selected and mechanically collected using pipette. These neural rosette-forming cells were used for the later experiments.

Expansion and differentiation of hNPCs

Neural-rosette forming NPCs were harvested and seeded on LM-1/PLO-coated dishes at a density of 2.0×10^4 cells/cm². For the expansion of hNPCs, cells were cultured in DMEM/F12 (1:1) containing 2% (v/v) B27 supplement, 5 µg/mL heparin, 100 U/mL penicillin, 100 µg/mL streptomycin, 20 ng/mL EGF, and 20 ng/mL bFGF. Cells were subcultured onto LM-1/PLO-coated dishes every 5 days. Cells at passage 4 were subjected to differentiate into dopamine neurons. First, cells were cultured in DMEM/F12 (1:1) containing 2% (v/v) B27 supplement, 100 ng/mL sonic hedgehog (R&D systems. Inc., Minneapolis, MN), 100 ng/mL FGF-8 (Wako) 100 U/mL penicillin, and 100 µg/mL streptomycin on the LM-1/PLO-coated dishes. After 7 days, medium was changed to DMEM/F12 (1:1) containing 2% (v/v) B27 supplement, 10 ng/mL brain derived neurotrophic factor (BDNF, Wako), 10 ng/mL glial cell-derived neurotrophic factor (GDNF, Wako), 1 ng/mL transforming growth factor β3 (TGF-β3, PeproTech, Rocky Hill, NJ), 0.5 mM dibutyryl cyclic AMP (Sigma), 0.2 mM ascorbic acid (Nacalai Tesque, Kyoto, Japan), 100 U/mL penicillin, and 100 µg/mL streptomycin, and cells were further cultured for 14 days.

Immunostaining

Cells were fixed with PBS containing 4% paraformaldehyde and then permeabilized by treating with 0.2% Triton X-100 solution for 15 min at room temperature. Then, the cells were treated with a Blocking One reagent (Nacalai Tesque) for 90 min to block nonspecific adsorption of antibodies, followed by binding of primary antibodies to octamer-binding transcription factor 3/4 (Oct3/4, 1:50, mouse monoclonal, Santa Cruz Biotechnology, Inc., Santa Cruz, CA), stage-specific embryonic antigen-4 (SSEA-4, 1:200, mouse monoclonal, Merck Millipore, Billerica, MA, USA), green fluorescent protein (GFP, 1:1000, chicken polyclonal, Millipore), nestin (1:200, mouse monoclonal, BD Biosciences), β -tubulin III (1:500, rabbit monoclonal, Covance, Princeton, NJ), sex determining region Y-box 1 (Sox1, 1:200, rabbit polyclonal, Cell signaling Technology, Inc., Danvers, MA), glial fibrillary acidic protein (GFAP, 1:200, mouse monoclonal, Millipore), and neuron-glia antigen 2 (NG2, 1:200 mouse monoclonal, Millipore) for 1 h at room temperature. After washing with PBS containing 0.05% Tween 20, cells were treated with Alexa Fluor 594 anti-mouse IgG and Alexa Fluor 488 anti-rabbit IgG Alexa Fluor 488 anti chicken IgG (Invitrogen) at a dilution of 1:500 for 1 h at room temperature and washed with PBS containing 0.05% Tween 20. Then, cell nuclei were counterstained with 1 μ g/mL Hoechst 33258 (Dojindo Laboratories, Kumamoto, Japan). The localization of secondary antibodies was analyzed with a fluorescent microscope (BX51 TRF, Olympus Optical Co., Ltd., Tokyo, Japan). The cells reactive for antibodies to nestin were counted on the merged images with nuclei staining. The original images were recorded at a magnification of $\times 200$, and individual cells were carefully identified on the merged images enlarged with a computer software.

Reverse transcriptase-polymerase chain reaction (RT-PCR)

Total RNA was extracted by SV total RNA Isolation System (Promega Corp., Madison, WI), and then total RNA was reverse-transcribed using Transcriptor First Strand complementary DNA (cDNA) Synthesis Kit (Roche Applied Science, Mannheim, Germany) primed by oligo(dT)₁₈. First-strand cDNA was then amplified by polymerase chain reaction (PCR) using the following specific primers [22]: Tyrosine hydroxylase (TH): sense; 5'-GAG TAC ACC GCC GAG GAG ATT G-3', antisense; 5'-GCG GAT ATA CTG GGT GCA CTG G-3'; Nurr 1: sense; 5'-CTC CCA GAG GGA ACT GCA CTT CG-3', antisense; 5'-CTC TGG AGT TAA GAA ATC GGA GCT G-3'; Lmx1b, sense: 5'-GCA GCG GCT GCA TGG AGA AGA TCG C-3', antisense; 5'-GGT TCT GAA ACC AGA CCT GGA CCA C-3'; glyceraldehyde-3-phosphate dehydrogenase (GAPDH): sense; 5'-ACC ACA GTC CAT GCC ATC AC-3', antisense; 5'-TCC ACC ACC CTG TTG CTG TA-3'. The reaction mixtures (20 μ L) containing 1 μ L cDNA template, 5 unit Takara Ex Taq DNA polymerase (Takara Bio Inc., Shiga, Japan), 1 μ M sense primer, and 1 μ M antisense primer were subjected to PCR under the following thermal cycling conditions: denaturation at 94 °C for 30 s, annealing at 56 °C for 30 s, and extension at 72 °C for 30 s, 30 cycles. RT-PCR products were analyzed by 2% agarose gel electrophoresis with ethidium bromide staining.

Reverse phase high performance liquid chromatography (HPLC)

After washing with PBS containing 0.33 mM Mg²⁺ and 0.9 mM Ca²⁺, cells were incubated for 15 min in 56 mM KCl /Hank's balanced salt solution to induce

depolarization of neurons. The supernatant was then collected and stabilized by adding 0.1 mM EDTA and 0.1 M perchloric acid. The sample solution was analyzed by high-performance liquid chromatography (HPLC) using a TSK-GEL Super-ODS column (100×4.6 mm; TOSOH, Tokyo, Japan) and an EC8020 electrochemical detector (TOSOH). The mobile phase was composed of 0.1 M citrate buffer solution (pH 2.5) containing 0.1 mM EDTA, 5 mM sodium 1-octanesulfonate, and 3% (v/v) methanol. The flow rate of the mobile phase was 1.2 mL/min.

4.3 Results

Immobilization of ECM proteins

Nine kinds of ECM (collagen I (Col-I, Col-IV, GE, LN-1, Matrigel, FN, VN, LN-5, and ProNectin F) were immobilized on the glass surfaces. As shown in Fig. 1, The amount of immobilized ECM determined after extensive washing with PBS was 0.05–0.5 $\mu\text{g}/\text{cm}^2$. The observed low density of LM-5 was probably caused by the fact that we used relatively low concentration of LM-5 solution (2 $\mu\text{g}/\text{mL}$ for LM-5 and 50 $\mu\text{g}/\text{mL}$ for the other proteins).

Induction of miPS cells to neural lineage

miPS cell used in this study expresses green fluorescent protein (GFP) gene driven by Nanog promoter (Fig. 2). miPS cells were maintained on a feeder layer of MEF and differentiated to a neural lineage during floating culture in a serum-free

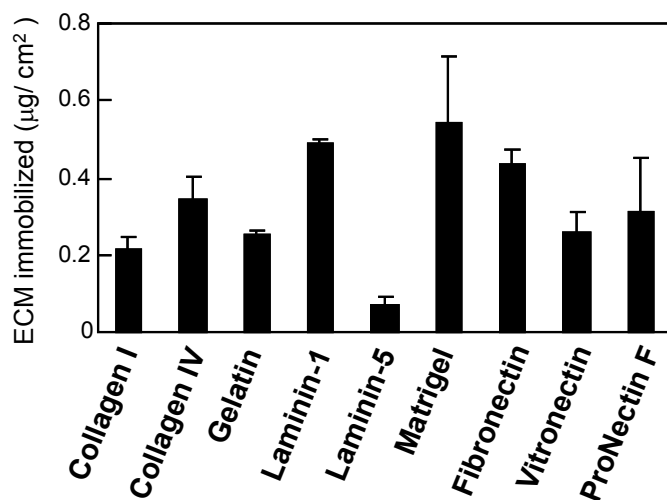


Fig. 1. Quantification of immobilized ECMs.

medium. To differentiate miPS cells to a neural lineage, undifferentiated miPS cells were detached from a feeder cell layer, and cultured as embryoid body-like aggregate in the presence of low concentration of retinoic acid [23]. The details of the experimental protocol for differentiation culture is shown in Fig. 3A. Although GFP expression of cells in aggregates was gradually decreased within 5 days, most of cells still expressed undifferentiated marker Oct 3/4 in primary aggregate culture (Fig. 4A, B). To induce differentiation into NPCs, aggregates were dissociated to single cells and additionally cultured in the presence of retinoic acid. During the formation and dissociation of cell aggregates, the expression of GFP and Oct 3/4 gradually decreased (Fig. 3). On the other hand, the expression of nestin, a marker for NPCs, increased. In contrast to primary aggregates, majority of cells in the forth aggregates expressed nestin and β -tubulin III. During the formation and dissociation of aggregates, the population of NPCs was enriched, and nestin-positive cells reached more than 70% of total cells at the end

of forth aggregate culture (Fig. 4E). The forth aggregates were used for the following array-based assays.

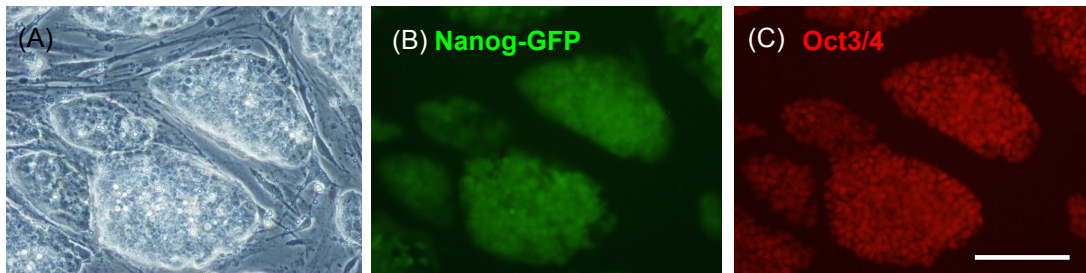


Fig.2. MiPS culture. (A) Phase contrast image of miPS on MEF feeder cell. (B, C) Fluorescent micrographs of cells immunologically stained with antibodies against anti-GFP (B) and anti-Oct 3/4 (C). Scale bar: 100 μ m.

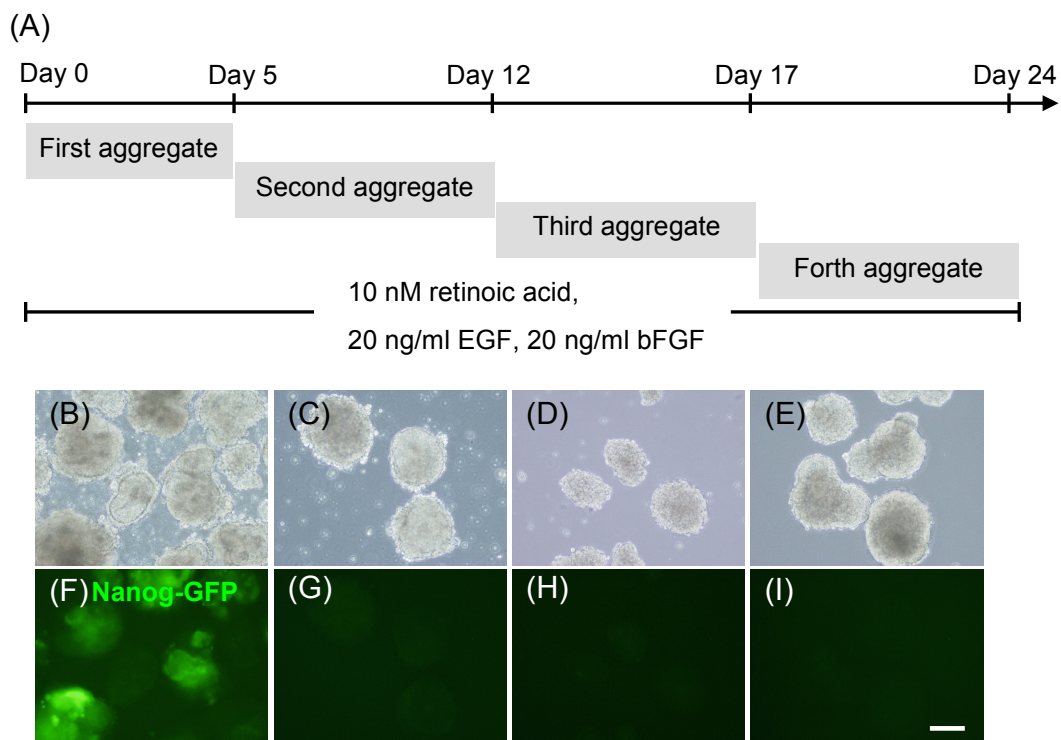


Fig.3. Differentiation of miPS cells into mNPCs. (A) Experimental protocol of differentiation culture. (B – E) Phase contrast images of cell aggregates at Day 5 (B), day 12 (C), day 17 (D), and day 24 (E). (F – H) Fluorescent micrographs of cells at Day 5 (F), day 12 (G), day 17 (H), and day 24 (I). Scale bar: 100 μ m.

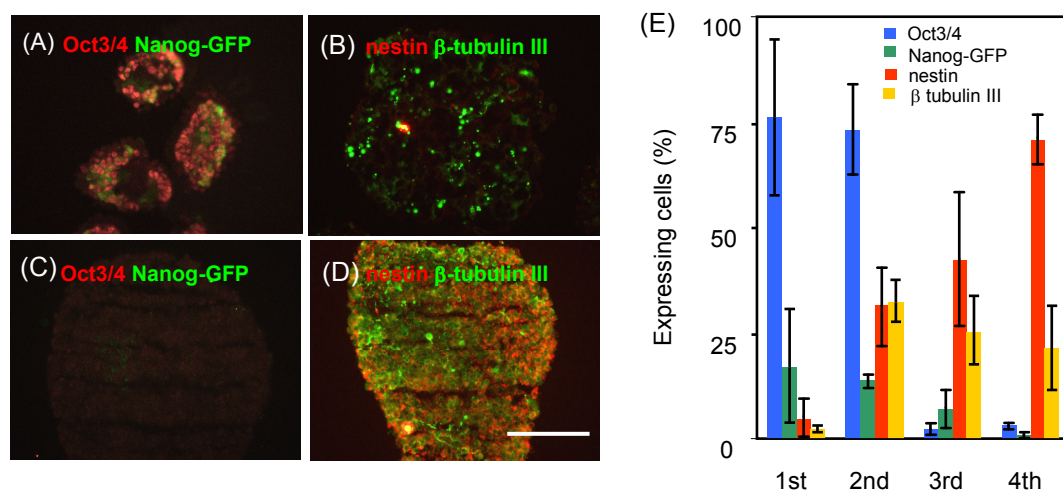


Fig. 4. Differentiation of miPS cells into NPCs. (A, B) Fluorescent micrographs of primary aggregates and (C, D) fourth aggregates. (A, C) Cells were stained for Oct 3/4 and GFP-Nanog, (B, D) nestin and β -tubulin III. Scale bar: 100 μ m. (E) Quantification of Oct 3/4⁺, Nanog⁺, nestin⁺, and β -tubulin III⁺ cells.

Array-based screening of ECMs for NPC expansion

To examine the effects of ECMs on NPC proliferation, fourth aggregates were dissociated into single cells and seeded to an ECM array. Figure 5A shows cell numbers adhering to substrates with different ECMs determined 24 h after cell seeding. As is seen, LM-1, LM-5, FN, and Matrigel were effective for initial cell adhesion, but Col-I, Col-IV, and Gel were ineffective. Figure 6 shows the fluorescent micrograph of cells cultured on an ECM array and then immunologically stained for nestin and β -tubulin III. As can be seen, a majority of cells were positive for nestin but not for β -tubulin III on all of the ECM immobilized. After 3 days of culture, cells expanded ten-fold on most of the ECMs in the presence of EGF and bFGF in a medium. Especially, nestin positive cells effectively proliferated on LM-1, LM-5, and Matrigel (Fig. 5B), yielding a population rich in nestin positive cells (more than 95% of total cells).

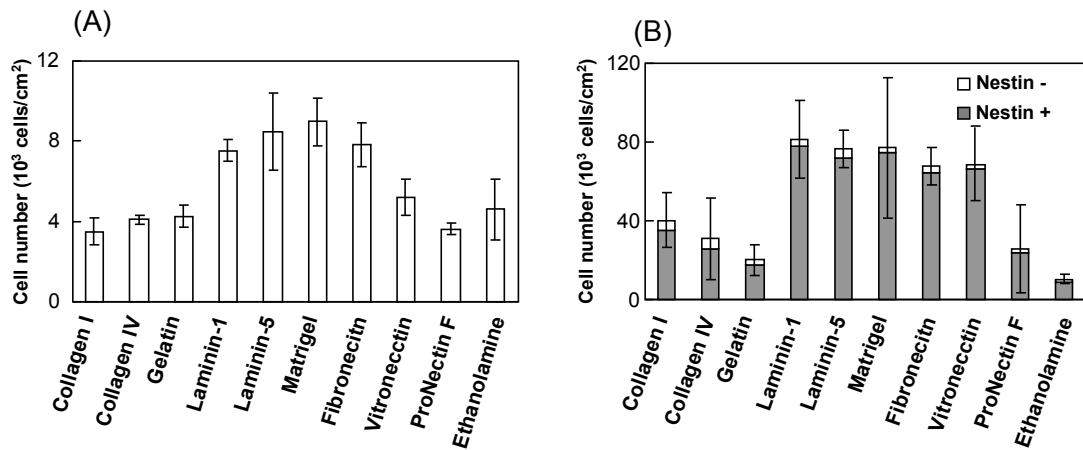


Fig. 5. The number of cells on various ECMs (A) 1 day and (B) 3 days after seeding. Gray and white boxes indicate the fraction of nestin positive and negative cells, respectively.

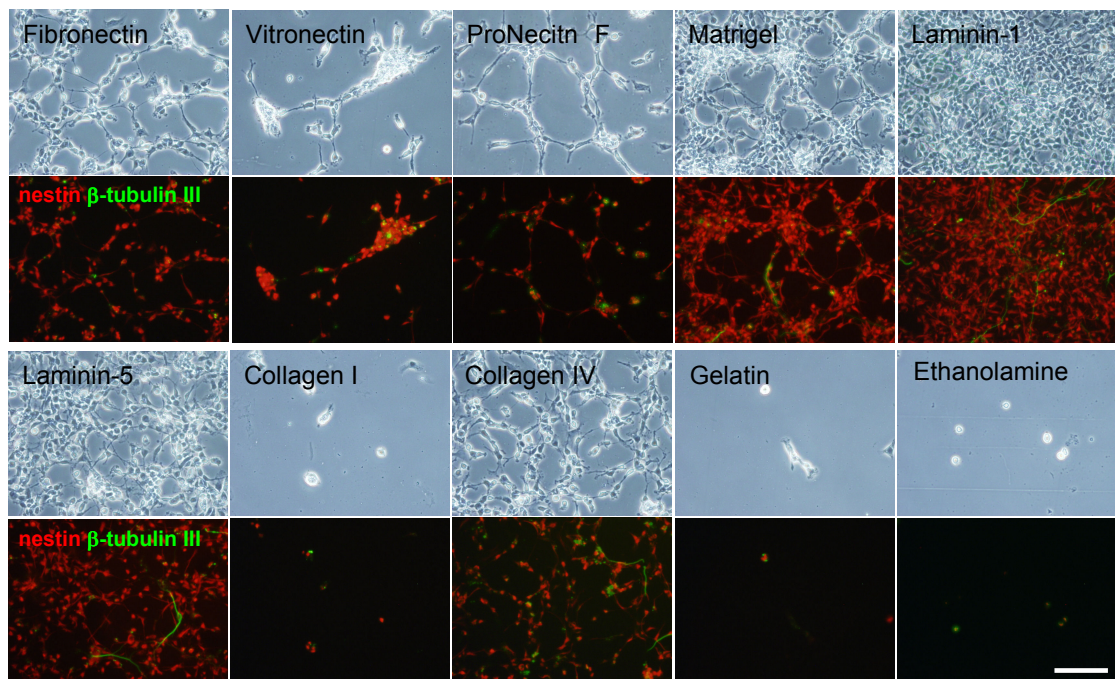


Fig. 6. Effect of various ECMs on NPC proliferation. NPC derived from miPS cells were cultured for 3 days on an array and stained using antibody to nestin (red) and β -tubulin III (green). Scale 100 μ m.

Expansion of hiPS-derived NPC on laminin substrate

Based on the results obtained from the array-based assays, a substrate with immobilized LM-1 was selected as one of the best candidates and tested for the expansion of NPCs derived from hiPS cells. In this case, LM-1 was physically coated to polystyrene tissue culture dish pre-coated with PLO for convenience.

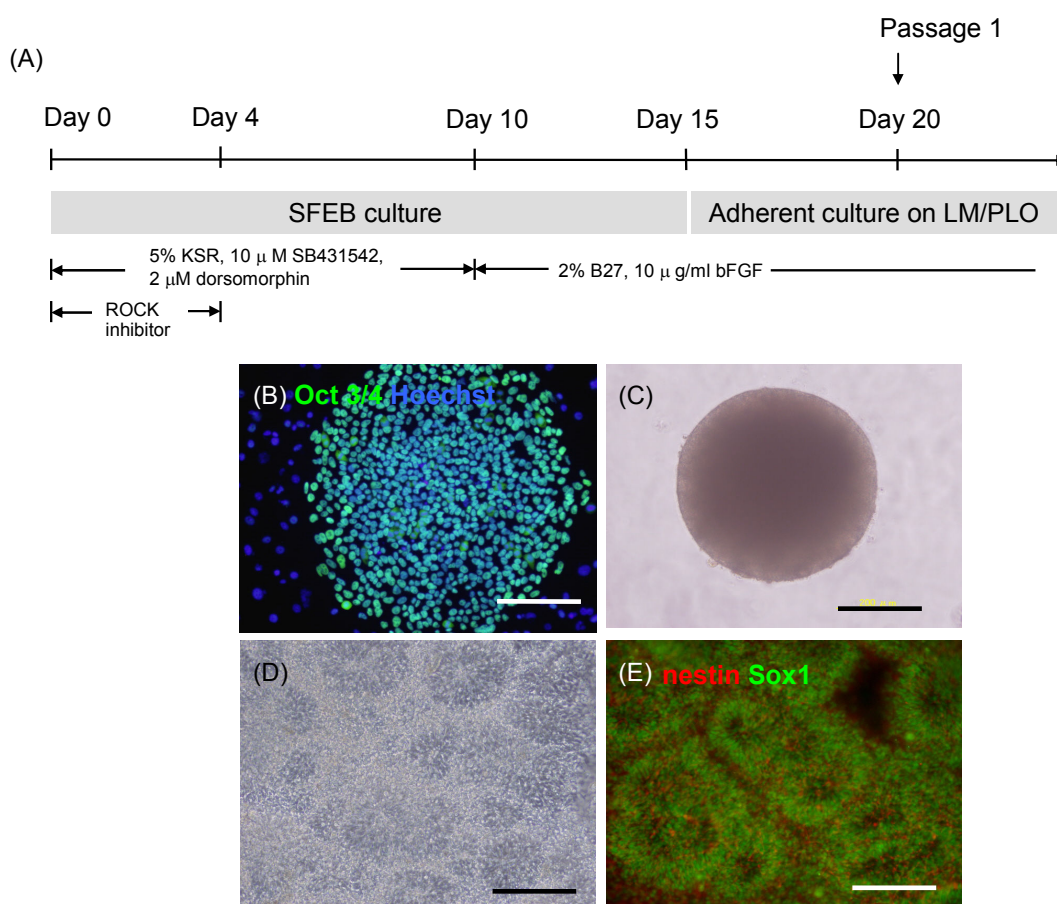


Fig. 7. Differentiation of hiPS cells into NPCs. (A) Experimental protocol of differentiation culture. (B) Fluorescent micrograph of undifferentiated human iPS cells. hiPS cells were maintained on feeder cells and immunologically stained with antibody against Oct 3/4 (green). Cell nuclei were stained by using Hoechst 33258 (blue). (C) Phase contrast image of embryoid body-like aggregate at day 15. (D) Phase contrast image of cells after seeding on LM/PLO. (E) Fluorescent micrographs of neural rosette forming cells. Cells were immunologically stained with antibody against nestin (red) and Sox 1 (green). Scale bar: 200 μ m.

hiPS cells were differentiated to NPCs by dual-SMAD inhibition (Fig. 7A) [24]. First, hiPS cells were cultured as floating aggregates to induce neural differentiation in a serum-free medium for 15 days (Fig. 7B, C). Then, the aggregates were seeded to a LM-1/PLO dish and cultured for 5 days. At day 20, neural-rosette structures were observed (Fig. 7D). This structure is typical for rosette-type NPCs derived from embryonic stem (ES) cells and iPS cells [25]. The rosette-forming cells expressed NPC markers such as nestin and Sox1 (Fig. 7E).

Then, neural-rosette forming cells were collected and seeded to the LM-1/PLO substrate. Figure 8A shows the phase contrast image of cells culture on the LM/PLO substrate. It is seen that NPCs derived from hiPS cells adhered well on the LM-1/PLO substrate and expanded on this substrate while expressing nestin and Sox1 (Fig. 8B). Although some of the cells expressed β -tubulin III (Fig. 8C), Oct 3/4 and SSEA-4 positive cells were not observed. It was observed that, after six times of subculture, the proliferation rate of NPCs did not decrease and that most of cells still expressed nestin.

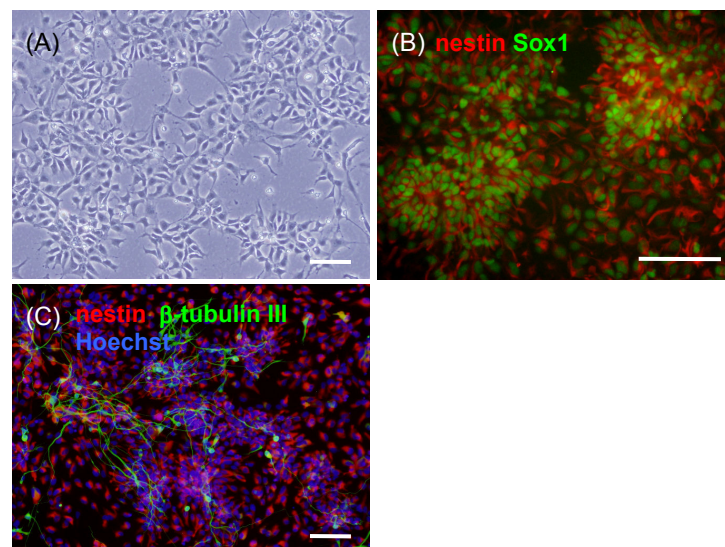


Fig. 8. Expansion of hiPS-derived NPCs on a substrate with LM-1. (A) Phase contrast images of cells cultured for 3 days. (B, C) Fluorescent micrograph of cells stained for (B) nestin (red) and Sox1 (green), (C) nestin (red), β -tubulin III (green), and cell nuclei (blue). Scale bar: 100 μ m.

In addition, NPCs could be cryopreserved by using a commercially-available serum-free freezing medium and recovered after thawing. Furthermore, expanded NPCs could be differentiated to neurons, astrocytes, and oligodendrocytes under the appropriate conditions.

Differentiation of hNPC into dopamine neurons

Expanded hNPCs at passage 4 were subjected to differentiation culture for inducing dopamine neurons. Figure 9A shows the fluorescent micrograph of cells cultured after 28 days and then immunologically stained for β -tubulin III and TH. As can be seen, expanded NPCs could be effectively differentiated to TH positive-cells. RT-PCR analysis showed that differentiated cells also expressed other marker genes of dopamine neurons such as Nurr1 and Lmx1b (Fig. 9B). Furthermore, dopamine released from the differentiated cells could be detected by HPLC (Fig 9C).

4.4 Discussion

Many protocols have been reported for the induction of NPCs from ES and iPS cells [24–26]. However, effective methods have not been established for the expansion and maintenance of NPCs derived from ES and iPS. Such methods are absolutely important for instantly supplying transplantable NPCs for clinical applications. Array-based assay showed that substrates with immobilized LM-1, LM-5, and Matrigel are effective for the expansion and maintenance of NPCs derived from miPS cells. Among these candidates, a substrate with LM-1 was tested using hiPS cells and finally found

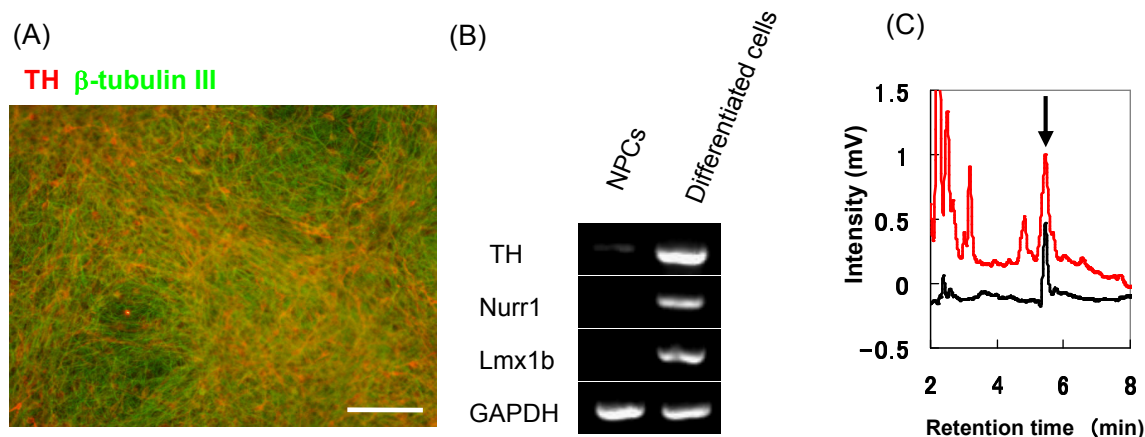


Fig. 9. Differentiation of expanded hNPC into dopamine neurons. (A) Fluorescent micrograph of cells immunologically stained using antibody to TH (red) and β -tubulin III (green). Scale bar: 100 μ m. (B) The results of RT-PCR analysis for NPCs and differentiated cells derived from hiPS cells. (C) The result of HPLC analyses of dopamine released from differentiated cells. Cells were treated with 56 mM potassiumchloride/Hanks' balanced salt solution for 15 min (red line). The black line shows the dopamine standard. Arrow indicates a peak of dopamine.

that this substrate is effective for the expansion and maintenance of NPCs induced from hiPS cells. Furthermore, these expanded hNPC could be efficiently differentiated to functional dopamine neurons.

To date, various research groups have studied different types of ECMs such as Matrigel [27], gelatin [28], fibronectin [29], and laminin [30] as a culture substrate for NPCs. In the present study, 9 different EMCs were systematically examined using array-based method. Array-based assay enables a high-throughput screening of materials such as proteins, DNAs, and synthetic polymers [31]. MmiPS cells differentiated most efficiently into a neural lineage on a substrate with LM-1, LM-5, or Matrigel. In contrast, adhesion of mouse NPCs was poor on the substrates with Col-I, Col-IV, or Gel. The observed difference between EMCs might be due to dissimilarity in

the expression of integrins. It is reported that neural stem cells derived from fetal brain tissue express integrin $\beta 1$, $\alpha 3$, $\alpha 6$, and $\alpha 7$, and integrin complexes specific for laminin such as $\alpha 3\beta 1$, $\alpha 6\beta 1$, and $\alpha 7\beta 1$ [32, 33].

Substrates for stem cell culture have been extensively studied [34-36] especially for the large-scale expansion of ES and iPS cells. In these cases, ECM proteins [34], synthetic polymers [35], and short peptides [36] were used for the preparation of culture substrates. From the clinical point of view, one of the most important aspects of such functional substrates is the requirements for xeno-free conditions, chemically-defined systems, and low-cost production. For these reasons, it is worth studying further for laminin-derived small domains or short peptides that can replace full-length LM-1 as used in this study.

References

- [1] Dyson SC, Barker RA. Cell-based therapies for Parkinson's disease. *Expert Rev Neurother* 2011;11:831–44.
- [2] Tetzlaff W, Okon EB, Karimi-Abdolrezaee S, Hill CE, Sparling JS, Plemel JR, et al. A Systematic Review of Cellular Transplantation Therapies for Spinal Cord Injury. *J Neurotrauma* 2011;28:1611–82.
- [3] Gögel S, Gubernator M, Minger SL. Progress and prospects: stem cells and neurological diseases. *Gene Ther* 2011;18:1–6.
- [4] Freed CR, Greene PE, Breeze RE, Tsai WY, DuMouchel W, Kao R, et al. Transplantation of embryonic dopamine neurons for severe Parkinson's disease. *N Engl J Med* 2001;344:710–9.
- [5] Robinton DA, Daley GQ. The promise of induced pluripotent stem cells in research and therapy. *Nature* 2012;481:295–305.
- [6] Solbakk JH, Zoloth L. The tragedy of translation: the case of "first use" in human embryonic stem cell research. *Cell Stem Cell* 2011;8:479–81.
- [7] Schwartz SD, Hubschman JP, Heilwell G, Franco-Cardenas V, Pan CK, Ostrick RM, et al. Embryonic stem cell trials for macular degeneration: a preliminary report. *Lancet* 2012;379:713–20.
- [8] Czepiel M, Balasubramanian V, Schaafsma W, Stancic M, Mikkers H, Huisman C, et al. Differentiation of induced pluripotent stem cells into functional oligodendrocytes. *Glia* 2011;59:882–92.

- [9] Kriks S, Shim JW, Piao J, Ganat YM, Wakeman DR, Xie Z, et al. Dopamine neurons derived from human ES cells efficiently engraft in animal models of Parkinson's disease. *Nature* 2011;480:547–51.
- [10] Nori S, Okada Y, Yasuda A, Tsuji O, Takahashi Y, Kobayashi Y, et al. Grafted human-induced pluripotent stem-cell-derived neurospheres promote motor functional recovery after spinal cord injury in mice. *Proc Natl Acad Sci* 2011;108:16825–30.
- [11] Rhee YH, Ko JY, Chang MY, Yi SH, Kim D, Kim CH, et al. Protein-based human iPS cells efficiently generate functional dopamine neurons and can treat a rat model of Parkinson disease. *J Clin Invest* 2011;121:2326–35.
- [12] Bellin M, Marchetto MC, Gage FH, Mummery CL. Induced pluripotent stem cells: the new patient? *Nat Rev Mol Cell Biol.* 2012;13:713–26.
- [13] Nakajima M, Ishimuro T, Kato K, Ko IK, Hirata I, Arima Y, et al. Combinatorial protein display for the cell-based screening of biomaterials that direct neural stem cell differentiation. *Biomaterials* 2007;28:1048–60.
- [14] Soen Y, Mori A, Palmer TD, Brown PO. Exploring the regulation of human neural precursor cell differentiation using arrays of signaling microenvironments. *Mol Syst Biol.* 2006;2:37.
- [15] Kim SH, Turnbull J, Guimond S. Extracellular matrix and cell signalling: the dynamic cooperation of integrin, proteoglycan and growth factor receptor. *J Endocrinol* 2011;209:139–51.
- [16] Wojcik-Stanaszek L, Gregor A, Zalewska T. Regulation of neurogenesis by extracellular matrix and integrins. *Acta Neurobiol Exp* 2011;71:103–12.

- [17] Okita K, Ichisaka T, Yamanaka S, Generation of germline-competent induced pluripotent stem cells. *Nature* 2007;448:313–7.
- [18] Takahashi K, Tanabe K, Ohnuki M, Narita M, Ichisaka T, Tomoda K, et al, Induction of pluripotent stem cells from adult human fibroblasts by defined factors. *Cell* 2007;131:861–72.
- [19] Nakagawa M, Koyanagi M, Tanabe K, Takahashi K, Ichisaka T, Aoi T, et al. Generation of induced pluripotent stem cells without Myc from mouse and human fibroblasts. *Nature Biotechnonology* 2008;26:101–6.
- [20] Nishigaki T, Teramura Y, Nasu A, Takada K, Toguchida J, Iwata H. Highly efficient cryopreservation of human induced pluripotent stem cells using a dimethyl sulfoxide-free solution. *Int J Dev Biol* 2011;55:305–11.
- [21] Watanabe K, Kamiya D, Nishiyama A, Katayama T, Nozaki S, Kawasaki H, et al. Directed differentiation of telencephalic precursors from embryonic stem cells. *Nat Neurosci* 2005;8:288–96.
- [22] Ando T, Yamazoe H, Moriyasu K, Ueda Y, Iwata H. Induction of dopamine-releasing cells from primate embryonic stem cells enclosed in agarose microcapsules. *Tissue Eng* 2007;13:2539–47.
- [23] Okada Y, Matsumoto A, Shimazaki T, Enoki R, Koizumi A, Ishii S, et al. Spatiotemporal Recapitulation of Central Nervous System Development by Murine Embryonic Stem Cell-Derived Neural Stem/Progenitor. *Cells Stem Cells* 2008;26:3086–98.
- [24] Chambers SM, Fasano CA, Papapetrou EP, Tomishima M, Sadelain M, Studer L. Highly efficient neural conversion of human ES and iPS cells by dual inhibition of SMAD signaling. *Nat Biotechnol.* 2009;27:275–80.

- [25] Elkabetz Y, Panagiotakos G, Al Shamy G, Socci ND, Tabar V, Studer L. Human ES cell-derived neural rosettes reveal a functionally distinct early neural stem cell stage. *Genes Dev.* 2008 Jan 15;22:152–65.
- [26] Cai C, Grabel L. Directing the differentiation of embryonic stem cells to neural stem cells. *Dev Dyn.* 2007;236:3255–66.
- [27] Colleoni S, Galli C, Giannelli SG, Armentero MT, Blandini F, Broccoli V, et al. Long-term culture and differentiation of CNS precursors derived from anterior human neural rosettes following exposure to ventralizing factors. *Exp Cell Res* 2010;316:1148–58.
- [28] Axell MZ, Zlateva S, Curtis M. A method for rapid derivation and propagation of neural progenitors from human embryonic stem cells. *J Neurosci Methods* 2009;184:275–84.
- [29] Hong S, Kang UJ, Isacson O, Kim KS. Neural precursors derived from human embryonic stem cells maintain long-term proliferation without losing the potential to differentiate into all three neural lineages, including dopaminergic neurons. *J Neurochem* 2008;104:316–24.
- [30] Koch P, Opitz T, Steinbeck JA, Ladewig J, Brüstle O. A rosette-type, self-renewing human ES cell-derived neural stem cell with potential for in vitro instruction and synaptic integration. *Proc Natl Acad Sci* 2009;106:3225–30.
- [31] Underhill GH, Bhatia SN. High-throughput analysis of signals regulating stem cell fate and function. *Curr Opin Chem Biol* 2007;11:357–66.
- [32] Prowse AB, Chong F, Gray PP, Munro TP. Stem cell integrins: implications for ex-vivo culture and cellular therapies. *Stem Cell Res* 2011;6:1–12.
- [33] Barczyk M, Carracedo S, Gullberg D. Integrins. *Cell Tissue Res* 2010;339:269–80.

- [34] Rodin S, Domogatskaya A, Ström S, Hansson EM, Chien KR, Inzunza J, et al. Long-term self-renewal of human pluripotent stem cells on human recombinant laminin-511. *Nat Biotechnol* 2010;28:611–5.
- [35] Melkounian Z, Weber JL, Weber DM, Fadeev AG, Zhou Y, Dolley-Sonneville P, et al. Synthetic peptide-acrylate surfaces for long-term self-renewal and cardiomyocyte differentiation of human embryonic stem cells. *Nat Biotechnol* 2010;28:606–10.
- [36] Villa-Diaz LG, Nandivada H, Ding J, Nogueira-de-Souza NC, Krebsbach PH, O'Shea KS, et al. Synthetic polymer coatings for long-term growth of human embryonic stem cells. *Nat Biotechnol* 2010;28:581–3.

Chapter 5

Induction of dopamine neurons from human induced pluripotent stem cells in agarose microbeads

5.1. Introduction

Parkinson's disease (PD) is a neurodegenerative disease mainly caused by selective loss of dopamine (DA) neurons in the substantia nigra [1]. L-3,4-dihydroxyphenylalaninedopa and DA receptor agonists have been administered to patients in pharmaceutical treatments of PD [2-4]. Unfortunately, these treatments cannot always be implemented for long periods due to their side effects, such as dyskinesia; the efficacy of these treatments gradually decreases. In recent years, cell replacement therapy has been considered as an alternative method to treat PD. Brain tissues from aborted fetuses have been transplanted into PD patients. Methods for engrafting DA neurons and the associated physiological recoveries have differed between reports [5-7], possibly due to immature DA neurons in the fetal brain tissue or to an insufficient number of DA neurons in the graft. In addition, the shortage of donors and ethical concerns make it difficult to accept cell replacement therapy as the normal course of treatment for PD.

Pluripotent stem cells, such as embryonic stem (ES) cells and induced pluripotent stem (iPS) cells, have been regarded as new sources for cell transplantation therapy [8, 9]. The cells can expand in number without limit under the undifferentiated

condition, and can be differentiated into multiple cell types. Differentiation protocols to turn pluripotent cells into DA neurons have been reported [10-12]; differentiated DA neurons from ES cells and iPS cells were previously transplanted into PD model animals to demonstrate the efficacy of these cells in the treatment of PD [10-12].

Although DA neurons derived from pluripotent stem cells are considered to have utility in human PD patients, various difficulties still remain to be overcome. First, tumor formation must be carefully considered in cell transplantation therapy using iPS-derived cells [13,14]. Undifferentiated pluripotent stem cells and neural progenitors contained in transplants may proliferate and overgrow in the host brain [15]. It has been claimed that the risk of tumor formation can be reduced by maturing cells for a long period *in vitro* before transplantation [16, 17]. Second, graft rejection by the host immune system is unavoidable in transplantation therapy and should be carefully controlled. When DA neurons derived from ES cells are used, the graft is expected to be recognized as allogeneic tissue and thus will be rejected by the host immune system [18, 19]. Even when iPS cells are derived from a patient, the reprogramming protocols may affect the immunogenicity of the grafts [20, 21]. In addition, approximately 100 iPS cell lines with HLA homozygotes [22] are planning to be established and banked; due to economic reasons, these cells will be used as sources for cell preparations for patient treatments. Third, although a small number of DA neurons is sufficient to demonstrate the efficacy of cell replacement therapy in PD model mice and cynomolgus monkeys, a large number of cells is needed to treat human PD patients. Sufficient numbers of matured DA neurons are not usually collected from cells adhered on dishes, because matured neurons are very fragile and are easily damaged by mechanical and enzymatic stress. Fourth, when a patient will be treated by transplantation, sufficient amounts of

DA neurons should be supplied in a timely fashion, requiring a method of preservation for DA neurons.

It was reported that microencapsulated islets of Langerhans effectively protects the cells from rejection in the transplantation model and from mechanical stress [23, 24]. In this chapter, the utility of this cell encapsulation technique was examined for overcoming the abovementioned difficulties with applying DA neurons to PD patients.

5.2. Materials and methods

Human iPS cell culture and differentiation to dopamine neuron

Two lines of hiPS cells (201B7 [25] and 253G1 [26], RIKEN Cell Bank, Ibaraki, Japan) were used in this study. Undifferentiated hiPS cells were maintained on SNL 76/7 cells (ECACC, Salisbury, UK) as a feeder layer, as previously described [27]. hiPS cells were differentiated into DA-releasing cells via a previously reported method [10]. Details of the differentiation culture are shown in Scheme 1. Undifferentiated hiPS cells were seeded on Matrigel (BD Bioscience, San Jose, CA, USA)-coated cell culture dishes. Cells were cultured in DMEM/F12 medium (Invitrogen, Carlsbad, CA, USA) supplemented with 2.5 mM GlutaMax, 15% KnockOut Serum Replacement (Invitrogen), and 0.1 mM 2-mercaptoethanol (Nacalai Tesque, Inc., Kyoto, Japan) at 37 °C under 5% CO₂. Ten micromolar SB 431542 (Wako Pure Chemical Industries, Osaka, Japan.), 100 nM LDN193189 (Wako), 3 μM CHIR99021 (Wako), 100 ng/mL sonic hedgehog N-terminus (R&D Systems, Minneapolis, MN, USA), 2 mM pumorphamine (Wako), and 100 ng/mL fibroblast growth factor-8 (Wako) were added to culture

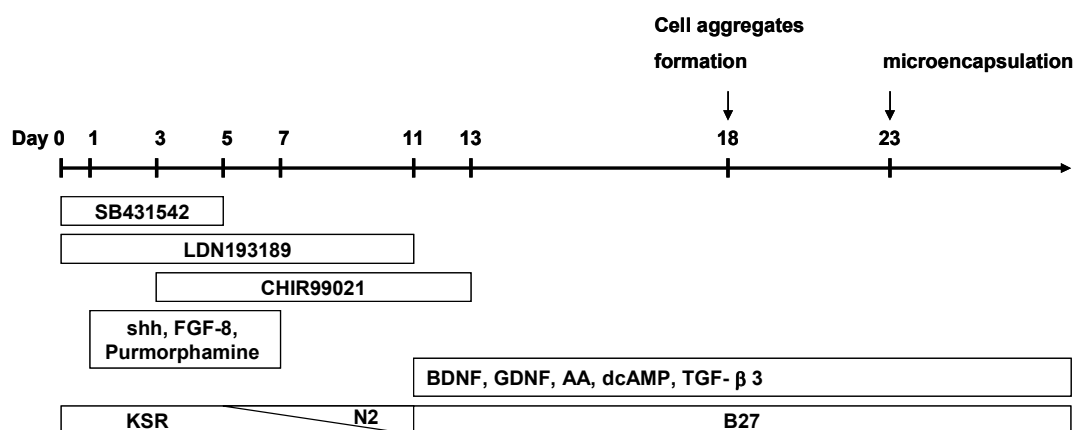
medium in a time-dependent fashion. KnockOut Serum Replacement was gradually shifted to N2 supplement (Invitrogen) from day 5 to day 11. On day 11, the culture medium was changed to DMEM/F12 supplemented with 2.5 mM GlutaMax, 2% B27 supplement (Invitrogen), 10 ng/mL brain-derived neurotrophic factor (BDNF, Wako), 10 ng/mL glial cell line-derived neurotrophic factor (GDNF, Wako), 0.2 mM ascorbic acid (Nacalai Tesque), 0.5 mM dibutyryl cyclic AMP (dcAMP, Nacalai Tesque), 1 ng/mL transforming growth factor β 3 (TGF- β 3, R&D Systems), 100 U/mL penicillin, and 100 μ g/mL streptomycin. The cells were cultured for an additional week for the maturation of neuronal cells. On day 18, subpopulations of the cells were used for the following experiments. The remaining cells were subcultured on a laminin/poly-L-ornithine (LM/PLO)-coated dish for further maturation.

Formation of cell aggregates

On day 18, cells were detached from culture dishes by treatment with Accumax (Innovative Cell Technologies, Inc., San Diego, CA, USA) for 3 min. Cells were suspended in DMEM/F12 containing 2.5 mM GlutaMax, 2% B27 supplement, 10 ng/mL BDNF, 10 ng/mL GDNF, 0.2 mM ascorbic acid, 0.5 mM dcAMP, 1 ng/mL TGF- β 3, 100 U/mL penicillin, and 100 μ g/mL streptomycin. U-bottom 96-well plates were pre-coated with 2% pluronic F127 overnight to inhibit cell adhesion. After washing with PBS five times, the cells were seeded into the wells at a density of 6000 cells/well and centrifuged at 1000 rpm for 3 min. The cells were cultured in an incubator at 37 °C in a 5% CO₂ atmosphere for 5 days to induce the formation of cell aggregates.

Agarose microencapsulation

Cell aggregates were enclosed in agarose microbeads as previously reported [23]. Briefly, approximately 2000 cell aggregates were mixed with 3 mL of 5% agarose (Taiyo Agarose, AG LT-600, Shimizu Shokuhin KK, Shizuoka, Japan)/PBS at 40 °C in a glass centrifuge tube. Then, 15 mL of liquid paraffin (Nacali Tesque) at 40 °C were added to the centrifuge tube. The tube was shaken on ice to form small droplets of the agarose solution and to induce gelation. The microbead suspension was centrifuged at 2000 rpm for 5 min, and the liquid paraffin was removed. The suspension was washed twice with PBS, and the microbeads containing cell aggregates were selected under a microscope. Encapsulated cells were cultured in DMEM/F12 containing 2.5 mM GlutaMax, 2% B27 supplement, 10 ng/mL BDNF, 10 ng/mL GDNF, 0.2 mM ascorbic acid, 0.5 mM dcAMP, 1 ng/mL TGF- β 3, 100 U/mL penicillin, and 100 μ g/mL streptomycin. Culture medium was replaced with fresh medium every three days.



Scheme 1. Experimental protocol. hiPS cells were differentiated into DA neurons in culture medium supplemented with several inhibitors and cytokines. Cells were collected from the dish and applied to U-bottom 96-well plates that were pretreated with pluronic F127 at a density of 6000 cells/well to form cell aggregates on day 18. The cell aggregates were encapsulated in agarose microbeads on day 23.

DA secretion and high-performance liquid chromatography (HPLC)

Microencapsulated cell aggregates (1200) were washed twice with PBS supplemented with 0.33 mM Mg²⁺ and 0.9 mM Ca²⁺. The cells were incubated for 30 min in 56 mM KCl/ Hanks' balanced salt solution (HBSS) supplemented with 0.33 mM Mg²⁺ and 0.9 mM Ca²⁺ to induce depolarization of cells. The supernatant was collected, and 0.1 mM ethylenediamine- N,N,N',N'-tetraacetic acid (EDTA) and 0.1 M perchloric acid were added to the supernatant to inhibit DA degradation. Non-encapsulated cell aggregates cultured on LM/PLO were used as a control.

A TSK-GEL Super-ODS column (100×4.6 mm; TOSOH, Tokyo, Japan) and an EC8020 electrochemical detector (TOSOH) were used for HPLC of the supernatant. The mobile phase was composed of 0.1 M citrate buffer solution (pH 2.5), 0.1 mM EDTA, 5 mM sodium 1-octanesulfonate, and 3% (v/v) methanol. The flow rate of the mobile phase was 1.2 mL/min.

Immunofluorescence

Antibodies against Oct3/4 (1:50, mouse monoclonal, Santa Cruz Biotechnology, Inc., Santa Cruz, CA, USA), SSEA-4 (1:200, mouse monoclonal, Merck Millipore, Billerica, MA, USA), β-tubulin III (1:500, rabbit monoclonal, Covance, Princeton, NJ, USA), tyrosine hydroxylase (TH, 1:200, mouse monoclonal, Millipore, and 1:200, mouse monoclonal, Covance), and GFAP (1:200, mouse monoclonal, Millipore) were used for immunohistochemistry. Cells were fixed with 4% paraformaldehyde in PBS for 1 h at 4 °C, and then sequentially soaked in 5%, 10%, and 20% sucrose in PBS for 12 h

at 4 °C. The cells were embedded in Tissue-Tek (Sakura Finetechnical Co. Ltd., Tokyo, Japan) and frozen. Frozen specimens of 10 µm thickness were prepared.

The specimens were treated with 0.2% Triton X-100 solution for 15 min at room temperature to permeabilize the cells, and were treated with Blocking One Reagent (Nacalai Tesque) for 90 min to block nonspecific adsorption of antibodies. Antibody solutions were applied to the specimens and incubated for 1 h at room temperature. After washing with PBS containing 0.05% Tween 20, the specimens were treated with Alexa Fluor 594 anti-mouse IgG and Alexa Fluor 488 anti-rabbit IgG (Invitrogen) at a dilution of 1:500 for 1 h at room temperature, then washed with PBS containing 0.05% Tween 20. The cell nuclei were counterstained with 1 µg/mL Hoechst 33258 (Dojindo Laboratories, Kumamoto, Japan). The localization of secondary antibodies was analyzed with a fluorescent microscope (BX51 TRF, Olympus Optical Co., Ltd., Tokyo, Japan). To determine the ratio of TH-positive cells, cells were carefully identified on merged images enlarged with computer software. Cells were counted at three sites on the same sample, and these data were averaged.

Reverse transcription polymerase chain reaction (RT-PCR)

On days 25, 40, and 68 of culture, encapsulated cells were collected into a centrifuge tube and washed with cold PBS. The microcapsules were homogenized on ice with a sonicator (VP-30S, Titec, Saitama, Japan). Total RNA was extracted with the SV Total RNA Isolation System (Promega Corp., Madison, WI, USA). First-strand cDNA was prepared from the RNA by reverse transcription using the Transcriptor First Strand cDNA Synthesis Kit (Roche Applied Science, Mannheim, Germany) primed by

oligo(dT)₁₈. cDNA was then amplified by PCR using the following specific primers [29]: Oct 3/4, 5'-ATT CAG CCA AAC GAC CAT CT-3' and 5'-ACA CTC GGA CCA CAT CCT TC-3'; Nanog, 5'-AGC ATC CGA CTG TAA AGA ATC TTC AC-3' and 5'-CGG CCA GTT GTT TTT CTG CCA CCT-3'; E-cadherin, 5'-CGA CCC AAC CCA AGA ATC TA-3' and 5'-AGG CTG TGC CTT CCT ACA GA-3'; tubulin β III, 5'-ACC TCA ACC ACC TGG TAT CG-3' and 5'-TGC TGT TCT TGC TCT GGA TG-3'; TH, 5'-GAG TAC ACC GCC GAG GAG ATT G-3' and 5'-GCG GAT ATA CTG GGT GCA CTG G-3'; Nurr1, 5'-CTC CCA GAG GGA ACT GCA CTT CG-3' and 5'-CTC TGG AGT TAA GAA ATC GGA GCT G-3'; Lmx1b, 5'-GCA GCG GCT GCA TGG AGA AGA TCG C-3' and 5'-GGT TCT GAA ACC AGA CCT GGA CCA C-3'; glyceraldehyde 3-phosphate dehydrogenase, 5'-ACC ACA GTC CAT GCC ATC AC-3' and 5'-TCC ACC ACC CTG TTG CTG TA-3'. The reaction mixtures (20 μ L) containing 1 μ L cDNA template, 5U Takara Ex Taq DNA polymerase (Takara Bio Inc., Shiga, Japan), 1 μ M sense primer, and 1 μ M antisense primer were subjected to PCR under the following thermal cycling conditions: denaturation at 94 °C for 30 s, annealing at 56 °C for 30 s, and extension at 72 °C for 30 s. PCR products were analyzed by 2% agarose gel electrophoresis with ethidium bromide staining.

Collection of cell aggregates from microbeads and adherent culture

Agarose microbeads were mechanically disrupted with a scalpel under a microscope to collect cell aggregates. The cell aggregates were seeded on a LM/PLO-coated dish and cultured in DMEM/F12 containing 2.5 mM GlutaMax, 2% B27 supplement, 10 ng/mL BDNF, 10 ng/mL GDNF, 0.2 mM ascorbic acid, 0.5 mM

dcAMP, 1 ng/mL TGF- β 3, 100 U/mL penicillin, and 100 μ g/mL streptomycin. After 14 days of culture, the cells were fixed with paraformaldehyde and immunostained.

Function of cell aggregates in microbeads after cryopreservation

Cell aggregates in agarose microbeads were cryopreserved as previously reported [18]. Chilled KYO-1 solution (5.38 M ethylene glycol, 2 M dimethyl sulfoxide, 0.1 M polyethylene glycol 1000, and 0.00175 M polyvinylpyrrolidone (molecular weight 10,000) in Euro-Collins solution) was used for vitrification. Briefly, on day 23, 800 cell aggregates in agarose microbeads were suspended in 100 μ L of Euro-Collins solution in a cryotube. Chilled KYO-1 solution was sequentially added and the suspension was incubated as follows: addition of 10 μ L KYO-1 and incubation for 10 min at room temperature, addition of 5 μ L KYO-1 and incubation for 15 min at room temperature, addition of 15 μ L KYO-1 and incubation for 15 min on ice, and addition of 980 μ L KYO-1 and incubation for 5 min at 0 °C. After these procedures, the cryotube was quickly immersed in liquid nitrogen for 3 min, then stored in the vapor phase of liquid nitrogen. After 24 h of cryopreservation, the cryotube was immersed into a 30% dimethyl sulfoxide-water solution at room temperature to thaw the suspension rapidly. The suspension was transferred to a conical tube containing 10 mL Euro-Collins solution and centrifuged at 1000 rpm for 3 min. The supernatant was discarded and the microbeads were resuspended in 0.75 M sucrose solution (DMEM/F12, 2% B27 supplement) and incubated at 0 °C for 30 min to remove intracellular vitrification solution. Then, ice-cold culture medium (1 mL DMEM/F12 plus 2% B27 supplement) was added every 5 min for 20 min. The final suspension was centrifuged at 1000 rpm

for 3 min and resuspended in culture medium. Cells were cultured for 17 days for maturation. Seven hundred cell aggregates in microbeads were used for the analysis of DA secretion.

5.3. Results

Differentiation of human iPS cells into dopamine neuron

The dual-SMAD inhibition and floor-plate induction protocol [10], which was developed for effective differentiation of human ES cells into midbrain DA neurons, was used to induce differentiation of hiPS cells into DA neurons (Scheme 1). Briefly, undifferentiated hiPS cells were seeded on a Matrigel-coated dish and cultured in medium containing inhibitors and cytokines for 18 days. Morphological changes in the iPS cells were observed after a few days in culture. Expression of pluripotent markers such as SSEA-4 and Oct 3/4 rapidly decreased and was hardly detectable at day

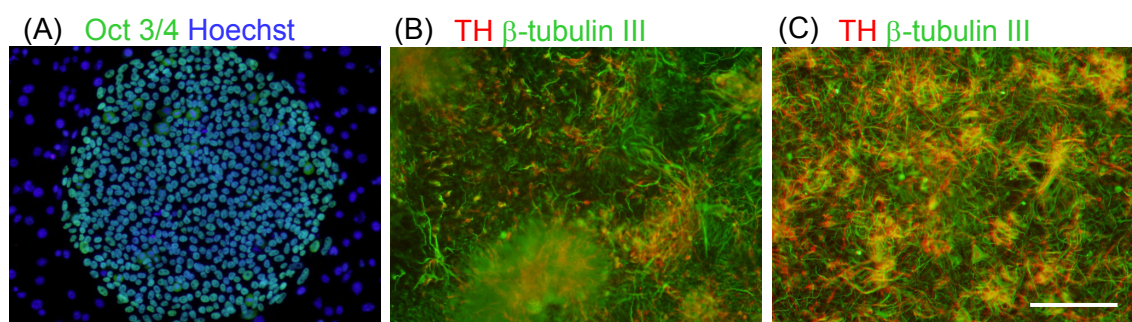


Fig. 1. Differentiation of hiPS cells into DA neurons. A: Fluorescent micrograph of undifferentiated hiPS cells on SNL feeder cells. The cells were immunologically stained with an antibody against Oct 3/4, and nuclei were stained with Hoechst 33258. B, C: Fluorescent micrographs of cells on day 18 (B) and on day 25 (C). Cells were immunologically stained with antibodies against TH and β -tubulin III. Scale bar: 200 μ m.

10 by immunohistochemistry (data not shown). On day 18, half of the cells were positive for β -tubulin III, a marker of both immature and mature neurons, but most cells were negative for TH, a marker of DA neurons (Fig. 1B). Progenitor cells and immature neurons coexisted in the culture. The cells were subcultured onto LM/PLO substrate and cultured for an additional week to assess lineage-specific differentiation. Approximately 20% of the cells became TH-positive by day 25 (Fig. 1C). These observations indicate that the hiPS cells were successfully differentiated into the DA neuron lineage.

Agarose microencapsulation

On day 18 of culture, cells that were insufficiently matured were easily collected from the culture dishes without damaging the cells. The cells were seeded into U-bottom 96-well plates pretreated with pluronic F127 at a density of 6000 cells/well to

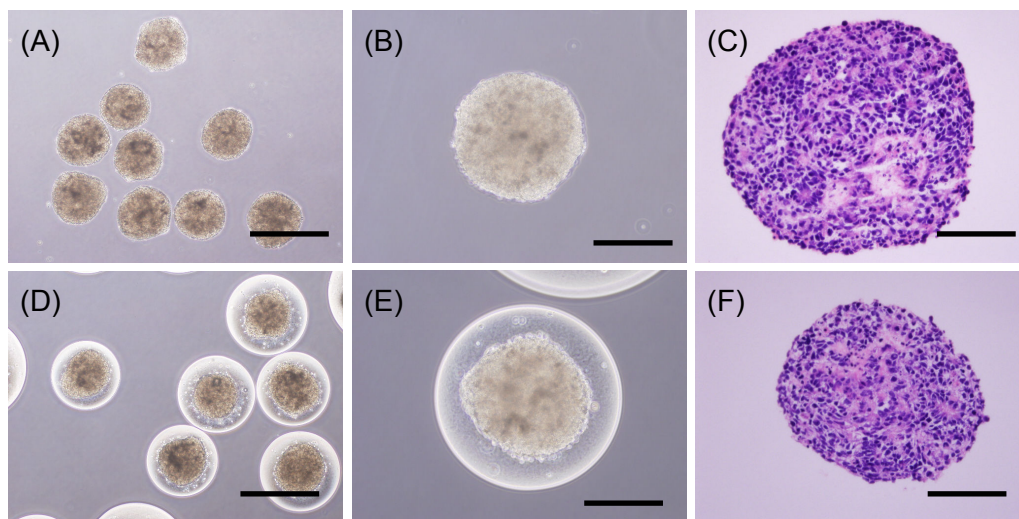


Fig. 2. Effect of microencapsulation on the morphology of cell aggregates derived from hiPS cells. Phase contrast micrographs of cell aggregates before (A, B) and after (D, E) microencapsulation. C, F: Hematoxylin and eosin staining of cell aggregates before (C) and after (F) microencapsulation. Scale bars: 500 μ m (A, C), 200 μ m (B, E), and 100 μ m (C, F).

induce cell aggregate formation. After 5 days, a cell aggregate with diameter of 300-400 μm was found in each well. The cell aggregates were collected from the plates and microencapsulated in agarose microbeads as previously reported [18]. Figure 2 contains phase contrast micrographs of microencapsulated cell aggregates and images of hematoxylin and eosin staining of thin sections before and immediately after microencapsulation. Cells exhibited a compact multicellular morphology; apparent cell death was not observed even after encapsulation.

Long-term culture

Cell aggregates were cultured for an additional 45 days to induce maturation of DA neurons. Free cell aggregates that lacked microencapsulation gathered together, and large aggregates formed (Fig. 3A and B). The core of the aggregates became dark. Cell necrosis was seen in the core of an aggregate due to limited supplies of oxygen and nutrients. After long-term culture (Fig. 3C-F), formation of large aggregates was inhibited and cells located at the center of the aggregates were still living when the cell aggregates were microencapsulated.

Figure 4 contains immunofluorescent images of cell aggregates in microbeads. Most of the cells were tubulin βIII -positive, and some cells became TH-positive on days 40 and 68. The percentage of cells positive for both tubulin βIII and TH were $42.0 \pm 8.7\%$ and $66.3 \pm 7.1\%$ on days 40 and 68, respectively. GFAP-positive glial cells were hardly detectable at day 40, but a few GFAP-positive cells were observed on day 68.

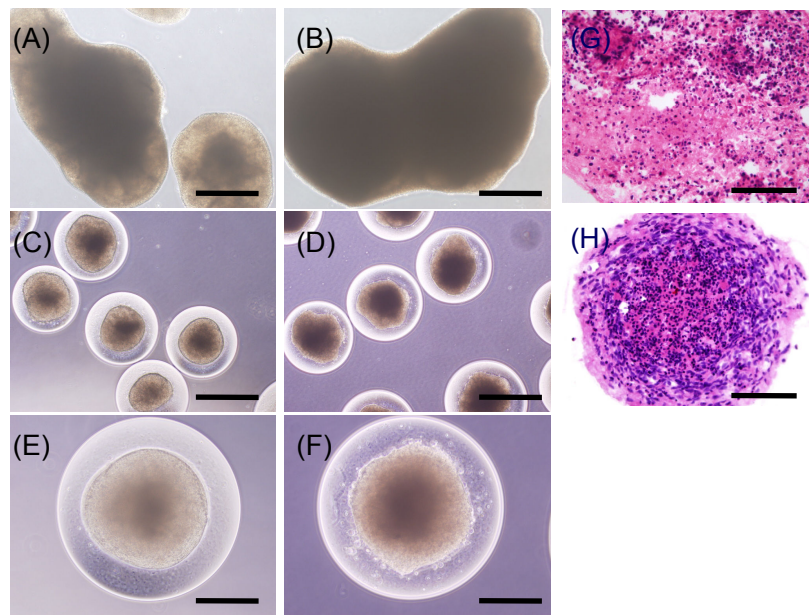


Fig. 3. Long-term culture of free cell aggregates and microencapsulated cell aggregates. A, B: Phase contrast microscopy of free cell aggregates on day 40 (A) and day 68 (B). C-F: Phase contrast microscopy of cell aggregates in agarose microbeads at day 40 (C, E) and day 68 (D, F). G: Hematoxylin and eosin staining of thin sections of free cell aggregates on day 68. H: Hematoxylin and eosin staining of cell aggregates in agarose microbeads on day 68. Scale bars: 500 μm (A-D), 200 μm (E-F), and 100 μm (G-H).

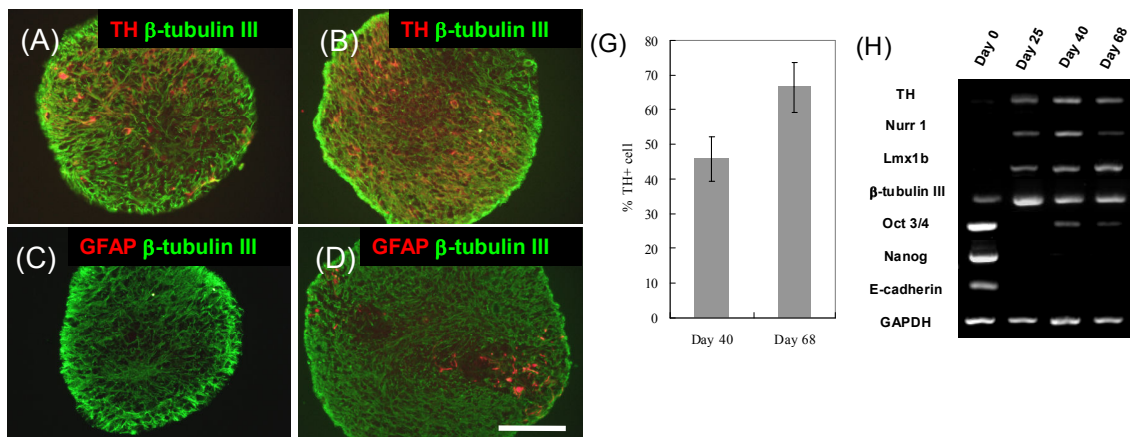


Fig. 4. Differentiation of hiPS cells in agarose microbeads into DA neurons. A, B: Fluorescent micrographs of cells immunologically stained using antibodies against TH and β -tubulin III on day 40 (A) and day 68 (B). C, D: Fluorescent micrographs of cells immunologically stained using antibodies against GFAP and β -tubulin III, (A, B) on day 40 (C) and day 68 (D). Scale bar: 100 μm . E: Percentage of TH-positive cells in cell aggregates on day 40 and day 68. F: RT-PCR of cells on day 0, day 25, day 40, and day 68.

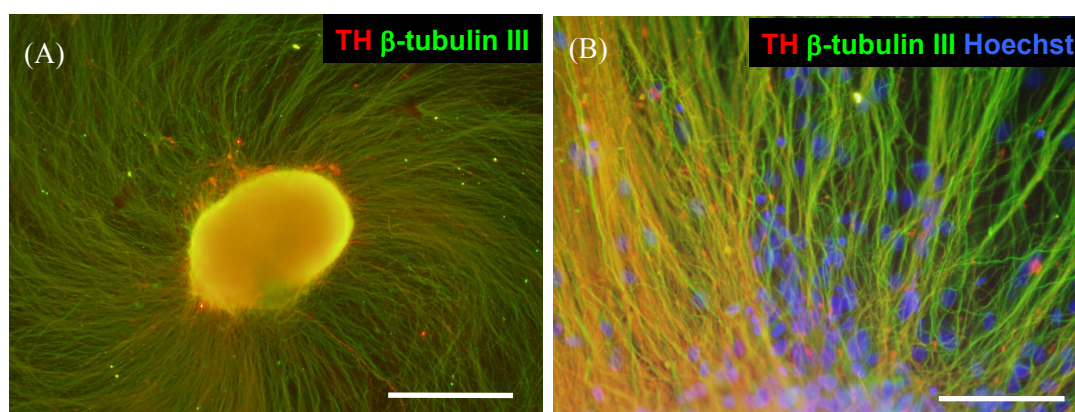


Fig. 5. Potential of cells in aggregates to extend neurites. Agarose microbeads were mechanically disrupted to collect cell aggregates on day 68, and the cell aggregates were cultured on LM/PLO substrate for 14 days. A: Fluorescent micrograph of cells immunologically stained using antibodies against TH (red) and β -tubulin III (green). B: High-magnification image of (A). Cell nuclei were stained with Hoechst 33258. Scale bars: 500 μ m (A) and 100 μ m (B).

RT-PCR of these cell aggregates revealed the expression of tubulin β III and TH (Fig. 4F). Expression of other DA neuron markers, such as Nurr1 and Lmx1b, were also detected by RT-PCR (Fig. 4F). These results indicate that the cells were differentiated into DA neurons, which were maintained in the cell aggregates after 68 days of culture. The pluripotent stem cell markers Oct 3/4 and SSEA-4 were not detected in immunofluorescent images of cell aggregates on day 40 and day 68. RT-PCR, however, indicated that expression of Oct 3/4 disappeared at day 25, but occurred on day 40 and day 68 (Fig. 4F).

Agarose beads were mechanically disrupted on day 68 to collect cell aggregates, which were seeded onto LM/PLO substrate. Many neurites extended from the aggregates within 1 day, and were elongated over 1 mm after 2 week.

Dopamine production

DA production by cells in microbeads was studied by depolarization in 56 mM KCl. Twelve hundred cell aggregates were incubated for 30 min in 0.5 mL 56 mM KCl in HBBS. The supernatants were collected and analyzed by HPLC (Fig. 6A). The DA peak was small on day 26, but became large and clearly visible after 61 days of cell culture (Fig. 6B). The amounts of DA produced by the microencapsulated cells gradually increased during culture; DA production was sustained to the end of culture. The low level of DA production at day 26 was due to insufficient maturation of cells, and coincided with a small ratio of TH-positive cells in the cell aggregates at day 26.

DA production by cells that were differentiated on LM/PLO substrate was also examined to assess the effects of cell aggregation formation and microencapsulation on

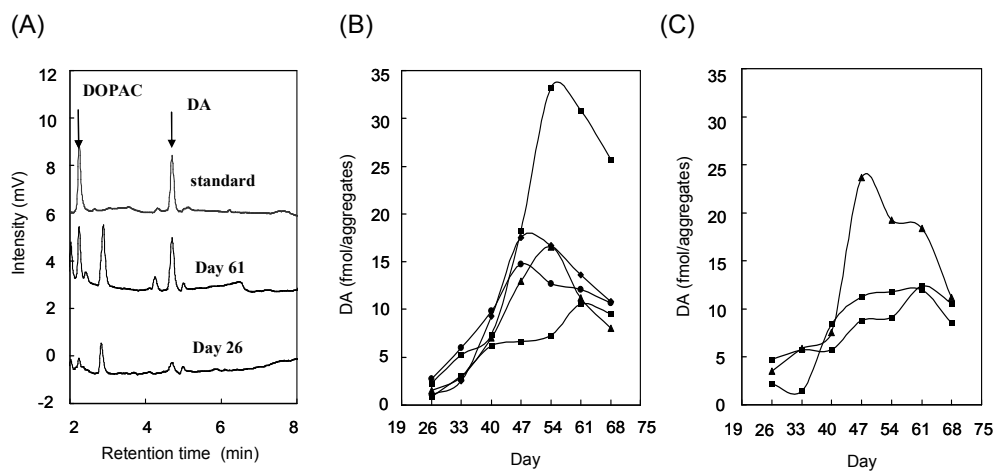


Fig. 6. DA production by cell aggregates in agarose microbeads. Microencapsulated cell aggregates (1200) were depolarized in 56 mM KCl for 30 min. The supernatants were analyzed by reverse-phase HPLC. A: Representative HPLC output: upper line, standard solution of 20 nM DA and 20 nM 3,4-dihydroxyphenylacetic acid (DOPAC); middle line, supernatant from microencapsulated cell aggregates on day 68; bottom line, supernatant from microencapsulated cell aggregates on day 26. Arrows indicate the peaks for DA and 3,4-dihydroxyphenylacetic acid (DOPAC), respectively. B: Temporal changes in DA production levels of microencapsulated cell aggregates (n = 4). C Temporal changes in DA production levels of cells adhered on LM/PLO substrate (n = 3).

DA production. DA production by cells in adherent culture gradually increased throughout the culture period; the amounts of production were similar to those of the encapsulated cells (Fig. 6B and C). No clear difference in DA production was observed between cells on LM/PLO substrate and cells in agarose beads.

Cryopreservation of encapsulated DA neuron

Vitrification was examined for cryopreservation of cell aggregates in agarose microbeads to avoid intracellular ice formation and to preserve the integrity of agarose capsules [18]. Cell aggregates from day 23 were used for cryopreservation. Microbeads and cell aggregates exhibited no morphological differences before and after freezing and thawing (Fig. 7A, B). These cells were further cultured to induce maturation; after 17 days, no morphological changes or cell death in the cell aggregates were observed (Fig. 7C). TH-positive cells were observed on day 40 (Fig. 7D). The amounts of DA secreted from cryopreserved cells were the same as those secreted by non-cryopreserved cells (Fig. 7E).

5.4. Discussion

The floor-plate induction protocol [10] was employed to induce differentiation of iPS cells into DA neurons. On day 18, cells were detached from culture dishes and applied to U-bottom 96-well plates to form cell aggregates. The cell aggregates were enclosed into agarose microbeads and cultured for differentiation into DA neurons. Approximately 66% of all cells became DA neurons (Fig. 4E) Although LM/PLO

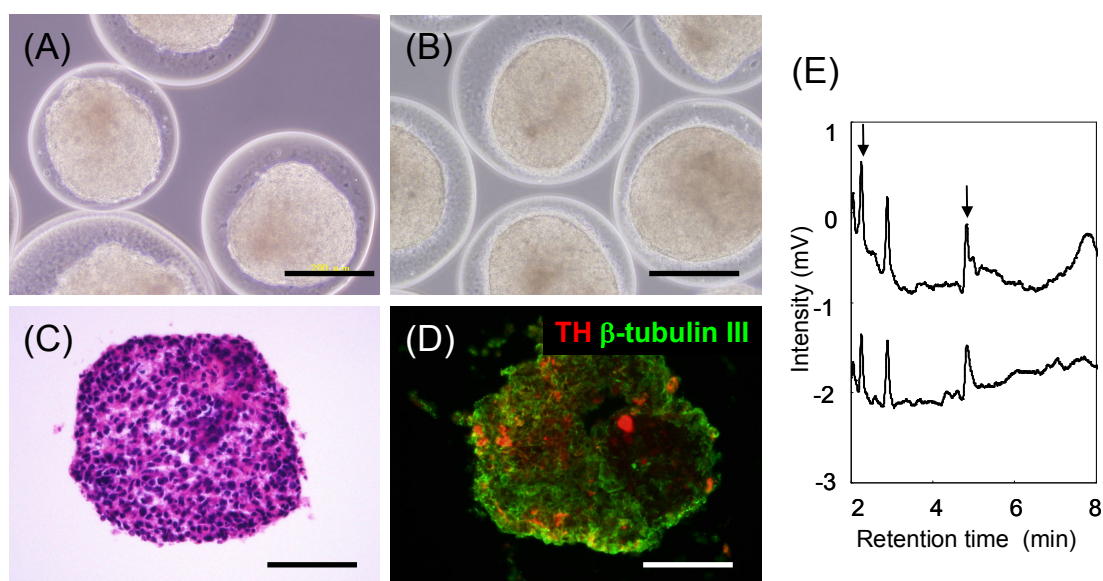


Fig. 7. Cryopreservation of cell aggregates in agarose microbeads. A, B: Phase contrast microscopy of cryopreserved cell aggregates immediately after thawing (A) and on day 40 (B). C, D: Hematoxylin and eosin staining of thin sections of cell aggregates immediately after thawing (C) and on day 40 (D). E: Fluorescent micrograph of cells at day 40 immunologically stained with antibodies against TH (red) and β -tubulin III (green). F: HPLC chromatograms of supernatants from depolarization studies of the cell aggregates in 56 mM KCl for 30 min on day 40. The lower and upper lines indicate data from cell aggregates with and without cryopreservation, respectively. Scale bars: 200 μ m (A) and 100 μ m (B).

substrate was employed to mature cells into DA neurons in the original protocol, hiPS cells in aggregates efficiently differentiated into DA neurons in agarose microcapsules. Cell aggregates without encapsulation adhered each to other and formed large aggregates, and the amount of DA produced from these aggregates was much smaller than that produced by the cell aggregates in microbeads due to necrosis in the core of the large cell aggregates. Agarose microbeads effectively inhibited formation of large cell aggregates and did not disrupt the differentiation of hiPS cells into DA neurons. No clear difference in DA production was observed between cells on LM/PLO substrate and cells encapsulated in agarose beads (Fig. 6). DA from DA neurons rapidly passed

through the agarose layer of the microbeads and was released into the medium, suggesting that the microbeads did not hinder DA release. Additionally, DA neurons in the microbeads could be handled without specific protocols, since the microbeads protected the fragile DA neurons from mechanical stress.

Once cells have been encapsulated, it is relatively easy to maintain them in large quantities. More than 1000 capsules can be cultured in a flask without the need for special protocols. Cell aggregates in microbeads can be cryopreserved (Fig. 7). DA-releasing cells should be supplied at the time of patient transplantation; cryopreservation of DA neurons is one way to realize this goal. Attention should be paid to graft volume, as there is limited space in the substantia nigra. When DA neurons are enclosed into microbeads, the volume of the graft will become several times larger than that of cells without microencapsulation. It was reported that more than 100,000 surviving DA neurons in each putamen are required for the treatment of PD [9]. Each microbead contained $3 \times 10^3 - 4 \times 10^3$ DA neurons, as estimated from the number of TH-positive cells (Fig. 4) and from the measurements of DA release (Fig. 6). Approximately 25-40 microbeads are required to treat a human patient, for a total graft volume of less than 0.01 mL. It will not be difficult to transplant such a small volume of microbeads. Taken together, these properties indicate that agarose microbeads are suitable for preparing a large number of DA neurons for treatment of human PD patients.

Tumor formation is a substantial problem during cell transplantation therapy using iPS derived-cells [13, 14]. Undifferentiated pluripotent stem cells and neural progenitors contained in transplants may proliferate and overgrow in the host brain [15]. The risk of tumor formation can be reduced by maturing cells for a long period *in vitro*

before transplantation, as previously reported [16, 17]. However, our RT-PCR analyses indicated that expression of Oct 3/4 disappeared at day 25, but was again detectable at day 40 and day 68 (Fig. 4F). It is uncertain as to the significance of the reoccurrence of Oct 3/4 expression at this point. Another pluripotent stem cell marker, Nanog, was not detected by RT-PCR after differentiation culture.

Graft rejection by the host immune system is unavoidable in transplantation therapy; DA neurons derived from ES cells are expected to be recognized as allogeneic tissue in patients. Reprogramming protocols for the preparation of iPS cells may affect the immunogenicity of iPS cells [18, 19]. The host immune system responds to cells derived from these cells [20, 21]. Immune reactions against banked DA neurons from iPS cells should be carefully controlled. Given the observations reported here, it is expected that agarose microbeads will provide an environment favorable to the survival of DA neurons, as agarose microbeads effectively protect allogeneic islet grafts from rejection in mice diabetes models [23, 24].

Some researchers have claimed that DA release in the substantia nigra is not sufficient to treat PD, that DA neurons should be integrated with the host brain, and that DA release is regulated through synaptic connections [9]. If these claims were valid, agarose microcapsulation could become an obstacle. Careful examination is needed to assess the functions of microencapsulated DA neurons *in vivo*.

References

- [1] Dauer W, Przedborski S. Parkinson's Disease: Review Mechanisms and Models. *Neuron* 2003;39:889–909.
- [2] Nurt JG, Wooten Gf. Diagnosis and initial management of Parkinson's disease. *N Engl J Med* 2005;353:1021–7.
- [3] Cools R. Dopaminergic modulation of cognitive function-implications for L-DOPA treatment in Parkinson's disease. *Neurosci Biobehav* 2006;30:1–23.
- [4] Rascol O, Brooks DJ, Korczyn AD, De Deyn PP, Clarke CE, Lang AE. A five-year study of the incidence of dyskinesia in patients with early Parkinson's disease who were treated with ropinirole or levodopa. *N Engl J Med* 2000;342:1484–91.
- [5] Freed CR, Greene PE, Breeze RE, Tsai WY, DuMouchel W, Kao R, et al. Transplantation of embryonic dopamine neurons for severe Parkinson's disease. *N Engl J Med* 2001;344:710–9.
- [6] Hauser RA, Freeman TB, Snow BJ, Nauert M, Gauger L, Kordower JH, et al. Long-term evaluation of bilateral fetal nigral transplantation in Parkinson disease. *Arch Neurol* 1999;56:179–87.
- [7] Mendez I, Sanchez-Pernaute R, Cooper O, Viñuela A, Ferrari D, Björklund L, et al. Cell type analysis of functional fetal dopamine cell suspension transplants in the striatum and substantia nigra of patients with Parkinson's disease. *Brain* 2005;128:1498–510.
- [8] Robinton DA, Daley GQ. The promise of induced pluripotent stem cells in research and therapy. *Nature* 2012;481:295–305.
- [9] Lindvall O, Kokaia Z. Prospects of stem cell therapy for replacing dopamine

- neurons in Parkinson's disease. *Trends Pharmacol Sci* 2009;30:260–7.
- [10] Kriks S, Shim JW, Piao J, Ganat YM, Wakeman DR, Xie Z, et al. Dopamine neurons derived from human ES cells efficiently engraft in animal models of Parkinson's disease. *Nature* 2011;480:547–51.
- [11] Rhee YH, Ko JY, Chang MY, Yi SH, Kim D, Kim CH, et al. Protein-based human iPS cells efficiently generate functional dopamine neurons and can treat a rat model of Parkinson disease. *J Clin Invest* 2011;121:2326–35.
- [12] Swistowski A, Peng J, Liu Q, Mali P, Rao MS, Cheng L, et al. Efficient generation of functional dopaminergic neurons from human induced pluripotent stem cells under defined conditions. *Stem Cells* 2010;281:893–904.
- [13] Hentze H, Graichen R, Colman A. Cell therapy and the safety of embryonic stem cell-derived grafts. *Trends Biotechnol* 2007;25:24–32.
- [14] Fong CY, Gauthaman K, Bongso A. Teratomas from pluripotent stem cells: A clinical hurdle. *J Cell Biochem* 2010;111:769–81.
- [15] Li JY, Christophersen NS, Hall V, Soulet D, Brundin P. Critical issues of clinical human embryonic stem cell therapy for brain repair. *Trends Neurosci* 2008;31:146–53.
- [16] Brederlau A, Correia AS, Anisimov SV, Elmi M, Paul G, Roybon L, et al. Transplantation of human embryonic stem cell-derived cells to a rat model of Parkinson's disease: effect of in vitro differentiation on graft survival and teratoma formation. *Stem Cells* 2006;24:1433–40.
- [17] Seminatore C, Polentes J, Ellman D, Kozubenko N, Itier V, Tine S, et al. The postischemic environment differentially impacts teratoma or tumor formation after transplantation of human embryonic stem cell-derived neural progenitors. *Stroke*

2010;41:153–9.

- [18] Drukker M, Benvenisty N. The immunogenicity of human embryonic stem-derived cells. *Trends Biotechnol* 2004;22:136–41.
- [19] Bradley JA, Bolton EM, Pedersen RA. Stem cell medicine encounters the immune system. *Nat Rev Immunol* 2002;2:859–71.
- [20] Taylor CJ, Bolton EM, Bradley JA. Immunological considerations for embryonic and induced pluripotent stem cell banking. *Philos Trans R Soc Lond B Biol Sci* 2011;366:2312–22.
- [21] Zhao T, Zhang ZN, Rong Z, Xu Y. Immunogenicity of induced pluripotent stem cell. *Nature* 2011;474:212–5.
- [22] Nakatsuji N, Nakajima F, Tokunaga K. HLA-haplotype banking and iPS cells. *Nat Biotechnol*. 2008;26:739–40.
- [23] Iwata H, Takagi T, Amemiya H, Shimizu H, Yamashita K, Kobayashi K, et al. Agarose for a bioartificial pancreas. *J Biomed Mater Res* 1992;26:967–77.
- [24] Teramura Y, Iwata H. Bioartificial pancreas microencapsulation and conformal coating of islet of Langerhans. *Adv Drug Deliv Rev* 2010;62:827–40.
- [25] Agudelo CA, Teramura Y, Iwata H. Cryopreserved agarose-encapsulated islets as bioartificial pancreas: a feasibility study. *Transplantation* 2009;87:29–34.
- [26] Takahashi K, Tanabe K, Ohnuki M, Narita M, Ichisaka T, Tomoda K, et al. Induction of pluripotent stem cells from adult human fibroblasts by defined factors. *Cell* 2007;131:861–872.
- [27] Nakagawa M, Koyanagi M, Tanabe K, Takahashi K, Ichisaka T, Aoi T, et al. Generation of induced pluripotent stem cells without Myc from mouse and human fibroblasts. *Nature Biotechnol* 2008;26:101–106.

- [28] Nishigaki T, Teramura Y, Nasu A, Takada K, Toguchida J, Iwata H. Highly efficient cryopreservation of human induced pluripotent stem cells using a dimethyl sulfoxide-free solution. *Int J Dev Biol* 2011;55:305–11.
- [29] Ando T, Yamazoe H, Moriyasu K, Ueda Y, Iwata H. Induction of dopamine-releasing cells from primate embryonic stem cells enclosed in agarose microcapsules. *Tissue Eng* 2007;13:2539–47.

Summary

Chapter 1

To gain insights into the effect of various growth factors on the behaviors of NSCs, cell culture assays were performed on the array that displayed five different growth factors. The array-based analyses showed that bFGF-His and EGF-His as a single component promoted the proliferation of NSCs. In contrast, IGF1-His and BDNF-His promoted neuronal differentiation of NSCs, while CNTF-His did glial differentiation. The array-based analysis further provided new insights into the combinatorial effects of growth factors. In the case that two different growth factors were co-displayed on a single spot, the behaviors of NSCs could not be simply predicted from their individual effects. A multivariate cluster analysis was carried out for the quantitative data on cell proliferation and differentiation. It was shown that the effect of two growth factors co-displayed was competitive, synergistic, or destructive depending on the combinations. In other peculiar cases, the effect of growth factors was totally different from those of individual factors.

Chapter 2

Currently, the most standard method to obtain NSCs is neurosphere culture. However, there are still limitations with this method. The most critical problems may be heterogeneity of cells in a neurosphere. To overcome these limitations, culture substrates were designed to selectively expand hNSCs in adherent culture. Based on the results of chapter 1, EGF-immobilized culture substrates were designed for the expansion of NSC. Engineered EGF fused with His or PSt peptide can be

Summary

surface-anchored to glass plates or polystyrene dishes, respectively. The culture module fabricated with the EGF-His/glass substrate enables to selectively expand rat NSCs in a closed system. The EGF-PSt/polystyrene dish also permits selective expansion of NSCs. Rat NSCs could be selectively captured on the EGF-immobilized surface most likely through EGF-EGFR interactions. The captured NSCs proliferated on the substrate on account of mitogenic activity of EGF while keeping the undifferentiated state. As a result, highly pure NSCs could be obtained 2-times faster than in neurosphere culture. With the culturewares developed here, one can prepare 1×10^7 NSCs within 5 d at a reasonably high purity. EGF-immobilized substrates practically provide a straightforward means to acquire large quantity of pure NSCs in standard laboratories.

Chapter 3

In this chapter, the surface-anchoring method was further applied to the expansion of human NSC. Because of an observed difference in the expression pattern of growth factor receptors between rat NSCs and human NPCs, two growth factors, EGF or bFGF, were immobilized on the glass substrates as a single component or the combination of two factors. Adhesion and proliferation of hNPCs took place most efficiently on the surface with both EGF and bFGF compared to surfaces with either factor as well as a bare glass surface. The rate of cell proliferation was more than 2-fold higher in the adherent culture on the substrate developed here than in the standard neurosphere culture. A population obtained after 5-day culture on the substrate contained nestin-expressing progenitors at a content of approximately 90%. The culture substrate with immobilized both EGF and bFGF is effective for the selective expansion of hNPCs.

Chapter 4

This chapter describes the investigation of nine kinds of ECM, including collagen I, collagen IV, gelatin, laminin-1, laminin-5, Matrigel, fibronectin, vitronectin, and ProNectin F, for their efficacy as a culture substrate for iPS-derived NPCs. Mouse iPS cells were differentiated into NPCs with the serum-free, floating culture method. The NPCs obtained were cultured on an array that displayed different types of ECMs. The results showed that NPCs derived from mouse iPS cells efficiently proliferated on a substrate with immobilized laminin-1, laminin-5, and Matrigel. Consequently, a laminin-1-immobilized substrate was tested for efficacy in supporting NPCs derived from human iPS cells. The human NPCs also proliferated selectively on this substrate without impairment of multipotent differentiation capability. Thus, immobilized laminin-1 was an effective substrate for the selective expansion of NPCs derived from mouse or human iPS cells.

Chapter 5

Dopamine neurons derived from induced pluripotent stem cells have been widely studied for the treatment of Parkinson's disease. However, various difficulties remain to be overcome, such as tumor formation, fragility of dopamine neurons, difficulty in handling large numbers of dopamine neurons, and immune reactions. In this chapter, human induced pluripotent stem cell-derived precursors of dopamine neurons were encapsulated in agarose microbeads. Approximately 66% of all cells differentiated into tyrosine hydroxylase-positive neurons in agarose microbeads. The cells released dopamine for more than 40 days. Dopamine neurons in microbeads could be handled without specific protocols, because the microbeads protected the fragile

Summary

dopamine neurons from mechanical stress. In addition, microbeads containing cells can be cryopreserved. Agarose microencapsulation therefore provides a good supporting environment for the preparation and storage of dopamine neurons.

List of Publications

- Chapter 1 Konagaya S, Kato K, Nakaji-Hirabayashi T, Arima Y, Iwata H. Array-based functional screening of growth factors toward optimizing neural stem cell microenvironments. *Biomaterials* 2011;32;5015–22.
- Chapter 2 Konagaya S, Kato K, Nakaji-Hirabayashi T, Iwata H. Design of culture substrates for large-scale expansion of neural stem cells. *Biomaterials* 2011;32;992–1001.
- Chapter 3 Konagaya S, Kato K, Nakaji-Hirabayashi T, Iwata H. Selective and rapid expansion of human neural progenitor cells on a substrate with terminally-anchored growth factors. In preparation.
- Chapter 4 Konagaya S, Kato K, Komura T, Iwata H. Effect of surface-immobilized extracellular matrices on the proliferation of neural progenitor cells derived from induced pluripotent stem cells. In preparation.
- Chapter 5 Konagaya S, Iwata H. Induction of dopamine neurons from human induced pluripotent stem cells in agarose microbeads. *Biomaterials* Submitted.

List of papers presented at international meetings

Kato K, Konagaya S, Nakaji-Hirabayashi T, Iwata H. Culture substrates with immobilized growth factors for use in in vitro expansion of human neural progenitor cells. Tissue Engineering and Regenerative Medicine International Society (TERMIS), 2010 Asia Pacific Meeting, Sydney, Australia (15–17 September 2010)

Konagaya S, Kato K, Komura T, Iwata H. Culture substrate for the expansion of neural progenitor cells derived from induced pluripotent stem cells. 3rd TERMIS World Congress, Vienna, Austria (6-9 September, 2012)

Acknowledgements

The present research was carried out from 2008 to 2013 under the continuous guidance of Dr. Hiroo Iwata, Professor of the Institute for Frontier Medical Sciences, Kyoto University. The author is deeply indebted to Professor Iwata for his constant guidance, encouragement, valuable discussion, and detailed criticism on the manuscript throughout the present work. The completion of the present research has been an exiting project and one which would not have been possible without his guidance.

The author is very grateful to Dr. Koichi Kato, Professor of Institute of Biomedical & Health Sciences, Hiroshima University for his constant guidance, helpful suggestions, and detailed criticism.

The author would like to express his great thank to Dr. Tadashi Nakaji-Hirabayashi, Assistant Professor of Frontier Research Core for Life Science, University of Toyama, for his valuable advice. The author also expresses his thanks to Mr. Edgar Yuji Egawa and Mr. Takashi Komura, Institute for Frontier Medical Sciences, Kyoto University, for their kind cooperation and useful suggestions.

General acknowledgments are due to Miss Yoshiko Suzuki, Dr. Yusuke Arima, Dr. Narifumi Kitamura, Dr. Tomonobu Kodama and other members of Professor Iwata's laboratory for their kind help.

Finally, the author likes to take the opportunity to extend hearty thanks to his parents, Yoshihiro and Noriko Konagaya, and his brother, Takuro Konagaya for their cordial support and continuous encouragement.

January, 2013

Kyoto

Shuhei Konagaya

Acknowledgements